THE ROLE OF THE PROTEASOME-ASSOCIATED PROTEIN ECM29 IN QUALITY CONTROL OF THE PROTEASOME

by

ALINA M. DE LA MOTA-PEYNADO

B.S., University of Puerto Rico-Mayaguez Campus, 1999
M.S., University of Puerto Rico-Mayaguez Campus, 2004

AN ABSTRACT OF A DISSERTATION

submitted in partial fulfillment of the requirements for the degree

DOCTOR OF PHILOSOPHY

Division of Biology
College of Arts and Sciences

KANSAS STATE UNIVERSITY
Manhattan, Kansas

2014

Abstract

The ubiquitin-proteasome pathway is the major pathway of selective protein degradation in the cell. Disruption of this pathway affects cellular protein homeostasis and contributes to diseases like cancer, and neurodegeneration. The end point of this pathway is the proteasome, a complex protease formed by 66 polypeptides. Structurally, it can be subdivided into the Core Particle (CP) and the Regulatory Particle (RP). The CP harbors the proteolytic sites, whereas, the RP contains six orthologous AAA-ATPases, the Rpt proteins. These Rpt's are essential for proteasome function and are at the interface between RP and CP. The work in this thesis focuses on the Rpt subunit Rpt5 from yeast. The C-terminal tail of Rpt5 has been shown to contribute to the binding with the CP. However, our study showed it is also essential for the interaction with Nas2, one of nine proteasome-specific chaperones. Thus, Nas2 might function as a regulator of the Rpt5-CP interaction. Further analyses suggested that Nas2 has an additional function in assembly, and that mutating the tail of Rpt5 results in increased binding of the proteasome-associated protein Ecm29 to the proteasome. We showed that Ecm29 binds Rpt5 directly, thereby inducing a closed conformation of the CP substrate entry channel, and inhibiting proteasomal ATPase activity. Consistent with these activities, several proteasome mutant strains showed Ecm29-dependent accumulation of unstable substrates. Thus, Ecm29 is an inhibitor of the proteasome in vivo and in vitro. Interestingly, besides the Rpt5 mutants, several other proteasome mutants show increased levels of Ecm29, suggesting Ecm29 has a role in quality control. Consistent with this, we observed that Ecm29 associates preferably with specific mutants and nucleotide-depleted proteasomes.

Based on our data we propose a model, where early in assembly Nas2 binds to the Rpt5 tail inhibiting the Rpt5-CP interaction directly. Later in assembly Ecm29 performs a quality control function, where it recognizes and remains bound to defective proteasomes. By inhibiting these proteasomes Ecm29 prevents the aberrant degradation of proteins.

THE ROLE OF THE PROTEASOME-ASSOCIATED PROTEIN ECM29 IN QUALITY CONTROL OF THE PROTEASOME

by

ALINA M. DE LA MOTA-PEYNADO

B.S., University of Puerto Rico-Mayaguez Campus, 1999
M.S., University of Puerto Rico-Mayaguez Campus, 2004

A DISSERTATION

submitted in partial fulfillment of the requirements for the degree

DOCTOR OF PHILOSOPHY

Division of Biology
College of Arts and Sciences

KANSAS STATE UNIVERSITY
Manhattan, Kansas

2014

Approved by:

Major Professor
Dr. Jeroen Roelofs

Copyright

Abstract

The ubiquitin-proteasome pathway is the major pathway of selective protein degradation in the cell. Disruption of this pathway affects cellular protein homeostasis and contributes to diseases like cancer, and neurodegeneration. The end point of this pathway is the proteasome, a complex protease formed by 66 polypeptides. Structurally, it can be subdivided into the Core Particle (CP) and the Regulatory Particle (RP). The CP harbors the proteolytic sites, whereas, the RP contains six orthologous AAA-ATPases, the Rpt proteins. These Rpt's are essential for proteasome function and are at the interface between RP and CP. The work in this thesis focuses on the Rpt subunit Rpt5 from yeast. The C-terminal tail of Rpt5 has been shown to contribute to the binding with the CP. However, our study showed it is also essential for the interaction with Nas2, one of nine proteasome-specific chaperones. Thus, Nas2 might function as a regulator of the Rpt5-CP interaction. Further analyses suggested that Nas2 has an additional function in assembly, and that mutating the tail of Rpt5 results in increased binding of the proteasome-associated protein Ecm29 to the proteasome. We showed that Ecm29 binds Rpt5 directly, thereby inducing a closed conformation of the CP substrate entry channel, and inhibiting proteasomal ATPase activity. Consistent with these activities, several proteasome mutant strains showed Ecm29-dependent accumulation of unstable substrates. Thus, Ecm29 is an inhibitor of the proteasome *in vivo* and *in vitro*. Interestingly, besides the Rpt5 mutants, several other proteasome mutants show increased levels of Ecm29, suggesting Ecm29 has a role in quality control. Consistent with this, we observed that Ecm29 associates preferably with specific mutants and nucleotide-depleted proteasomes.

Based on our data we propose a model, where early in assembly Nas2 binds to the Rpt5 tail inhibiting the Rpt5-CP interaction directly. Later in assembly Ecm29 performs a quality control function, where it recognizes and remains bound to defective proteasomes. By inhibiting these proteasomes Ecm29 prevents the aberrant degradation of proteins.

Table of Contents

List of Figures

List of Tables

Acknowledgements

First, and foremost, I want to thank my advisor Jeroen, I could not have dreamed of having a better mentor. You are the perfect example of what a good scientist is. I thank life for the path that led me to your lab.

To my lab mates: Stella, Ranjit, Prashant, Ted, Mark, Eric, Alex, and specially Brianne, you have all been a great source of support and inspiration.

To all the wonderful graduate student friends I've made here: Thankfully you are too many to name, but you know who you are and I treasure your friendship and support immensely.

To the faculty and staff in the Division of Biology: Thanks for sharing your advice, knowledge, and support with me throughout my graduate career, it has been a great experience.

To Suranganie Dharmawardhane and Valance Washington: Thank you for giving me a chance, and teaching me to fall in love with science all over again.

To my family: Thank you because even though you all believe I am crazy, you still give me your love and support every day.

And last but not least, thanks to my husband Piti, for giving up the sun and surf of Puerto Rico so that I could pursuit my dreams.

Dedication

This work is dedicated to my mom Sandra, my grandmother Abali, and to the light of my life, Lucas. Los Amo.

Chapter 1 - Introduction

Protein homeostasis

For cellular proteins the levels inside the cell are determined both by the rate of protein synthesis and the rate of degradation. In the cell this is controlled by a network of pathways that tightly regulate the synthesis, folding, transport and degradation of proteins, known as protein homeostasis or proteostasis (Fig. 1.1). Maintenance of proteostasis is vital for cell function and ensures an organism will have successful development, healthy aging, the ability to resist environmental stress, and minimimal disruptions by pathogens. The loss of proteostatic control can lead to the accumulation and aggregation of misfolded proteins, or to the untimely degradation of proteins (1). These features are associated with numerous conditions including metabolic diseases, cancer and neurodegenerative disorders (15, 36).

The key to protein homeostasis is the balance between pathways involved in synthesis, post-translational modifications, and the degradation of proteins.

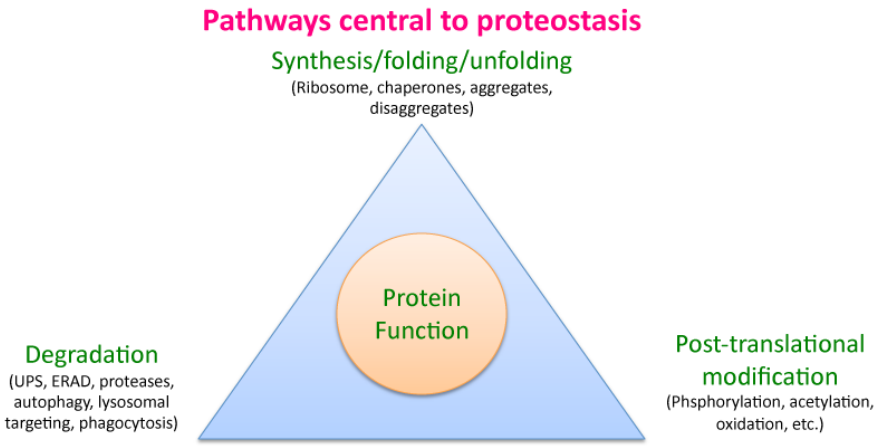

Figure 1.1 Cellular pathways essential to achieving homeostasis.

All cellular proteins are subjected to quality control mechanisms throughout their lifetime inside the cell (15, 21). Once proteins are synthesized at the ribosome, they need to acquire their tertiary (or quaternary) structure to be functional. Protein folding in vivo is accomplished through intrinsic factors of the folding polypeptide chain, often with the assistance of multiple classes of chaperones (1, 35). Different conditions can lead to protein degradation: abnormally synthesized proteins; de novo synthesized proteins that fail to spontaneously fold, or can't attain

their rightful conformation with the assistance of chaperones; previously folded proteins that unfold due to undesired post-translational modifications. Under such conditions proteins are delivered to the proteolytic machinery for degradation (15, 21).

Additionally, proteins could be targeted for degradation when they are present in excess (e.g. a protein that is part of a multimeric complex and is overexpressed will be unstable due to the inability to interact with a binding partner or chaperone); when the cell is going through different stages of the cell cycle; or when the cell requires changing its internal environment in response to external conditions (e.g. temperature, ion concentrations, pH) (19).

In all, there are multiple mechanisms involved in keeping proper protein homeostasis within the cell, including the degradation of proteins.

Protein degradation

Based on their turnover rate proteins can be classified as either "short-lived" proteins (with a fast degradation rate), or "long-lived" proteins (with a much slower degradation rate). Early studies that monitored protein kinetics together with lysosome inhibitors, suggested that long-lived and short-lived proteins were degraded differentially by either one of the two major pathways of protein degradation in the cell, the autophagy-lysosomal system (ALS) and the ubiquitin-proteasome system (UPS), respectively (4, 7). The assumption was that proteasome-mediated degradation had a high degree of specificity, because it involved specific labeling of substrates through the process of ubiquitination; whereas lysosomal degradation was non-selective in nature. However, more recent studies have shown that there is more complexity to these systems, and one has to consider not only the selectivity, and degradation kinetics, but also the purpose served by the degradation of the proteins (e.g. clearance, recycling) (7).

Figure 1.2 gives a general overview of how proteins are sorted for degradation. The UPS degrades two types of proteins: Fully functional proteins that are degraded as part of a regulatory mechanism (e.g. proteins involved in cell division, signal transduction) (11); and non-functional misfolded proteins that are degraded as part of a clearance mechanism (e.g. proteins degraded through the ER-associated degradation pathway (ERAD)) (12). Many short-lived proteins are degraded by the UPS. The proteolytic activity of the proteasome is not very specific, as it can degrade almost any protein. The specificity is achieved by selectively targeting substrates to the proteasome, this is done by labeling substrates through the covalent attachment of ubiquitin.

Thus, labeling with ubiquitin determines the specificity (4). There is one known exception to this rule, ornithine decarboxylase, a short-lived protein that is degraded by the proteasome without getting ubiquitinated.

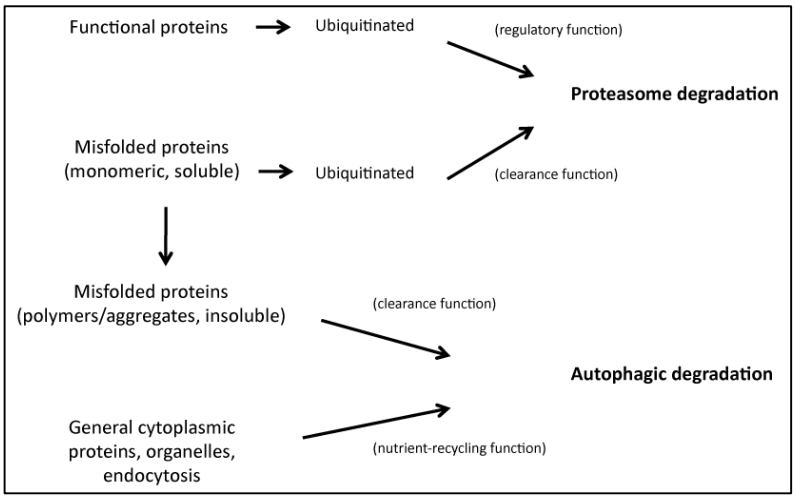

Figure 1.2 Sorting of proteins to be degraded in the cell

Proteins degraded by the ALS can be divided in two groups: First, proteins that are degraded in-bulk (e.g. during nutrient deprivation), as part of a nutrient recycling mechanism. The proteins that are degraded during this process would be functional proteins that are relatively long-lived (14, 18). This "in-bulk" degradation even includes whole organelles, and phagocytosed microbes (5); the second group of proteins that can be degraded by the ALS are non-functional misfolded proteins, these proteins are degraded as part of a clearance mechanism. The removal of these proteins requires a higher level of specificity. These proteins would likely be short-lived monomeric proteins that could turn long-lived due to aggregation (7).

The autophagy-lysosome system

Substrates of the ALS can be intra- and extracellular components. These substrates are degraded in an organelle known as the lysosome. The lysosome has an acidic lumen, and is limited by a single-lipid bilayer membrane. It contains 60 different types of acidic hydrolases that are devoted to the degradation of substrates. The hydrolases are activated by the acidic pH of the lumen, and can degrade a vast repertoire of biological substrates, including proteins, carbohydrates and DNA. Thus, the degradation is largely determined by what gets targeted to

the lysosome, and not by the enzyme specificity within the lysosome. Extracellular material that is destined for degradation reaches the lysosome mainly through the endocytic pathway, whereas intracellular components are transported to the lysosome by autophagy (28).

Autophagy is characterized by the formation of double-membrane vesicles called autophagosomes, which sequester the cytoplasmic structures destined for destruction. Three different forms of autophagy have been described: macroautophagy, microautophagy, and chaperone-mediated autophagy (CMA). They all differ in their mechanisms, and functions. (3, 23).

Both micro- and macroautophagy have the capacity to engulf large structures through both selective, and non-selective mechanisms, while CMA degrades only soluble proteins in a selective manner. A general overview of the three different types of autophagy is depicted in Figure 1.3.

Microautophay consists in the direct sequestration of cytosolic components by the lysosome. In microautophagy, the lysosomal/vacuolar membrane is randomly invaginated and differentiated to enclose portions of the cytosol. The formed vesicles are fused homotypically, and then bud into the lumen. The process has been well described in yeast. Two Atg7-dependent ubiquitin-like conjugation systems participate in microautophagy, mediating membrane tethering and vesicle fusion (20). The function and relevance of microautophagy in higher eukaryotes is not clear.

In macroautophagy, the cargo is sequestered within a unique double-membrane cytosolic vesicle called the autophagosome. Engulfment of the cargo can be either non-specific (bulk cytoplasm), or selective, targeting specific cargoes like organelles (ribophagy, mitophagy, etc.) (6). The autophagosome is a double-membrane vesicle, which captures cytosolic proteins and organelles during its transformation from a planar membrane disk into a sphere. The signals that trigger the formation of the autophagosome and the origin of the membrane are still under debate (8, 34), with evidence suggesting the ER, golgi and mitchondria can be providers of membrane for the autophagosome (10, 22). The autophagosome fuses with an endosome or a lysosome, where it acquires hydrolases. Lysis of the autophagosome inner membrane and breakdown of the contents occurs in the lysosome. The resulting breakdown products are released back into the cytosol, through amino acid transporters, to generate new cellular components and energy (6, 9, 27).

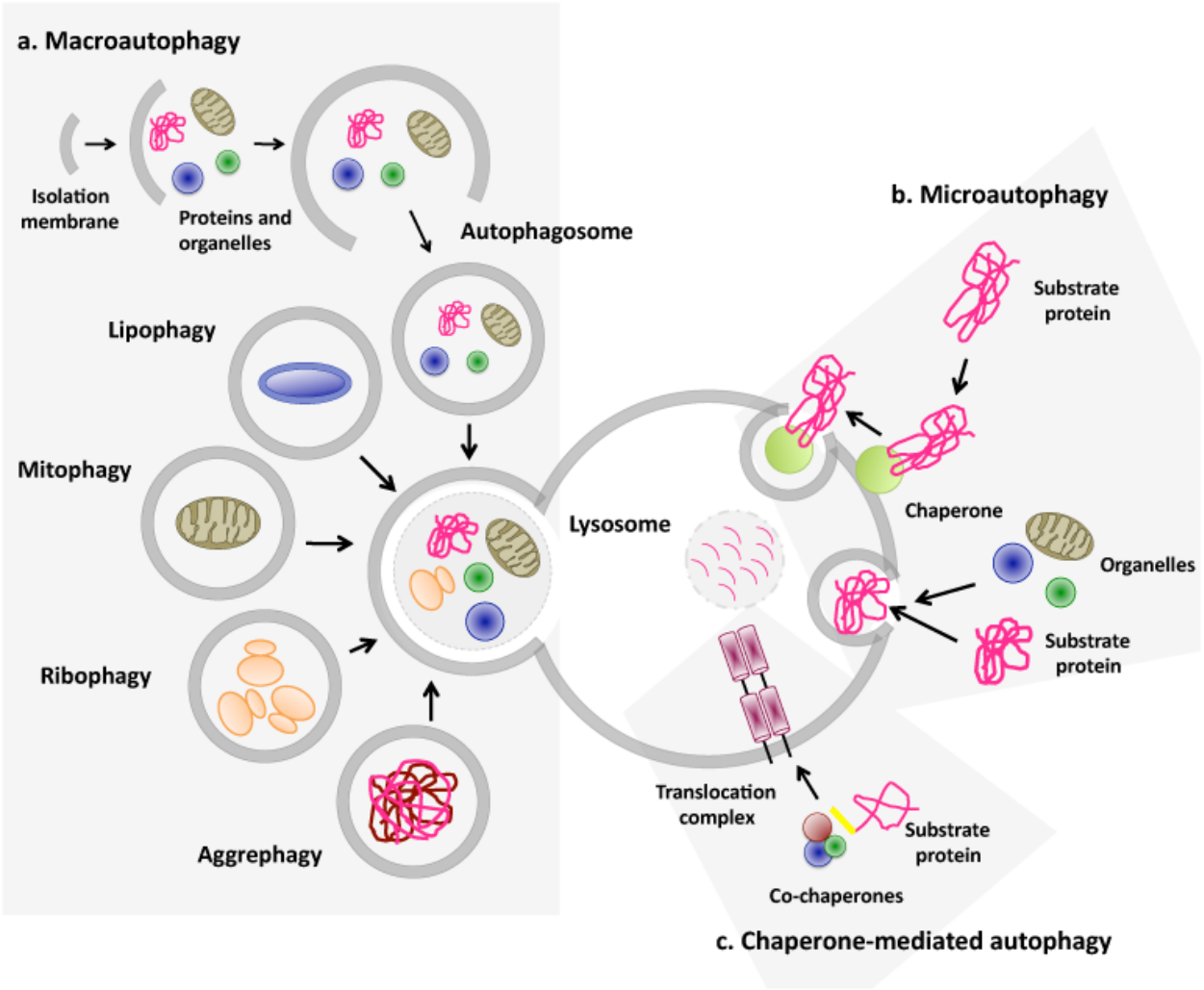

Figure 1.3 The different types of autophagy.

a. *Macroautophagy, proteins are sequestered along with other cytosolic components and organeles by a de novo-formed isolation membrane that expands and seals to form a double-membane vesicle, the autophagosome. Degradation occurs when autophagosomes fuse with the lyosome. Selective variations of this process, in which distinct substrates (aggregate protein or organelles) are targeted for degradation, and their names, are also depicted.* ***b.*** *Micoautophagy, invaginations at the surface of the lysosome or late endosomes trap cytosolic material, including proteins, and are then internalized after membrane scission and degraded in the lumen of the organelle. Cytosolic material can be sequestered 'in bulk' or selectively with the help of a cytosolic chaperone that recognizes the substrates.* ***c.*** *Chaperone-mediated autophagy, soluble cytosolic proteins containing a targeting motif are recognized by the cytosolic heat shock cognate 70 (HSC70) chaperone and its co-chaperones, which deliver the substrate to the membrane of the lysosome. After docking onto the cytosolic tail of the lysosomal receptor, the substrate protein unfolds and crosses the lysosomal membrane through a multimeric complex.*

Substrate translocation requires a lumenal HSC70 chaperone and is followed by rapid degradation in the lysosomal lumen (Adapted from (6)).

Finally, the third type of autophagy is chaperone-mediated autophagy (CMA). It involves the direct translocation of unfolded substrate proteins across the lysosome membrane through the action of a cytosolic form of the chaperone Hsc70, which recognizes a KFERQ-like peptide sequence in the substrate protein, where it binds. The chaperone-substrate complex then binds to the cytosolic tail of the membrane receptor LAMP-2A (lysosome-associated membrane protein type 2A), this binding induces the organization of the receptor into a multimeric complex. The substrate protein unfolds, and crosses the membrane through the translocation complex. A luminal form of the chaperone Hsc70 assists in the translocation of the substrate (6, 23).

The Ubiquitin-proteasome system

The ubiquiquitin-proteasome system degrades proteins in a two-step process. During the first step, proteins are marked for degradation by covalent attachment of multiple ubiquitin molecules. The resulting polyubiquitin chain serves as a marker for recognition by the 26S proteasome. In the second step, the 26S complex recognizes the ubiquitinated-protein and degrades it.

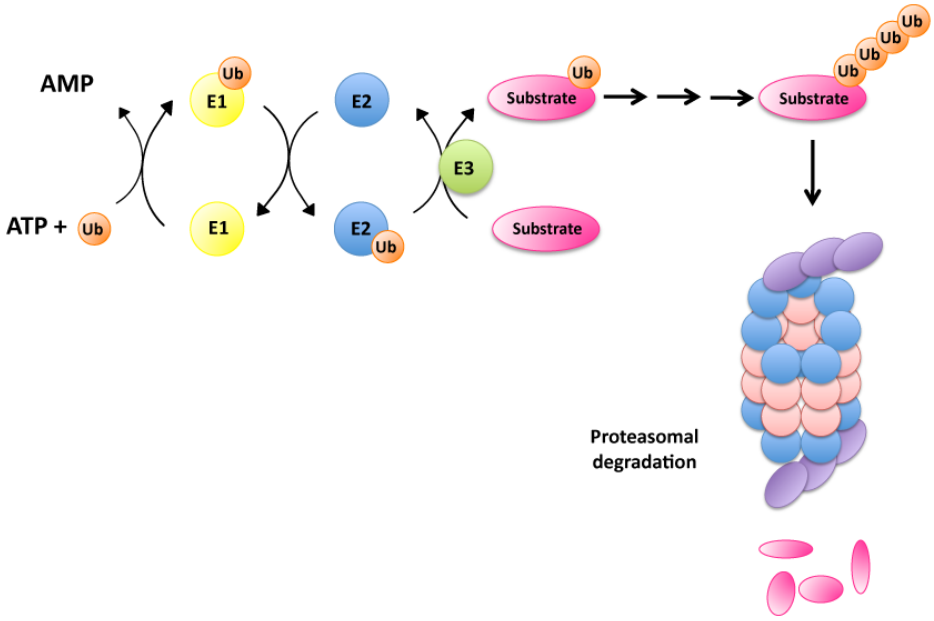

Figure 1.4 The ubiquitin-proteasome system.

During the ubiquitination process E1 binds to ubiquitin by consumption of one ATP to AMP in order to activate it. The ubiquitin-carrier enzyme E2 takes over the ubiquitin from E1. E2 transfers the ubiquitin to a protein substrate bound to the ubiquitin ligase, E3. The ubiquitin chain is extended. The ubiquitinated binds to the 26 S proteasome in order to be degraded.

Ubiquitin is a small protein composed of 76 amino acids. It is only found in eukaryotes, and is highly conserved from yeast to humans. It is a heat-stable protein that folds up into a compact globular structure. It is found throughout the cell (ubiquitous) and can exist either in free form or as part of a complex with other proteins. In the latter case, ubiquitin is conjugated to proteins through a covalent bond between the glycine at the C-terminal end of the ubiquitin molecule, and a lysine on the target protein. Conjugation of ubiquitin requires ATP hydrolysis,

and it can be attached as a single molecule (mono-ubiquitin) or as a chain of ubiquitin molecules (the more common form). To form chains, the ubiquitin molecules can attach to one another through seven lysine residues in positions 6, 11, 27, 29, 33, 48, and 63. The different forms of chains are named by which of the seven lysine amino acids in the ubiquitin molecule are used to link the chain together (17). Lysine 48-linked chains, linked by the 48th amino acid (a lysine) are the most common. They are the forms of chains that target proteins to the proteasome to be degraded (16). Lysine 63-linked chains, linked by the 63rd amino acid of ubiquitin (a lysine), regulate processes such as endocytic trafficking, inflammation, translation and DNA repair (30).

The conjugation of ubiquitin happens via a three-step cascade of reactions (Fig 1.4). First, the ubiquitin-activating enzyme (E1), activates ubiquitin in a reaction that requires ATP. Then one of several ubiquitin-conjugating enzyme (E2), transfer the activated ubiquitin to the substrate, which is bound to a member of the ubiquitin-protein ligase family (E3). The E3s catalyze the last step in the conjugation process, the covalent attachment of ubiquitin to the substrate.

Ubiquitin can be removed from substrate proteins by the action of deubiquitinating enzymes (DUBs). These are cysteine-proteases that cleave the amide bond between the two proteins. DUBs are highly specific, with only a few substrates per enzyme. DUBs have additional roles within the cell besides removing ubiquitin from substrate proteins. Ubiquitin is either expressed as one polypeptide with multiple copies in a row or a polypeptide with one ubiquitin fused to specific ribosomal subunits. Certain DUBs cleave these proteins to produce active monoubiquitin. Additionally, monoubiquitin is formed by DUBs that cleave ubiquitin from free polyubiquitin chains that have been previously removed from proteins (25, 26).

The Proteasome

The proteasome is a 66-polypeptide protease, which is structurally subdivided into the core particle (CP) and the regulatory particle (RP) (Fig 1.5). The proteolytically active sites reside within the 20S CP, a cylindrically shaped structure formed by four stacked rings, ordered α1-7, β1-7, β1-7, α1-7. Subunits β2, β5, and β1 have proteolytic activity, displaying trypsin-like, chymotrypsin-like, and caspase-like peptidase activity respectively. The proteolytic active sites are sequestered within the CP chamber, which is important to protect the cell from nonspecific

degradation. The N-termini of the α-subunits close the ends of the cylinder, often referred to as the gate. The CP can degrade some proteins, however, most proteasomal protein degradation depends on ATP (2). The only ATP hydrolyzing proteins in the proteasome are six AAA-ATPases located in the RP. These proteins form a ring that converts the chemical energy from ATP hydrolysis into a mechanical force. This force is used to unfold substrates, thereby allowing a polypeptide end or interior loop to be translocated into the central chamber of the CP (33). The 19 subunits of the RP are divided between two sub-structures, the base and lid complexes. The lid contains the Rpn11 subunit that has deubiquitinating activity. The base contains the afore mentioned AAA-ATPases. The C-termini of these ATPases dock into pockets present between the α-subunits of the CP (29). This results in a translocation of the α tails and an opening of the gate. The CP can associate with one or two RPs, but there are other activators that could also bind to the 20S CP particle. These are Blm10/PA200 protein, a large HEAT-repeat containing protein, and the 11S/PA28 complex, a heteroheptamer. Both activators can dock directly into the CP at the exclusion of the RP.

Assembly of the proteasome

Assembly of the 26S proteasome is not a simple process, there are at least 66 proteins that need to come together, each occupying a single, defined site within the final structure. There are at least nine dedicated chaperones that assist in assembly of the proteasome (Table 1.1). As expected from a chaperone, these molecules do not form part of the final biological functional complex. Five of these chaperones assist in assembly of the CP, and four are dedicated to RP assembly.

Four CP-chaperones play a role in assembly of the α-ring; yeast Pba (proteasome biogenesis associated protein) 1–4 or their probable orthologs in human PAC (proteasome assembly chaperone) 1–4. The assembly process seems largely conserved between yeast and humans. The proteins function as heterodimers: PAC1-PAC2 and PAC3-PAC4. The PAC3-PAC4 heterodimer is probably important early in assembly, when it attaches to α5 and assists in the recruitment and ordering of additional α-subunits. Once α-ring assembly is completed, the β-subunits are incorporated. Incorporation of the β-subunits requires dissociation of the PAC3-PAC4 heterodimer. The PAC1-PAC2 heterodimer also assists in the formation of the α-ring, but

unlike PAC3-PAC4 it remains associated with the complex upon incorporation of the β-subunits (2).

The fifth CP-chaperone Ump1, which has no role in α-ring formation, seems to function as a quality control agent. The Ump1 protein prevents stable dimerization of two half CPs until all seven β-subunits are assembled on the α-ring (creating the half CP). The formation of CP by two half CPs is accompanied by the maturation of the β-subunits and the degradation of Ump1 and PAC 1-PAC2 (24).

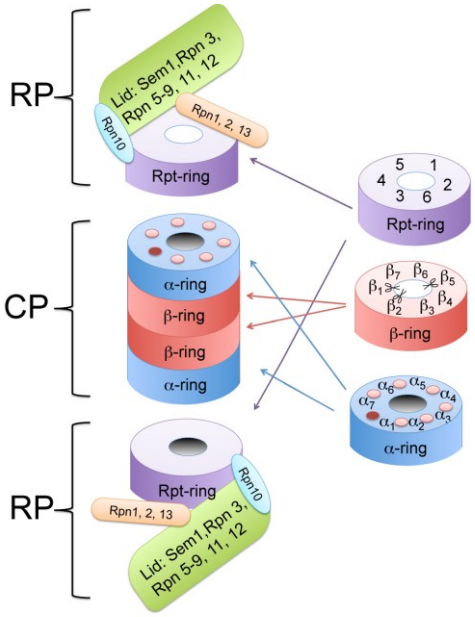

Figure 1.5 Proteasome structure

The proteasome is formed by two RPs abutting a cylindrically shaped CP. The CP is formed by two α-rings and two β-rings. The RP consists of a base complex and a lid complex. Rpn10 is at the interface between these complexes (shown in light blue). The lid (green) contains indicated subunits and its function is not well understood, with the exception of rpn11, which functions as a deubiquitinating enzyme. The base contains a ring formed by six AAA-ATPases, Rpt1–6 (purple ring), and the subunits Rpn1, Rpn2 and Rpn13 (shown as an orange box; see text for more details). The proteasome contains three heteromeric ring structures, each present twice. The α- and β-ring are formed by seven subunits; scissors indicate the active sites and the dots in the α ring show the binding pockets for the Rpt tails (see text). The pocket between α7 and α1 lacks a Lys typically found in the pocket and might not harbour an Rpt C-terminus. The Rpt-ring is formed by six AAA-ATPases (2) (Adapted from (2)).

The RP (19S) can be divided into two subcomplexes, the base and lid. In yeast, these subcomplexes assemble independent of each other. There are four RP dedicated chaperones that assist in assembly of the base (33). The base is composed of six related AAA + ATPase, Rpt1–Rpt6, and three non-ATPase subunits, Rpn1, Rpn2, and Rpn13 (Fig. 5). The six ATPase subunits are thought to form a ring structure that binds on the α-rings of the CP (Fig. 5). The chaperones involvd in RP assembly are Nas2/p27, Nas6/ gankyrin/p28, Rpn14/PAAF1, and Hsm3/S5b. Similarly to the CP chaperones they are not present in the mature 26S proteasome, and are evolutionarily conserved form yeast to humans (2, 24).

Table 1.1 Proteasome assembly chaperones

	Saccharomyces cerevisiae	***Homo sapiens***
Core Particle chaperones	Pba1 Pba2 Pba3 Pba4 Ump1	PAC1 PAC2 PAC3 PAC4 UMP1
Regulatory Particle chaperones	Hsm3 Nas2 Nas6 Rpn14	S5b P27 Gankyrin PAAF1

The four RP chaperones are structurally distinct but contain domains involved in protein–protein interactions: Nas2 has a PDZ domain, Nas6 has ankyrin repeats, Rpn14 has WD40 repeats, and Hsm3 is composed of HEAT repeats (fig 6). Interestingly, they all interact with the C-terminal tail of a specific Rpt subunit; Nas2 binds the C-terminal tail of Rpt5, Nas6 binds that of Rpt3, Rpn14 binds that of Rpt6, and Hsm3 binds that of Rpt1. Since the C-termini of Rpt subunits are necessary for docking onto the CP, it is probable that the base chaperones function to prevent premature binding of the Rpt subunits to the CP (2).

The RP lid consists of nine subunits, Rpn3, 5, 6, 7, 8 9, 11,12, and 15 (Sem1). Recent studies into the mechanisms of assembly of the lid have revealed that lid assembly does not require chaperones *in vitro,* and is likely to be independent of chaperones *in vivo* as well (32).

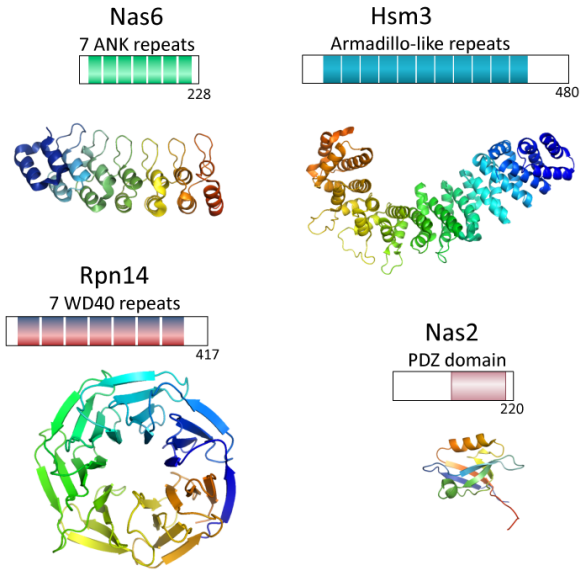

Figure 1.6 Domain topology of RP chaperones.

The RP chaperones bind to the C-terminal of their respective RP subunit. However, they are very different structurally (2).

In addition to the chaperones that assist in assembly, there are multiple proteins that associate with the proteasome. Table 2 provides an example of some of these proteins and their proposed function. Some of these proteins affect the substrate to be degraded, like Hul5 (ubiquitin ligase) and Ubp6 (DUB). Others have a broader range of functions, e.g. Blm10, which has been proposed to be involved in proteasome maturation, as well as to function as an activator of the proteasome (31). Another protasome-associated protein with a wide range of proposed functions is Ecm29. This 210 kD protein has been proposed to stabilize the proteasome, to remodel the proteasomes upon stress, and to work as a quality control factor of proteasome assembly. Together with the chaperones these proteasome-associated proteins provide additional control elements to proteasome assembly and function.

Table 1.2 Examples of proteasome-associated proteins and their functions

Protein	Proposed Function
Blm10	Proteasome maturation and DNA repair
Ecm29	RP-CP stabilization, quality control of proteasome assembly
Hul5	Ubiquitin-protein ligase
Ubp6	Deubiquiinating enzyme, proteasome inhibitor
Rad23	Delivers conjugates to proteasome

The existence of nine chaperones and a proposed quality control factor, suggests that the assembly of the proteasome is an error prone process. Therefore, understanding how the cell achieves efficient assembly of the proteasome requires a detailed understanding of the function of the individual chaperones that guide this process. While the interaction of three RP chaperones (Nas6, Hsm3, and Rpn14) with their respective RP subunits was previously elucidated, our understanding of Nas2 has been more limited. In vitro studies showed that the chaperones bind to a specific Rpt protein through their C-terminal domains. However, this interaction did not involve the residues at the C-terminal tail. These tail residues are known to directly interact with the CP. We hypothesized that Nas2 does require these tail residues to interact with Rpt5 and the work described in the second chapter of this thesis, shows that the interaction between Nas2 and Rpt5 happens through the C-terminal tail of Rpt5. The interaction requires the last three amino acids of the tail, suggesting that the binding of Nas2 prevents the docking of Rpt5 into the core particle. This not withstanding, our work indicates that Nas2 has cellular functions beyond this ability to block Rpt5 from docking onto CP. Furthermore, we observed an accumulation of Ecm29 on proteasome mutants in these studies, and this forms the focus of chapter 3.

The third chapter asks how is Ecm29 enriched in these mutants, and what it's doing to the proteasome. We found that Ecm29 preferentially binds to mutant or ATP-depleted proteasomes, and when it binds it inhibits proteasome function. Ecm29 binds to Rpt5

inhibiting ATPase activity, which in part contributes to the defect in degradation exhibited by these proteasomes. These suggest the existence of an additional quality control layer in proteasome assembly and function. Overall, our studies provide further understanding of the mechanisms of assembly and quality control of the proteasome.

References

1. Balch, W.E., Morimoto, R.I., Dillin, A., and Kelly, J.W. (2008) Adapting proteostasis for disease intervention. Science. 319, 916-919
2. Bedford, L., Paine, S., Sheppard, P.W., Mayer, R.J., and Roelofs, J. (2010) Assembly, structure, and function of the 26S proteasome. Trends Cell Biol. 20, 391-401
3. Boya, P., Reggiori, F., and Codogno, P. (2013) Emerging regulation and functions of autophagy. Nat.Cell Biol. 15, 713-720
4. Ciechanover, A. (2005) Proteolysis: from the lysosome to ubiquitin and the proteasome. Nat.Rev.Mol.Cell Biol. 6, 79-87
5. Clague, M.J., and Urbe, S. (2010) Ubiquitin: same molecule, different degradation pathways. Cell. 143, 682-685
6. Cuervo, A.M. (2011) Chaperone-mediated autophagy: Dice's 'wild' idea about lysosomal selectivity. Nat.Rev.Mol.Cell Biol. 12, 535-541
7. Ding, W.X., and Yin, X.M. (2008) Sorting, recognition and activation of the misfolded protein degradation pathways through macroautophagy and the proteasome. Autophagy. 4, 141-150
8. Ge, L., Baskaran, S., Schekman, R., and Hurley, J.H. (2014) The protein-vesicle network of autophagy. Curr.Opin.Cell Biol. 29C, 18-24
9. Goberdhan, D.C. (2010) Intracellular amino acid sensing and mTORC1-regulated growth: new ways to block an old target?. Curr.Opin.Investig Drugs. 11, 1360-1367
10. Hailey, D.W., Rambold, A.S., Satpute-Krishnan, P., Mitra, K., Sougrat, R., Kim, P.K., and Lippincott-Schwartz, J. (2010) Mitochondria supply membranes for autophagosome biogenesis during starvation. Cell. 141, 656-667
11. Hershko, A., and Ciechanover, A. (1998) The ubiquitin system. Annu.Rev.Biochem. 67, 425-479
12. Hoseki, J., Ushioda, R., and Nagata, K. (2010) Mechanism and components of endoplasmic reticulum-associated degradation. J.Biochem. 147, 19-25
13. Jung, T., and Grune, T. (2013) The proteasome and the degradation of oxidized proteins: Part I-structure of proteasomes. Redox Biol. 1, 178-182
14. Kamada, Y., Sekito, T., and Ohsumi, Y. (2004) Autophagy in yeast: a TOR-mediated response to nutrient starvation. Curr.Top.Microbiol.Immunol. 279, 73-84
15. Koga, H., Kaushik, S., and Cuervo, A.M. (2011) Protein homeostasis and aging: The importance of exquisite quality control. Ageing Res.Rev. 10, 205-215
16. Komander, D., and Rape, M. (2012) The ubiquitin code. Annu.Rev.Biochem. 81, 203-229
17. Kravtsova-Ivantsiv, Y., Sommer, T., and Ciechanover, A. (2013) The lysine48-based polyubiquitin chain proteasomal signal: not a single child anymore. Angew.Chem.Int.Ed Engl. 52, 192-198

18. Kristensen, A.R., Schandorff, S., Hoyer-Hansen, M., Nielsen, M.O., Jaattela, M., Dengjel, J., and Andersen, J.S. (2008) Ordered organelle degradation during starvation-induced autophagy. Mol.Cell.Proteomics. 7, 2419-2428

19. Kroemer, G., Marino, G., and Levine, B. (2010) Autophagy and the integrated stress response. Mol.Cell. 40, 280-293

20. Li, W.W., Li, J., and Bao, J.K. (2012) Microautophagy: lesser-known self-eating. Cell Mol.Life Sci. 69, 1125-1136

21. Liberek, K., Lewandowska, A., and Zietkiewicz, S. (2008) Chaperones in control of protein disaggregation. EMBO J. 27, 328-335

22. McEwan, D.G., and Dikic, I. (2010) Not all autophagy membranes are created equal. Cell. 141, 564-566

23. Mizushima, N., Levine, B., Cuervo, A.M., and Klionsky, D.J. (2008) Autophagy fights disease through cellular self-digestion. Nature. 451, 1069-1075

24. Murata, S., Yashiroda, H., and Tanaka, K. (2009) Molecular mechanisms of proteasome assembly. Nat.Rev.Mol.Cell Biol. 10, 104-115

25. Nijman, S.M., Luna-Vargas, M.P., Velds, A., Brummelkamp, T.R., Dirac, A.M., Sixma, T.K., and Bernards, R. (2005) A genomic and functional inventory of deubiquitinating enzymes. Cell. 123, 773-786

26. Reyes-Turcu, F.E., Ventii, K.H., and Wilkinson, K.D. (2009) Regulation and cellular roles of ubiquitin-specific deubiquitinating enzymes. Annu.Rev.Biochem. 78, 363-397

27. Russnak, R., Konczal, D., and McIntire, S.L. (2001) A family of yeast proteins mediating bidirectional vacuolar amino acid transport. J.Biol.Chem. 276, 23849-23857

28. Settembre, C., Fraldi, A., Medina, D.L., and Ballabio, A. (2013) Signals from the lysosome: a control centre for cellular clearance and energy metabolism. Nat.Rev.Mol.Cell Biol. 14, 283-296

29. Smith, D.M., Chang, S.C., Park, S., Finley, D., Cheng, Y., and Goldberg, A.L. (2007) Docking of the proteasomal ATPases' carboxyl termini in the 20S proteasome's alpha ring opens the gate for substrate entry. Mol.Cell. 27, 731-744

30. Sorkin, A. (2007) Ubiquitination without E3. Mol.Cell. 26, 771-773

31. Stadtmueller, B.M., and Hill, C.P. (2011) Proteasome activators. Mol.Cell. 41, 8-19

32. Tomko, R.J.,Jr, and Hochstrasser, M. (2014) The intrinsically disordered Sem1 protein functions as a molecular tether during proteasome lid biogenesis. Mol.Cell. 53, 433-443

33. Tomko, R.J.,Jr, and Hochstrasser, M. (2013) Molecular architecture and assembly of the eukaryotic proteasome. Annu.Rev.Biochem. 82, 415-445

34. Walker, S., Chandra, P., Manifava, M., Axe, E., and Ktistakis, N.T. (2008) Making autophagosomes: localized synthesis of phosphatidylinositol 3-phosphate holds the clue. Autophagy. 4, 1093-1096

35. Wiseman, R.L., Powers, E.T., Buxbaum, J.N., Kelly, J.W., and Balch, W.E. (2007) An adaptable standard for protein export from the endoplasmic reticulum. Cell. 131, 809-821

36. Wong, E., and Cuervo, A.M. (2010) Integration of clearance mechanisms: the proteasome and autophagy. Cold Spring Harb Perspect.Biol. 2, a006734

Chapter 2 - Loss of Rpt5 interactions with the core particle and Nas2 causes the formation of faulty proteasomes that are inhibited by Ecm29

Stella Yu-Chien Lee , Alina De La Mota-Peynado, and Jeroen Roelofs

Division of Biology, Kansas State University, Manhattan, Kansas, United States of America

*Published in the Journal of Biological Chemistry, Volume 286, Issue 42, 21 October 2011, Pages 36641-36651.

Republished with permission.

Abstract

The proteasome is a large and complex protease formed by 66 polypeptides. The assembly of the proteasome is assisted by at least nine chaperones. One of these chaperones, Nas2/p27, binds to the C-terminal region of the AAA-ATPase Rpt5. We report here that the tail of Rpt5 provides two functions. First, it facilitates the previously reported interaction with the proteasome core particle (CP). Second, it is essential for the interaction with Nas2. Deletion of the C-terminal amino acid of Rpt5 disrupts the CP interaction, but not the binding to Nas2. The later is surprising considering Nas2 contains a PDZ domain, which is often involved in binding to C-termini. Interestingly, deletion of the last three amino acids interferes with both functions. The disruption of the Rpt5-CP interactions gave distinct phenotypes different from disruption of the Nas2-Rpt5 interaction. Additinally, proteasomes purified from a *Saccharomyces Cerevisiae rpt5*-Δ3 strain show a strong enrichment of Ecm29. The function of Ecm29, a proteasome associated protein, is not well understood. Our data show that Ecm29 can inhibit proteasomes, as our Ecm29 containing proteasomes have reduced suc-LLVY-AMC hydrolytic activity. Consistent with this apparent role as negative regulator, the deletion of *ECM29* rescues the phenotypes of *rpt5*-Δ3 and *nas2*Δ in an *hsm3*Δ background. In sum, the interactions facilitated by the tail of Rpt5 act synergistically to minimize the formation of faulty proteasomes, thereby preventing recognition and inhibition by Ecm29.

Introduction

The proteasome is a large and complex molecular machine. It is responsible for the ATP dependent degradation of the majority of soluble cellular proteins destined for degradation in eukaryotic cells. It can biochemically be divided in two major subcomplexes, the core particle (CP) and the regulatory particle (RP). The CP is formed by four stacked rings, each consisting of seven subunits. The middle rings are formed by beta subunits and the outer rings by alpha subunits, creating an α_{1-7}-β_{1-7}-β_{1-7}-α_{1-7} structure. The proteolytic active sites are located on the inner surface of this hollow cylinder (1). The degradation of substrates requires the opening of a gate located at either end of the CP. This gate can be opened by activators such as the RP (1,2). The degradation of folded proteins generally requires the presence of the RP. RP is a 19 subunit complex that contains six AAA-ATPases. These ATPases form a ring where each subunit occupies a specific position (3,4). They are important for unfolding substrates, opening the gate of the CP, and substrate entry into the CP. At the outer surface of the CP surrounding the gate are seven pockets, each located at the interface between the α subunits. A number of these pockets can receive the C-terminal amino acids ("tails") of presumably specific AAA-ATPases (5-7). However, the positioning of the ATPase ring in respect to the CP α-ring is still unclear (3,5,7,8). Docking of the tail of two different AAA-ATPases, namely Rpt2 and Rpt5, can result in opening of the gate (5,6). The tails of Rpt4 and Rpt6 play an important role in the assembly of the proteasome in yeast (9), while in human the tails of Rpt5 and Rpt3 seem to be important for assembly (10).

The efficient assembly of the proteasome requires a number of chaperones. At least five chaperones assist in the assembly of the core particle (1,11). In addition to these, four chaperones have been identified that are important for the formation of the AAA-ATPase ring, known by their yeast/human names Hsm3/PSMD5 (a.k.a. S5B), Rpn14/PAAF1, Nas2/PSMD9 (a.k.a. p27), and Nas6/PSMD10 (a.k.a. gankyrin) (12-16). Each of these chaperones has been shown to bind to a specific AAA-ATPase present in the RP; Hsm3 binds to Rpt1, Nas2 to Rpt5, Rpn14 to Rpt6, and Nas6 to Rpt3. Although the chaperones lack sequence as well as structural homology amongst one another, they all bind to the same C-terminal region of their specific partner Rpt-protein (14,16-18). Our understanding of how these chaperones assist in assembly at the molecular level is limited. As is typical for chaperones, these proteins are not present on the final

functional complex, assembled proteasomes. The chaperones have been suggested to directly facilitate assembly of neighboring ATPases, provide stability or bring sub-assemblies together (4,19). For Nas6, structural data and molecular modeling in combination with experimental data suggest that there is a steric hindrance preventing simultaneous binding of Nas6 and CP to Rpt3 (9,14). Biochemical experiments suggest a similar property for Hsm3 and Rpn14 exists (9,14). Thus, one function of these chaperones might be to regulate the interactions of the Rpt proteins with the CP (20). For Nas2 this has not been studied in detail. Interestingly, Nas2 has a PDZ domain (15). Because PDZ domains often bind to the Cterminus of proteins, binding of Nas2 might directly prevent docking of Rpt5 to the CP (15).

Three other important regulators of proteasome in yeast that have been implicated in proteasome assembly are Ubp6, Ecm29 and Blm10. Each protein has a human orthologue; USP14, KIAA0368, and PSME4 (a.k.a.PA200) respectively. Ubp6 is a deubiquitinating enzyme that binds to the proteasome and regulates the degradation of ubiquitinated proteins (21). Interestingly it has been identified in an RP assembly subcomplex (9,16,22) and recent data suggest that it plays an active role in proteasome assembly (22). Blm10, like RP, binds to either end of the CP and has been found associated with CP or in a hybrid proteasome with CP and RP (23-25). Association of Blm10 with CP has been shown to increase suc-LLVY-AMC proteolytic activity and is required for the degradation of specific substrates (24,26,27). On the other hand it also has a function in assembly of the proteasome and has been observed in association with immature CP (28-30). Ecm29 is mainly found associated with RP-CP or RP_2-CP complexes. It has been shown to stabilize proteasomes in the absence of ATP presumably by binding to the CP as well as the RP (31,32), suggesting it might have a positive role in proteasome function. However, recent publications describe Ecm29 as a chaperone or protein that monitors the quality of assembled proteasomes (33-35). One of these studies found Ecm29 associated with proteasomes that lack the β3 subunit and have stalled CP maturation (33). How Ecm29 recognizes these proteasomes and how it regulates proteasomes remains unclear.

In this study we show that Nas2 binds to the C-terminal tail of Rpt5, but does not require the last amino acid of Rpt5 that is essential for functional Rpt5-CP interaction. While binding of Nas2 to Rpt5 is likely to cause steric hindrance for the Rpt5-CP interactions, our phenotypic

analyses suggest that Nas2 functions beyond regulating this interaction. In *rpt5*-Δ3 cells, which are disrupted for the interaction between Rpt5 and CP as well as Rpt5 and Nas2, we see a strong increase in Ecm29-associated assembled proteasomes. These proteasomes seem to be compromised in their functionality as they have reduced suc-LLVYAMC hydrolytic activity. Consistent with a role for Ecm29 as a negative regulator, deletion of *ECM29* rescues the phenotypes observed in *nas2*Δ or *rpt5*-Δ3 backgrounds.

Experimental Procedures

Yeast strains

See Supplementary Table 1 for genotypes of strains used. Standard methods for strain construction and cell culture were used. Plating assays were done as described before, using four-fold dilutions (14).

Plasmids and antibodies

For the expression of GST-Nas2 in *E.coli* we cloned the open reading frame of Nas2 into a pGEX-6P1 derived plasmid, creating plasmid pJR500. His-tagged full length Rpt5 or His-tagged Rpt5 C-domain (coding for amino acids 350 till 434) were cloned into the pRSFDuet-1 plasmid (Novagen) for expression in *E.coli*, creating plasmids pJR506 and pJR168 respectively. To express the truncations of Rpt5 in *E.coli* plasmid pJR506 was mutated such that the last (pJR507) or last three codons (pJR508) before the stop codon were deleted. Similarly, plasmid pJR168 was used to construct deletions of the last (pJR509) or last three codons (pJR510) of the C-domain. For the detection of His tagged proteins we used THE® His tag monoclonal antibody (Genscript). Ecm29 was detected using an Ecm29 polyclonal antibody, kindly provided by Dr. Dan Finley (Harvard Medical School, Boston MA).

Table 2.1 Yeast Strains

Strain	Genotype[a] (*lys2-801 leu2-3, 2-112 ura3-52 his3-Δ200 trp1-1)*	Figure	Source
SUB61	MATα	2.2,2.3,2.4a,2.6	(1)
sDL133	MAT*a rpn11::RPN11-TEVProA (HIS3)*	2.4b,c,2.5	(2)
sMK60	*MATα ecm29::TRP rpn11::RPN11-TEVProA (HIS3)*	2.5	(3)
sJR233	MATα *hsm3::KAN nas6::TRP*	2.6	(4)
sJR236	MATα *hsm3::KAN rpn14::HYG*	2.6	(4)
sJR239	*nas6::TRP rpn14::HYG*	2.6	(4)
sJR245	*hsm3::KAN*	2.6	(4)
sJR299	*hsm3::KAN nas6::TRP ecm29::TRP*	2.6	(5)
sJR301	*nas6::TRP rpn14::HYG ecm29::TRP*	2.6	(5)
sJR303	*hsm3::KAN rpn14::HYGRO ecm29::TRP*	2.6	(5)
sJR515	MAT*A hsm3::KAN*	2.3	(5)
sJR518	MATα *nas2::NAT, hsm3::KAN rpt5::rpt5Δ1-HYG*	2.3	(5)
sJR519	MAT*A nas2::NAT, hsm3::KAN rpt5::rpt5Δ3-HYG*	2.3	(5)
sJR528	MAT*A hsm3::KAN rpt5::rpt5Δ1-HYG*	2.3	(5)
sJR530	MAT*A hsm3::KAN rpt5::rpt5Δ3-HYG*	2.3	(5)
sJR534	*nas2::NAT*	2.2,2.3,2.4a	(5)
sJR535	*rpt5:: rpt5Δ1-HYG*	2.2,2.3,2.4a	(5)
sJR536	*rpt5:: rpt5Δ3-HYG*	2.2,2.3,2.4a	(5)
sJR539	*nas2::NAT, rpt5::rpt5Δ1-HYG*	2.3	(5)
sJR540	*nas2::NAT, rpt5::rpt5Δ3-HYG*	2.3	(5)
sJR544	MATα *ecm29::TRP rpt5::rpt5Δ3-HYG*	2.6	(5)
sJR545	MAT*a hsm3::KAN ecm29::TRP rpt5::rpt5Δ0-HYG*	2.6	(5)
sJR546	MAT*A hsm3::KAN ecm29::TRP rpt5::rpt5Δ3-HYG*	2.6	(5)
sJR548	*ecm29::TRP rpt5::rpt5Δ3-HYG rpn11::RPN11-TEVProA (HIS3)*	2.4b,c	(5)
sJR550	MAT*a hsm3::KAN ecm29::TRP rpt5::rpt5Δ3-HYG rpn11::RPN11-TEVProA (HIS3)*	2.4b,c	(5)
sJR552	*rpt5::rpt5Δ3-HYG rpn11::RPN11-TEVProA (HIS3)*	2.4b,c	(5)
sJR554	*hsm3::KAN rpt5::rpt5Δ3-HYG rpn11::RPN11-TEVProA (HIS3)*	2.4b,c	(5)
sJR555	*rpt5::rpt5Δ0-HYG*	2.6	(5)
sJR556	*rpt5::rpt5Δ3-HYG*	2.6	(5)
sJR557	*hsm3::KAN rpt5::rpt5Δ0-HYG*	2.6	(5)
sJR558	*hsm3::KAN rpt5::rpt5Δ3-HYG*	2.6	(5)
sJR559	MATα *ecm29::TRP*	2.6	(5)
sJR578	*nas2::NAT hsm3::KAN ecm29::TRP*	2.6	(5)
sJR579	*nas2::NAT hsm3::KAN*	2.6	(5)

a. All strains, except sJR387 and 388, have the DF5 background genotype[6] (*lys2-801 leu2-3, 2-112 ura3-52 his3-Δ200 trp1-1*

1. Finley, D., Ozkaynak, E., and Varshavsky, A. (1987) Cell 48, 1035-1046
2. Leggett, D. S., Hanna, J., Borodovsky, A., Crosas, B., Schmidt, M., Baker, R. T., Walz, T., Ploegh, H., and Finley, D. (2002) Mol Cell 10, 495-507
3. Kleijnen, M. F., Roelofs, J., Park, S., Hathaway, N. A., Glickman, M., King, R. W., and Finley, D. (2007) Nat Struct Mol Biol 14, 1180-1188
4. Roelofs, J., Park, S., Haas, W., Tian, G., McAllister, F. E., Huo, Y., Lee, B. H., Zhang, F., Shi, Y., Gygi, S. P., and Finley, D. (2009) Nature 459, 861-865
5. This study

Proteasome purifications and native gels

The affinity-purification of Rpn11-TeV-Protein A tagged proteasomes was performed as described before with minor modifications (36). Briefly, between 1 and 6 liter of overnight cultures (OD600 ~ 10) were spun down, washed in H2O, and a two-fold pellet volume of lysis buffer (50 mM Tris-HCl [pH 8], 1 mM EDTA, 5 mM MgCl2, 1 mM ATP) was added. Cells were lysed by French Press, and lysates were centrifuged at 12,000 rpm (SS34, Sorvall) at 4°C for 25 min. The supernatant was filtered through a cheesecloth, IgG beads (MP Biomedicals) were added (~0.5 ml / l culture), and the lysate was rotated at 4°C for one hour. The IgG beads were collected in an Econo Column (Biorad), and washed with ice-cold wash buffer (50 column volumes; 50 mM Tris- HCl [pH 7.5], 1 mM EDTA, 100 mM NaCl, 5 mM MgCl2, 1 mM ATP). Next, beads were washed with 15 column volumes of cleavage buffer (50 mM Tris-HCl [pH 7.5], 1 mM EDTA, 1 mM DTT, 5 mM MgCl2, 1 mM ATP). Followed by cleavage in the same buffer containing His-tagged TeV protease (Invitrogen), for 1 hour at 30°C. Talon beads were added for 20 minutes at 4°C to remove TeV protease, after which the preparation was concentrated in a 10 kDa concentrator (Millipore). Proteasome preparations were stored at –80°C. Proteasome preparations were analyzed using standard SDS-PAGE or on native gels prepared as described previously and run between 2 and 3 hours at 4ºC (37). Total lysates for analysis on native gel were prepared as described previously
(14).

Apyrase treatment

The apyrase treatment of purified proteasomes was performed as described previously with minor modifications (31). Purified proteasomes were diluted in 50mM Tris-HCl (pH 7.5), 5mM MgCl2, 1mM EDTA, and 0.25mM ATP. Samples were incubated for 45 min at 30°C with or without apyrase (20 mU µl-1 working concentration). After treatment proteasomes were analyzed using native gels.

Mass spectrometry

CBB stained gel pieces were excised from native gel and proteins were digested with trypsin, followed by a peptide extraction and Nano-HPLC and Electrospray Ionization Tandem Mass Spectrometry (ESI−MS/MS). Peptide masses were compared to Swiss Prot Database using MASCOT 2.2 (http://www.matrixscience.com). For more details see supplementary table 2.

GST pull down

GST-Nas2 and His-Rpt5, His- Rpt5-Δ1, or His-Rpt5-Δ3 were overexpressed in *E. coli* at 30°C for 3 hours. Cells were harvested and resuspended in lysis buffer (20mM Tris-HCl [pH8.0], 100mM NaCl, 1mM EDTA, 1% Triton X-100, and protease inhibitors). Lysates were prepared by French Press and cleared by centrifugation. Lysates of GST-Nas2 and his-tagged proteins were mixed and incubated at 4°C for 1.5 hours. Glutathione sepharose beads were added to the mix and incubated at 4°C for 30 minutes to bind GST-Nas2. Beads were collected by centrifugation and washed 3x with lysis buffer. Samples were separated on SDS-PAGE for analysis. For His-Rpt5 C domain series, GSTNas2 and his-tagged proteins were co-expressed in *E. coli* and purified as above.

Results

In vitro Nas2-Rpt5 binding

The proteasome contains six ATPases (the Rpt proteins) that belong to the AAA-ATPase family. AAAATPases typically have a C-domain (a.k.a. C-terminal domain) following the ATPase domain (38). Because the C-domain is in the C-terminal region of the Rpt proteins, it is generally considered to end at the C-terminus (14,16). However, crystal structure analysis of part of the archeal homolog of the proteasomal ATPases, the Proteasome-Activating Nucleotidase (PAN), show that the last twelve amino acids from the C-terminus are not structured (39). This suggests that these amino acids, referred to as the C-terminal tail or tail, are highly flexible and formally are not part of the preceding C-domain of PAN. A flexible tail is in agreement with the model that the tails of the Rpt proteins extend and partially dock into pockets located on the CP (5-7,40). The three C-terminal amino acids are tightly packed into the pockets upon docking (7,40). Thus, if binding of a chaperone requires these amino acids, it would suggest this chaperone directly interferes with docking of the Rpt tail into the CP pocket. For three of the four chaperones that bind to the C-domains of their respective Rpt protein, namely Nas6, Hsm3 and Rpn14, the last three amino acids are not required for binding to the C-domain (14). For the fourth chaperone, Nas2, two–hybrid studies have shown an interaction with the C-domain of Rpt5 (16). However it is unclear if this interaction requires any of the amino acids at the C-terminal tail (20). Interestingly, Nas2 consists largely of a PDZ domain (15,16) and a subset of PDZ domains has been shown to bind specifically to the C-terminus of their binding partners (41,42). Consistent with this, the tail of Rpt5 shows a consensus motif II sequence for PDZ binding (Fig. 2.1A and B). Moreover, docking of the C-terminus of Rpt5 into a pocket present on the CP surface results in opening of the CP gate (5,6). Therefore, mapping the precise binding of Nas2 on Rpt5 potentially provides important insights into the molecular mechanisms of assembly and proteasome function.

We set up an *in vitro* binding assay to analyze the interaction between Rpt5 and Nas2. Lysates expressing indicated proteins (Fig 2.1C, right panel) were mixed and incubated with glutathione resin. His-tagged Rpt5 specifically co-purified with GST-tagged Nas2, but not GST, (Fig. 2.1C, left panel, lane 1 and 4). To test if indeed the C-domain, including the tail, of Rpt5 binds to Nas2 we co-expressed GST-Nas2 or GST with His-tagged Rpt5 C-domain, followed by

a purification using glutathione-resin (Fig. 2.1D, left panel, lane 1 and 2). These data show that the C-domain of Rpt5, in agreement with previous 2-hybrid data (16), is sufficient for binding to Nas2. Our *in vitro* data also show that this is a direct interaction between Nas2 and Rpt5.

Next, we tested the requirement of the amino acids at the C-terminus of Rpt5 for Nas2 binding. Deleting the last amino acid (Ala, Δ1) or the last three amino acids (Phe-Tyr-Ala; Δ3) did not change the expression level or solubility of His-tagged Rpt5 or His-tagged Rpt5 C-domain in *E.coli* (Fig. 2.1 C and D, right panels). Nonetheless, hardly any Rpt5-Δ3 co-purified with GST-Nas2, while Rpt5-Δ1 and Rpt5 readily co-purified with GST-Nas2 (Fig. 2.1C and D, left panels). These results indicate that Nas2 depends on the C-terminal tail of Rpt5 for binding, but not on the C-terminal amino acid.

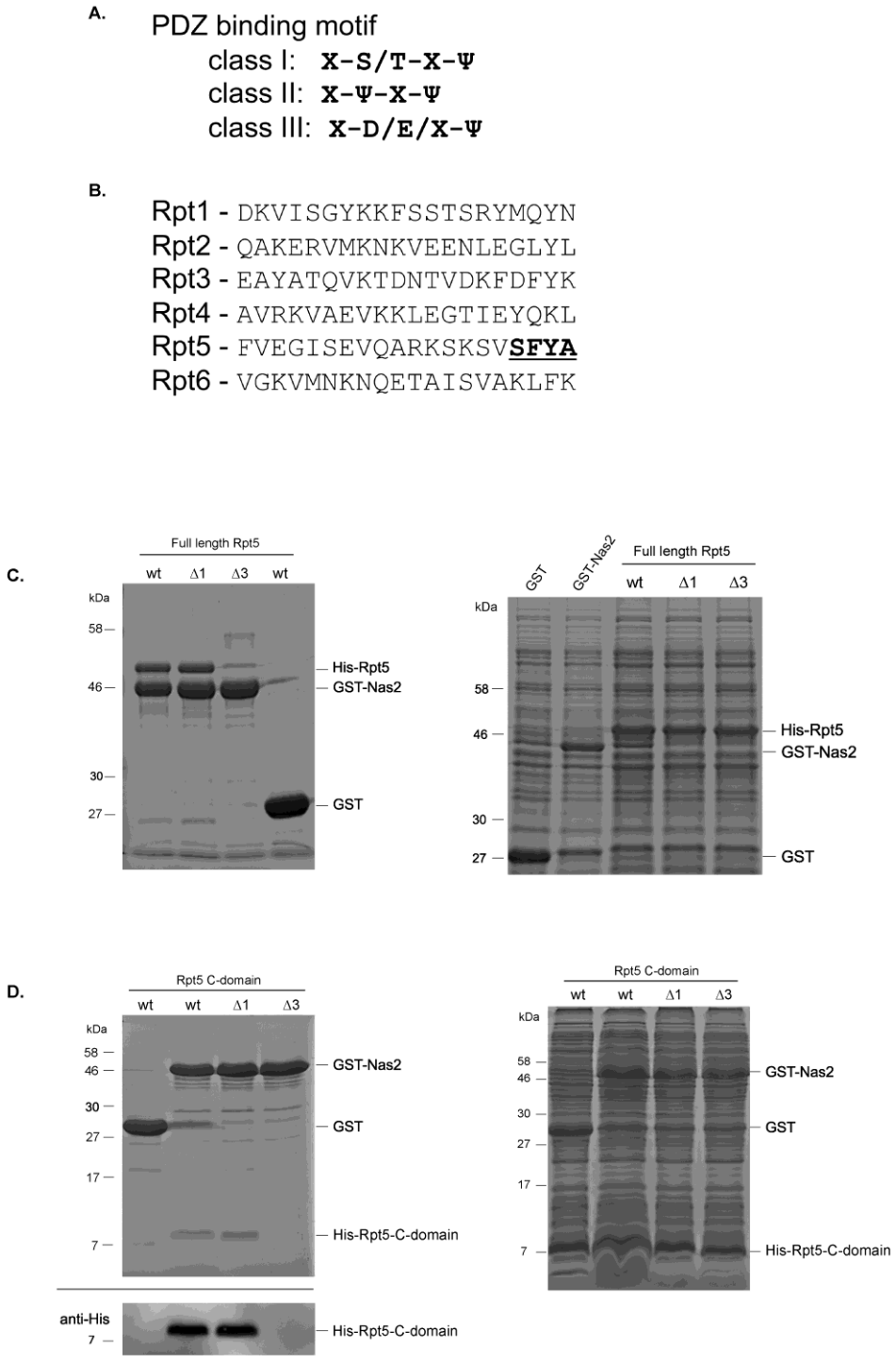

Figure 2.1 Nas2 binds to the tail of Rpt5 independent of the C-terminus.

A, a subset of PDZ-domain containing proteins has been shown to bind to the C-termini of their binding partner. Three classes of C-termini binding PDZ domains have been identified based on the motif they bind to. Shown is the consensus motif as reported by (41,42) with X for any amino

acid and ψ indicating a hydrophobic amino acid. B, Last twenty amino acids of the S.cerevisiae proteasomal AAA-ATPases, Rpt1-6. Bold and underlined is shows the putative class II recognition sequence found in Rpt5. C, E.coli lysates expressing His-tagged Rpt5, Rpt5-Δ1 or Rpt5-Δ3 (right panel) were mixed with lysates expressing GST or GST-tagged Nas2. Glutathione-Sepharose-purified samples were separated on SDS-PAGE followed by Coomassie blue staining (left panel). D, His-tagged C-domains of Rpt5, Rpt5-Δ1 or Rpt5-Δ3 were co-expressed with GST or GST-tagged Nas2 in E.coli (right panel). Glutathione-Sepharose-purified samples were separated on SDS-PAGE followed by either Coomassie blue staining ((left panel; top) or immunoblotting using a His-tag antibody (left panel; bottom). Comparable results were obtained with more than three independent purifications.

The binding of Nas2 to Rpt5-Δ1 is surprising, because the deletion of the C-terminal amino acid of the Rpt5 eliminates the class II binding motif at the C-terminus of Rpt5 (Figure 2.1A and B). However, this result is consistent with the absence of several amino acids, referred to as GLGF motif, in Nas2 (data not shown). The GLGF motif is normally conserved in C-terminus binding PDZ domains and involved in the binding of the C-terminus (42). Thus, although Nas2 binds very close to the C-terminus, it does not belong to the PDZ domains that bind C-termini.

Reduced 26S activity in Rpt5 mutants

The tail of Rpt5 seems to provide two important functions. First, it is involved in the binding of Nas2, suggesting it has an important role in the assembly of the proteasome. Second, part of the tail docks into a pocket present in the proteasome CP. The docking of the Rpt5 tail opens the CP gate as well as stabilizes the CP-RP interaction (5,6). When we compared total lysates on native gel of wildtype, *rpt5*-Δ1 and *rpt5*-Δ3 strains, we observed an increase in free CP in the *rpt5*-Δ1 and *rpt5*-Δ3 strains together with a decrease in the level of singly and doubly capped proteasomes (Fig. 2.2).

These observations can be explained by the compromised CP-RP interaction in the *rpt5*-Δ1 and the *rpt5*-Δ3 strains. Because we observed *in vitro* that the rpt5-Δ3 protein interacts poorly with Nas2 (Fig. 2.1), the more severe reduction in 26S activity as observed for the *rpt5*-Δ3 strain (Fig. 2.2 top panel, lane 4 versus 5) can most likely be contributed to the combined effect of a docking defect and an assembly defect. The later caused by the disruption of the interaction between Rpt5 and Nas2. Alternatively, the *rpt5*-Δ3 strain might show a more complete

impairment of the interaction with CP. However, both the *rpt5*-Δ1 mutation and the *rpt5*-Δ3 mutation are lethal in the *rpn4*Δ background as determined by tetrad analysis (data not shown), indicating that both the *rpt5*-Δ1 and the *rpt5*-Δ3 strains are severely compromised in an important role that the Rpt5 C-terminus performs in proteasome function. Rpn4 is a transcription factor for proteasome genes and at the same time is degraded by the proteasome, thereby providing an important feedback mechanism that is activated when proteasome function is compromised (43). In sum, both the *rpt5*-Δ1 and *rpt5*-Δ3 strains show phenotypes consistent with a defect in docking of Rpt5 onto the CP.

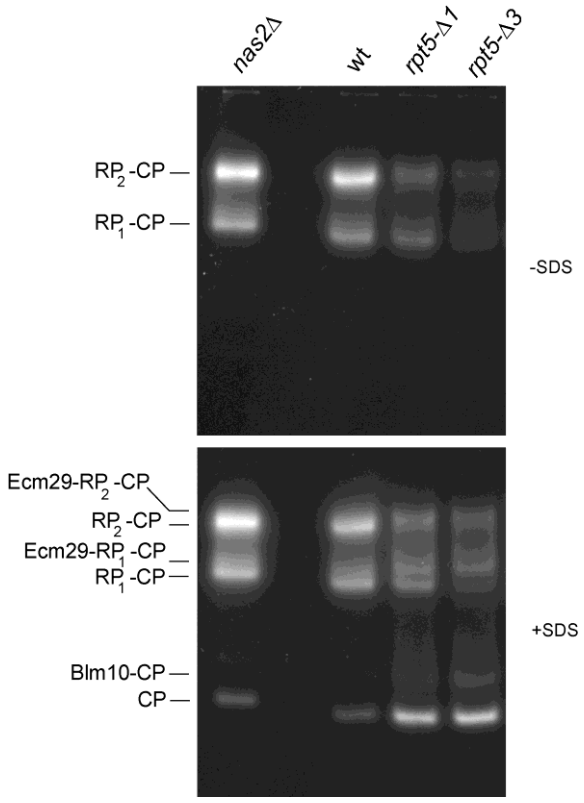

Figure 2.2 Reduced LLVY-AMC hydrolytic activity for proteasome complexes of Rpt5 mutants on antive gel.

A, Cell lysates of wildtype, nas2Δ, rpt5-Δ1 or rpt5-Δ3 were resolved on native gel (100 μg protein/lane). Gels were stained for hydrolytic activity using the fluorogenic substrate LLVY-AMC in the absence (top) or presence (bottom) of 0.02% SDS. The presence of SDS results in visualization of free CP, by opening the CP gate. The different CP containing complexes that can

be identified are indicated. The results shown are a representative example of more than three independent experiments.

Phenotypic analysis

How Nas2 and the other chaperones function at the molecular level in assembly is not well understood. One model, supported by some experimental data, is that binding of Nas6, Rpn14 and Hsm3 to the C-domain of their respective Rpt protein antagonizes docking of the Rpt tail onto the CP (9,14). Structural studies show that the hydrophobic amino acids of the Hb-Y-X motif present in the tail of a number of Rpt proteins fits snugly into the CP pocket (7,40), indicating that the binding of Nas2 to Rpt5 would prevent Rpt5 from docking onto CP. If Nas2 would function solely as a factor to prevent Rpt5-CP interaction one would predict that this function would become irrelevant when Rpt5 and CP do not interact, such as in the *rpt5*-Δ1. Thus if a deletion of *NAS2* in an *rpt5*-Δ1 strain would cause a more severe phenotype, it would suggest that Nas2 might perform roles in assembly beyond regulating the Rpt5-CP interaction. To test this we performed some phenotypic analysis. Using strains deleted for NAS2 or containing the *rpt5*-Δ1 or *rpt5*-Δ3 mutation we did not observe any sensitivity for high temperature (Fig. 2.3). When we tested our mutants in the *hsm3*Δ background, the *rpt5*-Δ1 strain did not show any sensitivity at 37ºC (Fig. 2.3). However, upon deletion of *NAS2* in this background, these cells became temperature sensitive. This suggests that Nas2 has additional, as of yet unidentified, functions during proteasome assembly. The *nas2*Δ *hsm3*Δ strain (15,16) and the *hsm3*Δ *rpt5*-Δ3 strain showed temperature sensitivity as well, since both grew poorly at 37ºC as well (Fig. 2.3). This is consistent with the notion that disruption of the Rtp5-Nas2 interaction in an *HSM3* deletion background causes temperature sensitivity. The *hsm3*Δ *rpt5*-Δ3 strain appears to be somewhat more sensitive compared with *nas2*Δ *hsm3*Δ. This can most likely be explained by the disrupted Rpt5-CP interaction in *hsm3*Δ *rpt5*-Δ3 strain.

As mentioned before, the disruption of the Rpt5-CP interaction, as observed in the *rpt5*-Δ3 or *rpt5*-Δ1 appears to be synthetic lethal with a deletion of *RPN4*. The deletion of *NAS2* in an *rpn4*Δ strain is not lethal and *nas2*Δ *rpn4*Δ cells do not show temperature sensitivity either (data not shown). This is similar to what has been observed for deletions of the other individual chaperones in combination with *RPN4* (14). In sum, strains in which the Nas2-Rpt5 interaction is

disrupted in the *hsm3*Δ background become sensitive for heat stress. Strains with compromised Rpt5 docking on the other hand display lethality in the *rpn4*Δ background.

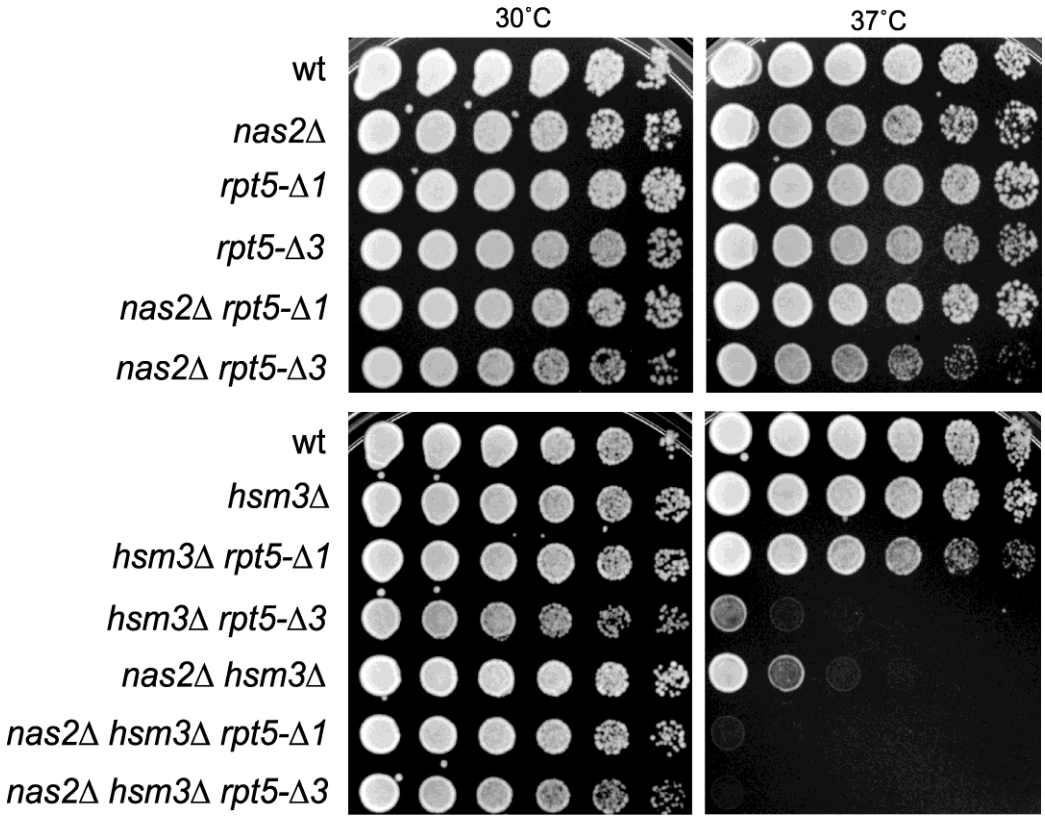

Figure 2.3 Growth phenotype of *nas2*Δ correlates with *rpt5*-Δ*3* mutation in the *hsm3*Δ background.

Strains with the indicated mutations or genes deleted were spotted on YPD plates in four- fold serial dilutions and grown at the indicated temperature for 2-3 days. Dilution assays were performed three times with at least two independent clones, each time showing similar growth patterns.

Enrichment in Ecm29

The lysate of *rpt5*-Δ1 strain shows a modest enrichment in a species that migrates slightly slower then RP-CP, while there also is a species migrating slightly slower than RP_2-CP (Fig. 2.2). This effect is consistently more pronounced in *rpt5*-Δ3 lysates, suggesting both the failure to interact with the CP as well as the failure to bind Nas2 contribute to this effect (Fig. 2.2). These slower migrating species can generally be attributed to retarded migration due to the binding of Ecm29 or Blm10 (24,31). Ecm29 can bind to RP_2-CP or RP-CP. Blm10 can only bind to RP-CP, because Blm10, like RP, interacts with the ends of CP, and the binding to the same end of the CP is mutually exclusive between RP and Blm10 (44).

To confirm that the slower migrating forms we observe are Ecm29 containing species, we used two approaches. First, we analyzed the presence of Ecm29 by performing immunoblots of the native gels (Fig. 2.4A). This experiment shows that the Ecm29 positive bands align with the retarded RP-CP and RP_2-CP, indicating these bands contain Ecm29. Furthermore, comparing the signal of Ecm29 with Rpt5 in Figure 2.4A, suggests the ratio of Ecm29 containing proteasome is strongly increased in *rpt5*-Δ1 and especially in the *rpt5*-Δ3 strains. Second, we introduced a protein A tagged proteasome subunit (36) in the different strains and used this to affinity-purify proteasomes. SDS-PAGE analysis of these purified proteasomes showed an enrichment of a band at a molecular weight similar to Ecm29 in the *rpt5*-Δ1 and *rpt5*-Δ3 (Fig. 2.4B, lane 1 versus 2, 4 and 6). This band was absent from *ecm29* deletion strains (Fig. 2.4B, lanes 3,5 and 7). To confirm this was indeed Ecm29 we did an immunoblot using the same Ecm29 antibody that was used in Figure 2.4A (Fig. 2.4C). Next, the purified proteasomes were treated with apyrase to reveal the proteasomes that have Ecm29 associated with it. Apyrase converts ATP and ADP into AMP and thereby causes dissociation of the RP-CP interaction unless Ecm29 is present (31). Therefore, the reduction of RP_2-CP or RP-CP levels and the concurrent increase in the level of free CP is an indication of the amount of proteasomes that did not have Ecm29 associated with it, while resistance to apyrase treatment reflect complexes that are associated with Ecm29. Wild-type proteasomes have little Ecm29 associated, as most of the RP_2-CP and RP-CP species disappear upon apyrase treatment and free CP dramatically increases (Fig. 2.4D lanes 1, 2, 11 and 12).

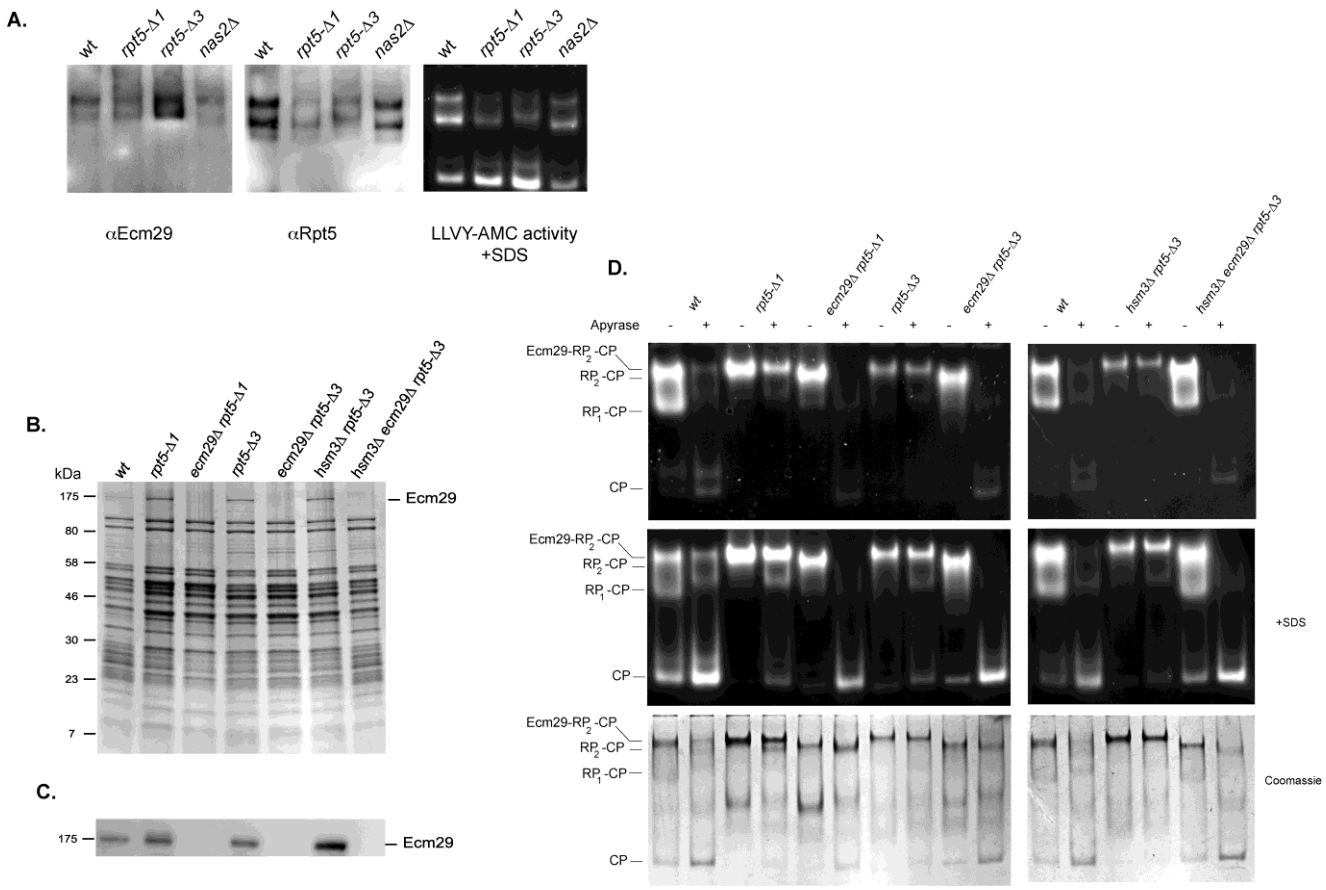

Figure 2.4 rpt5-□3 proteasomes are enriched in Ecm29.

A, Cell lysates of wildtype, nas2Δ, Rpt5-Δ1 or Rpt5-Δ3 were resolved on native gel (60 μg protein/lane) and stained for hydrolytic activity in the presence of 0.02% SDS using the fluorogenic substrate LLVY-AMC (right panel). Gels were also transferred to a membrane and probed with antibodies to Ecm29 or Rpt5. Two independent experiments showed similar results. B, Proteasomes were affinity-purified from strains with protein A-tagged Rpn11 in the presence of ATP. Samples were analyzed using SDS-PAGE and stained with CBB. C, Identical to B, only instead of CBB staining gels were transferred to a membrane and probed with an antibody to Ecm29. D, Proteasome preparations shown in (B) were incubated in the presence or absence of apyrase. Samples were subjected to native gel electrophoresis in the presence of ATP, and stained for LLVY-AMC hydrolytic activity in the presence or absence of 0.02% SDS. Third panel shows native gel stained with coomassie blue. Results shown in B-D are representative examples of at least three experiments using two independently purified proteasome preparations.

Proteasomes purified from *rpt5*-Δ1, *rpt5*-Δ3 and *hsm3*Δ *rpt5*-Δ3 strains show hardly an increase in free CP upon treatment with apyrase and almost all RP-CP species remain stably associated (Fig. 2.4 D, lanes 3, 4, 7,8, 13 and 14). This shows that these proteasomes are highly enriched in Ecm29, with almost every RP-CP species containing at least one Ecm29 molecule. This is consistent with what we saw for the lysates on native gel (Fig. 2.4A). To show that the observed stability upon apyrase treatment is indeed caused by Ecm29, we deleted *ECM29* in the *rpt5*-Δ1, *rpt5*-Δ3 and *hsm3*Δ *rpt5*-Δ3 strains. Upon treatment of proteasome from *ecm29*Δ strains with apyrase, the levels of RP_2-CP and RP-CP were strongly reduced, similarly to wildtype, with a concurrent increase in free CP (Fig. 2.4D; lanes 5,6,9,10, 15 and 16). Thus the *rpt5*-Δ1 and *rpt5*-Δ3 mutations cause a strong increase in proteasomes associated with Ecm29 and the majority of assembled proteasomes contain Ecm29.

Ecm29 induced closing of the gate

We observed a surprising SDS-induced increase in RP-CP and RP_2-CP suc-LLVY-AMC hydrolytic activity on native gels in the *rpt5*-Δ3 strain (Fig. 2.2 and Fig. 2.4D lane 7 and 8; compare top and middle panel) as well as the *rpt5*-Δ1 and wildtype strain after apyrase treatment (Fig. 2.4D). SDS induces a strong increase in free CP activity, because SDS causes an artificial opening of the gate of the CP (45). However, the association of RP with CP also results in gate opening. Thus RP_2-CP species normally do not display an increase of LLVY-AMC hydrolytic activity in the presence of SDS compared to the absence of SDS, while RP-CP might show an intermediate activation. The SDS stimulated activity seems to be exclusive for the proteasome species with retarded migration and more pronounced in the *rpt5*-Δ3 strain (Fig. 2.4D) suggesting this effect depends on the presence of Ecm29. Alternatively, it could be specific for the *rpt5*-Δ3 strain, as Rpt5 reportedly plays a role in gate opening (5,6). We favor the earlier, because the SDS stimulation was not observed for protesomes purified from a *rpt5*-Δ3 *ecm29*Δ strain (Fig. 2.4D) and a similar effect has been observed in other mutants strains as well (Park et al. JBC in press). Furthermore, *hsm3*Δ and *nas2*Δ strains show the same SDS activation for the Ecm29-RP-CP species (Fig. 2.2 and data not shown). Thus the activation by SDS seems specific for RP-CP complexes that have Ecm29 associated. To test if the association of Ecm29 might

affect SDS dependent stimulation of LLVY-AMC activity in strains without any other mutations, we compared wildtype proteasomes with and without Ecm29.

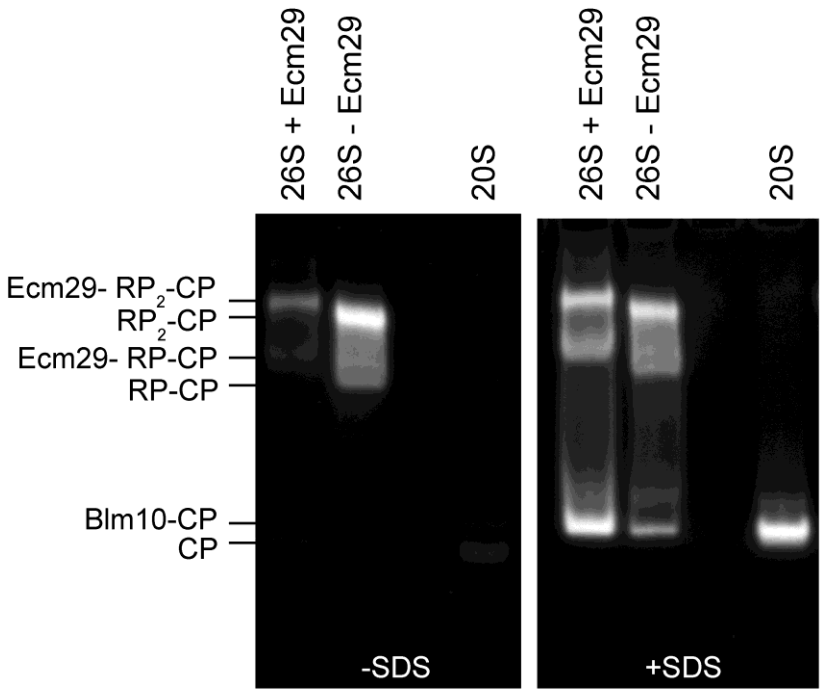

Figure 2.5 Ecm29-containing proteasomes have reduced activity in the absence of SDS.

Proteasomes were affinity-purified from cell lysates of wildtype in the absence of ATP, which results in the purification of Ecm29 containing RP-CP and RP_2-CP, or from ecm29Δ cells in the presence of ATP. As a control CP was affinity purified as well, using a strain with protein A tagged pre1 strain. Samples were subjected to native gel in the presence of ATP and stained for suc-LLVY-AMC hydrolytic activity in the presence or absence of SDS. Results shown represent one of two independent experiments that yielded similar results.

To do this, we purified proteasomes from an *ecm29*Δ strain in the presence of ATP or from wildtype cells in the absence of nucleotide. In the absence of nucleotide all the 26S proteasomes purified from the wildtype strain contain Ecm29 (31). Native gel analysis of these purified proteasome show that RP-CP species containing Ecm29 are strongly activated by SDS as is CP, while RP-CP species lacking Ecm29 are not (Fig. 2.5). Because the only known role of SDS is opening the gate, these data strongly suggest that Ecm29 containing proteasomes have the gate in a closed conformation. Proteasomes containing Ecm29 might therefore be less active and have reduced functionality, a property consistent with the recently proposed quality control function of Ecm29 (33).

Ecm29 proteasomes contain all subunits

In a paper proposing the quality control function of Ecm29, Lehman et al. suggest that the observed reduction of the relative hydrolytic activity for Ecm29-bound RP-CP species is caused by incomplete CP maturation (33). However, the observed hydrolytic activity of the Ecm29 containing proteins in our native gel assays, especially in the presence of SDS, suggest that these proteasomes have mature active sites. In addition to incompletely maturation of CP, Lehman et al. argue that all Ecm29 containing proteasomes lack the CP subunit β3 (33). To test if the Ecm29 containing proteasomes in our system lack β3 we purified proteasomes from a wildtype strain as well as an *rpt5*-Δ3 strain. Even though almost all 26S purified from the *rpt5*-Δ3 strain is associated with Ecm29 (see Fig. 2.4D), we treated *rpt5*-Δ3 strain derived proteasomes with apyrase to dissociate any RP-CP complexes that do not contain Ecm29. Next, samples were loaded on a native gel to separate RP_2-CP complexes from other proteasome complexes and analyzed the proteasome subunit composition of the Ecm29 containing RP_2-CP using mass spectrometry. Analysis of two independent purifications show the presence of all core particle subunits, including β3, in Ecm29 containing RP_2-CP proteasomes purified from *rpt5*Δ3 strain (Fig. 2.6). Thus, under our conditions the presence of Ecm29 does not correlate with the absence of β3.

		mass	WT score	matches	sequences	emPAI	*rpt5Δ3* score	matches	sequences	emPAI
Ecm29	ECM29_YEAST	211610	938	15	15	0.24	2319	52	40	0.77
alpha1	PSA6_YEAST	25759	361	7	6	1.11	332	6	6	0.7
alpha2	PSA2_YEAST	27145	305	10	5	1.42	263	6	4	0.74
alpha3	PSA4_YEAST	31688	366	7	6	1.08	379	9	8	1.31
alpha4	PSA7_YEAST	28697	289	6	5	0.52	266	6	4	0.52
alpha5	PSA5_YEAST	28770	36	1	1	0.11	38	1	1	0.11
alpha6	PSA1_YEAST	28154	357	5	5	0.79	452	9	7	1.26
alpha7	PSA3_YEAST	28650	394	7	7	0.95	258	7	5	0.46
beta1	PSB6_YEAST	26968	74	2	1	0.13	142	3	2	0.29
beta2	PSB7_YEAST	22560	101	2	2	0.23	60	1	1	0.11
beta3	PSB3_YEAST	22819	327	8	4	1.19	317	8	5	1.19
beta4	PSB2_YEAST	29425	87	2	2	0.3	174	3	3	0.49
beta5	PSB5_YEAST	31902	230	4	4	0.46	246	4	4	0.46
beta6	PSB1_YEAST	23761	161	3	3	0.25	174	4	4	0.56
beta7	PSB4_YEAST	28478	300	6	5	0.85	167	6	3	0.67
Rpt1	PRS7_YEAST	52293	472	15	12	1.13	288	6	6	0.34
Rpt2	PRS4_YEAST	49026	509	9	8	0.75	86	2	2	0.13
Rpt3	PRS6B_YEAST	47864	444	11	8	0.56	306	5	5	0.37
Rpt4	PRS10_YEAST	49492	319	8	5	0.36	95	2	2	0.13
Rpt5	PRS6A_YEAST	48283	687	13	10	1.13	289	6	6	0.37
Rpt6	PRS8_YEAST	45471	512	11	8	0.71	288	6	6	0.4
Rpn1	RPN1_YEAST	109880	512	12	12	0.4	537	10	10	0.32
Rpn2	RPN2_YEAST	104623	948	18	17	0.55	884	20	17	0.65
Rpn3	RPN3_YEAST	60754	235	4	4	0.16	399	7	6	0.42
Rpn5	RPN5_YEAST	51850	438	10	8	0.7	460	13	11	1.03
Rpn6	RPN6_YEAST	50085	219	7	7	0.36	146	4	4	0.28
Rpn7	RPN7_YEAST	49213	97	3	3	0.2	220	4	4	0.2
Rpn8	RPN8_YEAST	38460	525	8	8	0.88	559	10	9	1.2
Rpn9	RPN9_YEAST	45811	611	12	11	1.07	421	10	10	0.49
Rpn10	RPN10_YEAST	29786	205	3	2	0.36	249	4	3	0.5
Rpn11	RPN11_YEAST	34433	244	5	5	0.42	153	5	3	0.3
Rpn12	RPN12_YEAST	31956	407	8	8	0.76	304	7	6	0.76
Rpn13	RPN13_YEAST	18005	143	4	3	0.93	152	3	3	0.64

Figure 2.6 LC-MS/MS Analysis of Ecm29-Bound RP_2-CP

To determine the presence of the CP subunit β3 in Ecm29-RP2-CP proteasomes complexes derived from the rpt5-Δ3 strain, purified proteasomes samples were treated with apyrase and separated on a native gel. As a positive control wildtype proteasomes without apyrase treatment were loaded on gel. The band containing doubly capped proteasomes was excised from each lane and submitted for analysis by mass spectrometry. Mass spectormetry of samples from two independent purifications for both wildtype and Rpt3-Δ3 proteasomes proteasome showed very similar results. All proteasome subunits, with the exception of sem1, were identified in all fours sample. Sem1 was only detected in the second purification of wildtype and mutant proteasomes (data not shown). The initial absence can probably be explained by the small size of Sem1 which can hinder its detection, even if present. For Mass spectrometry analysis CBB stained gel pieces were destained using 50% acetonitrile (ACN) at 30 °C. After destaining, the gel pieces were shrunk by addition of 50 µl of 100% ACN for 10 min and solvent was discarded. The gel pieces were dried by speed vacuum concentrator. To rehydrate the gel in 20 µL 20 mM ammonium bicarbonate supplemented with 200 ng sequencing grade trypsin (Trypsin Gold, Promega, Madison, WI), was added. Next, 20 µL of 20 mM ammonium bicarbonate and 10% ACN was added, and gel pieces were incubated at 30°C for 17 h. Tryptic peptides were recovered from gel plugs by extraction with 100 µL of 50% ACN in 2% trifluoroacetic acid (TFA) at 30 °C for 30 min.

Extracted peptides were concentrated by speed vacuum concentrator and added to 100 µL of 2% ACN in 0.1% formic acid. 30 µL Peptide solution was loaded on a C18 reversedphase capillary column (75 µm ID Å~ 15 cm, PepMap: Dionex) in conjunction with an Acclaim C18 PepMap trapping column (300 µm idÅ~10 mm, Dionex) using Nano-HPLC was performed automatically

using a microcolumn switching device (Switchos; LC Packings) coupled to an autosampler (Famos: LC Packings) and a nanogradient generator (UltiMate Nano HPLC; LC Packings). . Peptides were separated by a nanoflow linear ACN gradient using buffer A (0.1% formic acid, 2% ACN) and buffer B (0.1% formic acid, 80% ACN) starting from 5% buffer B to 70% over 55 min at a flow rate of 200 nL/min. Then column was washed by 95% of buffer B for 5 min. The system control software, Hystar 3.2, was used to control the entire process. The eluted peptides were injected into an HCT Ultra Ion Trap Mass Spectrometer (Bruker Daltronics). The mass spectrometer was set up in the data dependent MS/MS mode to alternatively acquire full scans (m/z acquisition range from 300 to 1500 Da). The four most intense peaks in any full scan were selected as precursor ions and fragmented by collision energy. MS/MS spectra were interpreted and peak lists were generated by DataAnalysis 3.4 and Biotools 3.0 software (Bruker Daltronics).

Peptide masses were compared to Swiss Prot Database using MASCOT 2.2 (http://www.matrixscience.com). Saccharomyces Cerevisiae was selected for the taxonomy. The following parameters were used in all searches: the maximum number of missed cleavages allowed was 2; the mass tolerance was 1.2 Da for MS and 0.6 Da for MS/MS. Fixed modification was set on cystein with carbamidomethylation. Variable modification was done on methionine with oxidation. Positive protein identifications using a threshold of 0.05 were used. Peptides scoring <20 were automatically rejected, ensuring all protein identifications were based on the reliable peptide identifications.

Rescue by ECM29 deletion

The increased association of Ecm29 to *rpt5*-Δ3 derived proteasomes might fulfill one of two different functions based on the reported roles of Ecm29. First, Ecm29 binding might stabilize the RP-CP interaction for these compromised proteasomes. If Ecm29 would provide only stabilizing functions, its absence would attenuate proteasome function and presumably cause more severe phenotypes. On the other hand if Ecm29 would act as a negative regulator that inhibits faulty proteasomes, its absence might be beneficial for cells with large amounts of faulty proteasomes. We tested the effect of deleting *ECM29* on the phenotype to assess if it rescues or exacerbates the phenotypes of *hsm3*Δ *rpt5*-Δ3 strain. The deletion of *ECM29* in the *hsm3*Δ *rpt5*-Δ3 strains showed a rescue of the temperature sensitivity, suggesting Ecm29 actually functions as a negative regulator of proteasome assembly or function (Fig. 2.7 upper panel). If the observed effects of Ecm29 are in part related to the failure of Rpt5 binding to Nas2, the *nas2*Δ *hsm3*Δ cells should also be rescued by a deletion of *ECM29*. The deletion of *ECM29* indeed rescues the *nas2*Δ *hsm3*Δ temperature sensitivity, although the rescue is not as robust as for the *hsm3*Δ *rpt5*-Δ3 strain (Fig. 2.7 middle panel). To confirm that these phenotypic rescues are not the result of a rescue of *hsm3*Δ, we tested if the *hsm3*Δ *rpn14*Δ or the *hsm3*Δ *nas6*Δ are rescued by a deletion of *ECM29*. Both strains are not rescued by the deletion of *ECM29* (Fig. 2.7 lower panel), while they are rescued by overexpression of Rpt1 (14). Overexpression of Rpt1 is known to compensate for the absence of Hsm3 (14). Furthermore, the *nas6*Δ *rpn14*Δ strain is also not rescued by a deletion of *ECM29*, indicating that only deletions of *NAS2*, but not other RP chaperone genes, is rescued by a deletion of *ECM29*.

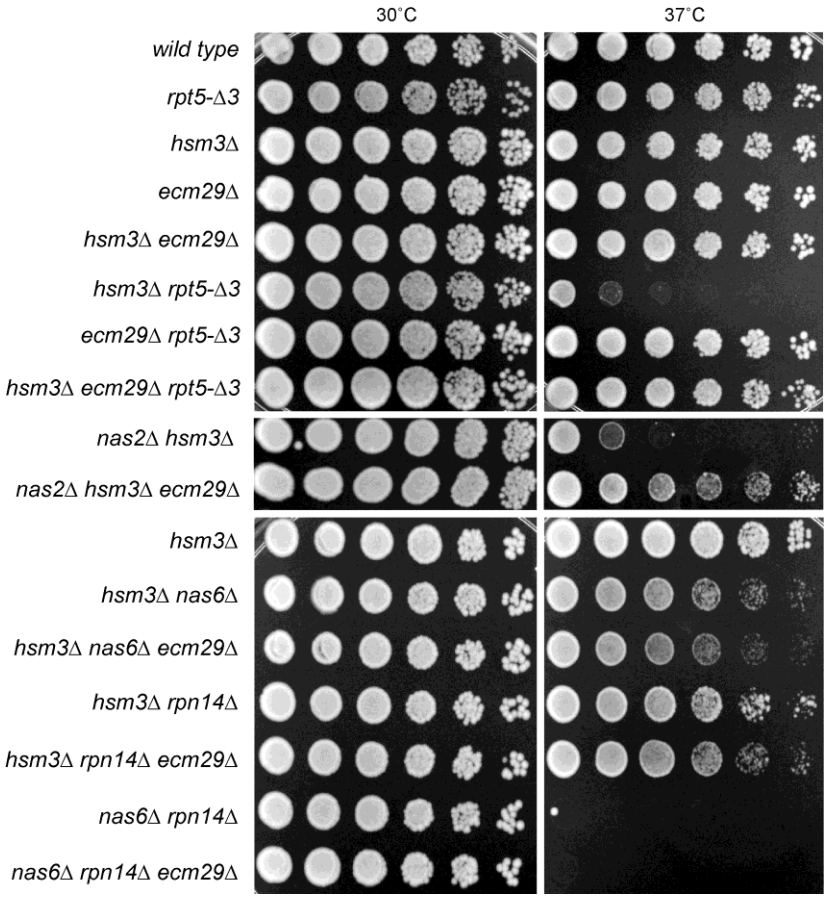

Figure 2.7 *rpt5*-Δ*3* and *nas2*Δ in the *hsm3*Δ background can be rescued by the deletion of Ecm29.

Strains with the indicated mutations or genes deleted were spotted on YPD plates in four-fold serial dilutions and grown at the indicated temperature for 2-3 days. Dilution assays were performed three times with at least two independent clones, each time showing similar growth patterns.

Discussion

The identification of four chaperones that assist in the assembly of the proteasome regulatory particle provides a remarkable example of convergent evolution (9,13-16), since these chaperones do not display any genetic or structural relatedness. Even more remarkable is that each of the four chaperones binds to the C-domain of a specific paralogous AAA-ATPase. The data presented here show that Nas2, unlike the other chaperones, requires the last three amino acids of the Rpt protein for its interaction with this protein. This suggests that Nas2 will interfere with the docking of the Rpt5 tail into the CP, because the C-terminal three amino acids of the tail of Rpt5 are tightly packed in a CP pocket upon docking (7,40). Thus Nas2, has the potential to regulate the interaction of the Rpt protein with the CP by a more direct mechanism as compared to Rpn14, Nas6 and maybe Hsm3 (9,14). Our data also suggests that when studying the *rpt5*-Δ3 mutant *in vivo* (10), one is looking at the cumulative effect of the disruption of two interactions. Using different mutants we were able to dissect the importance of the different interactions: the *rpt5*-Δ1 strain, which is compromised in Rpt5-CP interaction; the *nas2*Δ strain, which lacks the Rpt5-Nas2 interaction; and the *rpt5*-Δ3 strain, which is compromised in both Rpt5-CP and Rpt5-Nas2 interactions.

If the only function of Nas2 would be to prevent docking of Rpt5 tail into a pocket located on the CP, Nas2 function would become irrelevant in the *rpt5*-Δ1 strain, where the Rpt5-CP interaction is compromised. However, deletion of *NAS2* in the *hsm3*Δ *rpt5*-Δ1 strain results in temperature sensitivity, indicating Nas2 has functions beyond preventing the docking of Rpt5 into a CP pocket. We are currently investigating what other functions Nas2 has. Nas2 might e.g. facilitate the formation of specific intermediate assembly complexes or could prevent formation of off-pathway products. Alternatively Nas2 might stabilize Rpt5, as has been suggested for the human homolog p27 (12), although over-expression of Rpt5 in yeast does not rescue the temperature sensitivity of *nas2*Δ *hsm3*Δ strains (data not shown).

We observed that the combined failure of the Nas2-Rpt5 and the Rpt5-CP interaction by means of the *rpt5*−Δ3 mutant causes a dramatic accumulation of Ecm29 on the RP-CP and RP_2-CP proteasome species. There have been several publications showing Ecm29 is a stabilizing factor for the RP-CP interaction in the absence of ATP (31,32). However, more recent

publications suggest it is also a negative regulator or quality control protein for proteasome assembly (33-35). These roles might appear contradictory, but our data actually suggest that both phenomena happen synchronously. We observed that Ecm29-containing proteasomes remain stable upon removal of ATP and display reduced suc-LLVY-AMC hydrolytic activity in the absence of SDS. In the presence of SDS suc-LLVY-AMC hydrolytic activity is restored. The mechanism for SDS activation is generally believed to involve an artificial opening of the CP gate by disrupting the interaction between the N-termini of the CP α subunits, which then facilitates substrate entry. Therefore our data suggest that upon binding with proteasomes Ecm29 actually enforces a (partially) closed gate and thereby inhibits the proteasome. Thus, Ecm29 could function as a quality control protein, if it would recognize and inhibit "faulty" proteasomes.

Although we currently have no molecular insight into if and how Ecm29 recognizes defective proteasomes, there are data that suggest Ecm29 recognizes such proteasomes. First, we saw enrichment in Ecm29 containing proteasomes in our *rpt5*-Δ1 and *rpt5*-Δ3 backgrounds. Second, RP-CP complexes in which the β3 subunit is absent and the active sites of the CP not properly matured show association with Ecm29 (33). Finally, upon oxidative stress there is an increased association of Ecm29 with RP (34). While we favor a model with specific recruitment of Ecm29 to faulty proteasomes, increased cellular levels of Ecm29 might also directly contribute to the enrichment in Ecm29 on proteasomes (Park et al. JBC in press).

Earlier work suggested that Ecm29 association with proteasomes coincides with the absence of the CP β3 subunit (33). The absence of β3 also causes the lack of matured active sites. Under our conditions it seems unlikely that CP maturation defects cause the recruitment of Ecm29, because the Ecm29 containing proteasomes show robust proteolytic activity in the presence of SDS. It is more plausible that failure in CP as well as RP assembly can result in the recruitment of Ecm29. Ecm29 could specifically recognize conformations in each path, or it might be able to recognize a specific signal at some integration point. The later seems possible considering the interaction between RP and CP regulates gate opening and the binding of Ecm29 affects the gate. Interesting to note is the presence of an allosteric communication that occurs between the proteolytic active sites inside the CP and CP-RP interface (31,46). Thus, immature

active sites of the CP could affect the CP-RP interaction as well. Therefore, if Ecm29 would recognize some misalignment between CP and RP it would have the potential to be able to "sense" a variety of faulty proteasomes, even if the cause is from a different origin. Since Ecm29 has been reported to bind to the CP as well as the RP (32), one can envision subtle changes affecting the relative position of the two binding sites might function as a sensor of improper RP-CP alignment.

Although our data indicates a function of Ecm29 in recognizing and inhibiting faulty proteasomes, it is unclear if Ecm29 always inhibits the proteasome, since Ecm29 also appears to function as an adaptor that anchors proteasomes to specific cellular compartments (47,48). Furthermore, while we have shown *in vitro* that Ecm29 stabilizes proteasomes in the absence of ATP or ADP, other recent publication suggests that Ecm29 might cause dissociation of RP-CP complexes under different conditions (33,34). Ecm29 induced dissociation might make sense as part of a mechanism to recognize and restore faulty proteasomes.

Figure 2.8 explains our observations in respect to a model. In wildtype cells the majority of proteasomes are assembled correctly. Nas2 mediated assembly is normal and the Rpt5 tail can dock into the core particle. Thus, there is only a small population of proteasomes associated with Ecm29. It could be that during normal assembly there is a transient functional association with Ecm29, or there is always a low background of faulty proteasomes present. Upon deletion of the Rpt5 C-terminal amino acid (Fig. 2.8 second row) Rpt5 does not dock properly onto CP, but in the presence of Nas2 this does not cause a major defect in assembly. This results in an increase in association of Ecm29 with the proteasome, but there is a substantial pool of proteasomes that are not bound or recognized by Ecm29 and are fully active. This provides a medium level of activity that is sufficient to cope with stress conditions such as heat, especially when the cell is able to compensate for reduced proteasome function using the rpn4 based feedback mechanism. However, the combined mutation with *rpn*4Δ causes lethality, indicating the docking of the Rpt5-Δ1 protein into the CP pocket is severely compromised. In *rpt5*−Δ3 there is a defect in docking in combination with a defect in assembly since the interaction between Nas2 and Rpt5 is disrupted as well (Fig. 2.8 third row). This presumably causes an increase in faulty proteasomes.

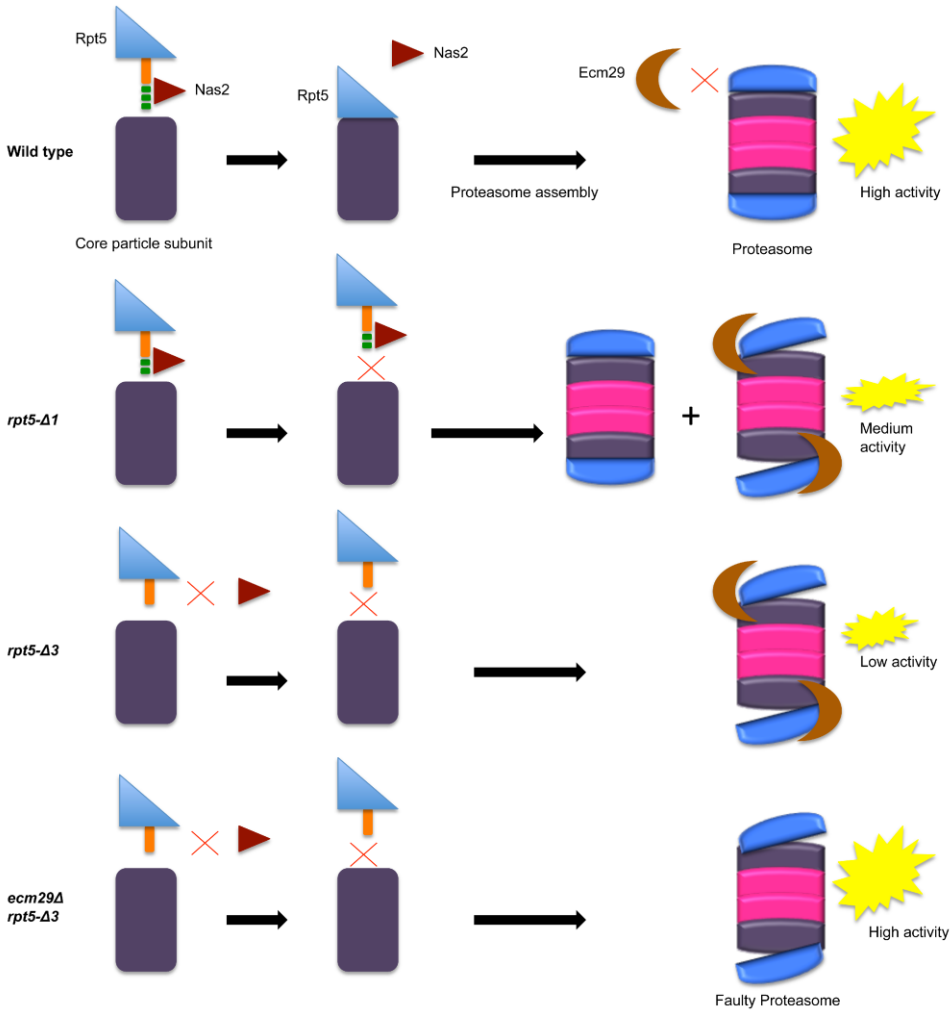

Figure 2.8 Model explaining and summarizing the role of the Rpt5 tail in proteasome assembly.

In wildtype cells Rpt5 (indicated with the blue triangle) contains a tail of about 12 amino acids that are predicted to be unstructured and not part of the preceding C-domain. The tail is depicted in orange with the last three amino acids shown as green blocks. This tail has two functions. First it interacts with the chaperone Nas2 (indicated with the red triangle). Second the tail contains a Hb-Y-X consensus motif and has been shown to dock into a pocket present on the CP. Both interactions are mutually exclusive. Without disruption of either function, proteasomes assemble normally and have little Ecm29 associated with them. These proteasomes display high hydrolytic activity towards the substrate suc-LLVY-AMC. B, Upon the deletion of the C-terminal amino acid of Rpt5, the functional binding to CP is disrupted, while the binding to Nas2 is still functional. Under these conditions there is a modest increase in the formation of faulty proteasomes (indicated by the misalignment of CP-RP) which have Ecm29 associated, but there is a substantial amount of proteasomes remaining that do not have Ecm29 associated with them. C, Deleting three amino acids from the C-terminal end of Rpt5, results in the loss of both Nas2 binding and proper CP docking. Under these conditions almost all proteasomes formed have Ecm29 associated with them. Although it is unclear what signal recruits Ecm29 to these

proteasomes, we propose that Ecm29 functions as a quality control protein that recognizes proteasomes because of a misalignment between CP and RP. These Ecm29 associated proteasomes show a strongly reduced LLVY-AMC hydrolytic activity, suggesting the function of Ecm29 might be to recognize and inhibit faulty proteasomes. D, This model predicts that the deletion of Ecm29 would remove inhibition of the proteasome and actually rescue cells with a substantial amount of faulty proteasomes, by increasing their cellular proteolytic potential.

These faulty proteasomes are then recognized by and bound to Ecm29 resulting in low proteasome activity. This prevents this strain from being able to cope with heat stress in e.g. the *hsm3*Δ background. Deleting *ECM29* in this background, does not restore the defective proteasomes, but removes the inhibition of the defective proteasomes (Fig. 2.8 fourth row). Thus these cells have again a substantial amount of proteasome activity that enables them to deal with a certain amount of heat stress.

In mutants where faulty proteasomes can be restored or make up a minor portion of the total proteasomes, it might be preferable to have Ecm29 inhibit these proteasomes. This will ensure the cell has a pool of proper proteasomes and no active faulty proteasomes. However, under conditions where large amounts of faulty proteasomes are formed, such as in our *rpt5*-Δ3 mutant, Ecm29 would be inhibiting a large fraction of proteasomes. Therefore, a particular cell might be better off to have fully active, albeit faulty, proteasomes. This would explain how the deletion of *ECM29* can rescue the phenotypes of specific strains. However, under conditions where the absence of Ecm29 would not restore proteolytic activity, e.g. because defects in core particle assembly caused the association of Ecm29, deleting *ECM29* might actually exacerbate the phenotype. Such an exacerbated phenotype has e.g. been reported for *ecm29*Δ *ump1*Δ and *ecm29*Δ *blm10*Δ (24,33).

From our data it is clear that both the Rpt5-CP and the Rpt5-Nas2 interaction are important for proper proteasome formation. Interestingly, the compromised interaction of Rpt5 with Nas2 does not simply cause a reduced or slower assembly of normal proteasomes, but causes the formation of proteasomes associated with Ecm29. Delineating the mechanism by which these proteasomes are recognized by Ecm29 will be important for understanding at the

molecular level how Rpt5 and Nas2 function in proteasome assembly as well as how Ecm29 plays a role as a negative regulator and putative quality control protein.

A.D.L.M., S.Y.L, and J.R. conceived the experiments, S.Y.L performed experiments in figures 1, 2 and 4a. A.D.L.M conducted all other experiments. A.D.L.M. , S.Y.L. and J.R. analyzed and interpreted the data. A.D.L.M., S.Y.L. and J.R. wrote the manuscript with input from all coauthors.

References

1. Gallastegui, N., and Groll, M. (2010) *Trends Biochem Sci* **35**, 634-642
2. Stadtmueller, B. M., and Hill, C. P. (2011) *Molecular Cell* **41**, 8-19
3. Forster, F., Lasker, K., Beck, F., Nickell, S., Sali, A., and Baumeister, W. (2009) *Biochem Biophys Res Commun* **388**, 228-233
4. Tomko Jr, R. J., Funakoshi, M., Schneider, K., Wang, J., and Hochstrasser, M. (2010) *Molecular Cell* **38**, 393-403
5. Gillette, T. G., Kumar, B., Thompson, D., Slaughter, C. A., and DeMartino, G. N. (2008) *J Biol Chem* **283**, 31813-31822
6. Smith, D. M., Chang, S. C., Park, S., Finley, D., Cheng, Y., and Goldberg, A. L. (2007) *Mol Cell* **27**, 731-744
7. Yu, Y., Smith, D. M., Kim, H. M., Rodriguez, V., Goldberg, A. L., and Cheng, Y. (2009) *The EMBO Journal* **29**, 692-702
8. Bohn, S., Beck, F., Sakata, E., Walzthoeni, T., Beck, M., Aebersold, R., Forster, F., Baumeister, W., and Nickell, S. (2010) *Proc Natl Acad Sci U S A* **107**, 20992-20997
9. Park, S., Roelofs, J., Kim, W., Robert, J., Schmidt, M., Gygi, S. P., and Finley, D. (2009) *Nature* **459**, 866-870
10. Kim, Y. C., and Demartino, G. N. (2011) *J Biol Chem* **286**, 26652-26666
11. Murata, S., Yashiroda, H., and Tanaka, K. (2009) *Nat Rev Mol Cell Biol* **10**, 104-115
12. Kaneko, T., Hamazaki, J., Iemura, S., Sasaki, K., Furuyama, K., Natsume, T., Tanaka, K., and Murata, S. (2009) *Cell* **137**, 914-925
13. Le Tallec, B., Barrault, M. B., Guerois, R., Carre, T., and Peyroche, A. (2009) *Mol Cell* **33**, 389-399
14. Roelofs, J., Park, S., Haas, W., Tian, G., McAllister, F. E., Huo, Y., Lee, B. H., Zhang, F., Shi, Y., Gygi, S. P., and Finley, D. (2009) *Nature* **459**, 861-865
15. Funakoshi, M., Tomko, R. J., Jr., Kobayashi, H., and Hochstrasser, M. (2009) *Cell* **137**, 887-899
16. Saeki, Y., Toh, E. A., Kudo, T., Kawamura, H., and Tanaka, K. (2009) *Cell* **137**, 900-913
17. Le Tallec, B., Barrault, M.-B., Guérois, R., Carré, T., and Peyroche, A. (2009) *Molecular Cell* **33**, 389-399
18. Dawson, S., Apcher, S., Mee, M., Higashitsuji, H., Baker, R., Uhle, S., Dubiel, W., Fujita, J., and Mayer, R. J. (2002) *J Biol Chem* **277**, 10893-10902
19. Bedford, L., Paine, S., Sheppard, P. W., Mayer, R. J., and Roelofs, J. (2010) *Trends Cell Biol* **20**, 391-401
20. Park, S., Tian, G., Roelofs, J., and Finley, D. (2010) *Biochem Soc Trans* **38**, 6-13

21. Finley, D. (2009) *Annu Rev Biochem* **78**, 477-513

22. Sakata, E., Stengel, F., Fukunaga, K., Zhou, M., Saeki, Y., Forster, F., Baumeister, W., Tanaka, K., and Robinson, C. V. (2011) *Mol Cell* **42**, 637-649

23. Sadre-Bazzaz, K., Whitby, F. G., Robinson, H., Formosa, T., and Hill, C. P. (2010) *Molecular Cell* **37**, 728-735

24. Schmidt, M., Haas, W., Crosas, B., Santamaria, P. G., Gygi, S. P., Walz, T., and Finley, D. (2005) *Nat Struct Mol Biol* **12**, 294-303

25. Iwanczyk, J., Sadre-Bazzaz, K., Ferrell, K., Kondrashkina, E., Formosa, T., Hill, C. P., and Ortega, J. (2006) *Journal of Molecular Biology* **363**, 648-659

26. Lopez, A. D., Tar, K., Kruegel, U., Dange, T., Ros, I. G., and Schmidt, M. (2011) *Mol Biol Cell* **22**, 528-540

27. Ortega, J., Heymann, J. B., Kajava, A. V., Ustrell, V., Rechsteiner, M., and Steven, A. C. (2005) *J Mol Biol* **346**, 1221-1227

28. Marques, A. J., Glanemann, C., Ramos, P. C., and Dohmen, R. J. (2007) *Journal of Biological Chemistry* **282**, 34869-34876

29. Fehlker, M., Wendler, P., Lehmann, A., and Enenkel, C. (2003) *EMBO reports* **4**, 959-963

30. Li, X., Kusmierczyk, A. R., Wong, P., Emili, A., and Hochstrasser, M. (2007) *EMBO J* **26**, 2339-2349

31. Kleijnen, M. F., Roelofs, J., Park, S., Hathaway, N. A., Glickman, M., King, R. W., and Finley, D. (2007) *Nat Struct Mol Biol* **14**, 1180-1188

32. Leggett, D. S., Hanna, J., Borodovsky, A., Crosas, B., Schmidt, M., Baker, R. T., Walz, T., Ploegh, H., and Finley, D. (2002) *Mol Cell* **10**, 495-507

33. Lehmann, A., Niewienda, A., Jechow, K., Janek, K., and Enenkel, C. (2010) *Molecular Cell* **38**, 879-888

34. Wang, X., Yen, J., Kaiser, P., and Huang, L. (2010) *Science Signaling* **3**, ra88-ra88

35. Panasenko, O. O., and Collart, M. A. (2011) *Molecular and Cellular Biology* **31**, 1610-1623

36. Leggett, D. S., Glickman, M. H., and Finley, D. (2005) *Methods Mol Biol* **301**, 57-70

37. Elsasser, S., Schmidt, M., and Finley, D. (2005) *Methods in Enzymology* **398**, 353-363

38. Ammelburg, M., Frickey, T., and Lupas, A. N. (2006) *J Struct Biol* **156**, 2-11

39. Zhang, F., Hu, M., Tian, G., Zhang, P., Finley, D., Jeffrey, P. D., and Shi, Y. (2009) *Mol Cell* **34**, 473-484

40. Stadtmueller, B. M., Ferrell, K., Whitby, F. G., Heroux, A., Robinson, H., Myszka, D. G., and Hill, C. P. (2009) *Journal of Biological Chemistry* **285**, 13-17

41. Songyang, Z., Fanning, A. S., Fu, C., Xu, J., Marfatia, S. M., Chishti, A. H., Crompton, A., Chan, A. C., Anderson, J. M., and Cantley, L. C. (1997) *Science* **275**, 73-77

42. Hung, A. Y., and Sheng, M. (2002) *J Biol Chem* **277**, 5699-5702

43. Xie, Y., and Varshavsky, A. (2001) *Proc Natl Acad Sci U S A* **98**, 3056-3061

44. Sadre-Bazzaz, K., Whitby, F. G., Robinson, H., Formosa, T., and Hill, C. P. (2010) *Mol Cell* **37**, 728-735

45. Rubin, D. M., Glickman, M. H., Larsen, C. N., Dhruvakumar, S., and Finley, D. (1998) *EMBO J* **17**, 4909-4919

46. Osmulski, P. A., Hochstrasser, M., and Gaczynska, M. (2009) *Structure* **17**, 1137-1147

47. Gorbea, C., Pratt, G., Ustrell, V., Bell, R., Sahasrabudhe, S., Hughes, R. E., and Rechsteiner, M. (2010) *J Biol Chem* **285**, 31616-31633

48. Gorbea, C., Goellner, G. M., Teter, K., Holmes, R. K., and Rechsteiner, M. (2004) *J Biol Chem* **279**, 54849-54861

Chapter 3 - The proteasome-associated protein Ecm29 inhibits proteasomal ATPase activity and *in vivo* protein degradation by the proteasome

Alina De La Mota-Peynado, Stella Yu-Chien Lee, Brianne Marie Pierce, Prashant Wani, Chingakham Ranjit Singh, and Jeroen Roelofs

Division of Biology, Kansas State University, Manhattan, Kansas, United States of America

*Published in the Journal of Biological Chemistry, Volume 288, Issue 41, 11 October 2013, Pages 29467-29481.

Republished with permission.

Abstract

Several proteasome-associated proteins regulate degradation by the 26S proteasome using the ubiquitin chains that mark most substrates for degradation. The proteasome-associated protein Ecm29, however, has no ubiquitin-binding or modifying activity and its direct effect on substrate degradation is unclear. Here, we show that Ecm29 acts as a proteasome inhibitor. Besides inhibiting the proteolytic cleavage of peptide substrates *in vitro,* it inhibits the degradation of ubiquitin-dependent and independent substrates *in vivo*. Binding of Ecm29 to the proteasome induces a closed conformation of the substrate entry channel of the core particle. Furthermore, Ecm29 inhibits proteasomal ATPase activity, suggesting the mechanism of inhibition and gate regulation by Ecm29 is through regulation of the proteasomal ATPases. Consistent with this, we identified through chemical crosslinking that Ecm29 binds to, or in close proximity to, the proteasomal ATPase subunit Rpt5. Additionally, we show that Ecm29 preferentially associates with both mutant and nucleotide depleted proteasomes. We propose that the inhibitory ability of Ecm29 is important for its function as a proteasome quality control factor by ensuring that aberrant proteasomes recognized by Ecm29 are inactive.

Introduction

The proteasome is the major cytosolic protease in eukaryotes. The 26S proteasome holoenzyme consists of a core particle (CP) with one or two regulatory particles (RPs), giving rise to a protease complex of about 2.5 MDa in size. Many proteasome substrates are marked for degradation by the covalent attachment of a polyubiquitin chain (1-3). The first step in degradation is the selection of substrates by a large number of E2 and E3 enzymes that mark specific proteins for degradation. However, additional steps of potential regulation are present at the proteasome. This includes substrate delivery to the proteasome, as well as recognition and deubiquitination by the proteasome. These are facilitated by proteasome-intrinsic ubiquitin receptors, like yeast Rpn10 (human PSMD4) and Rpn13 (ADRM1); shuttling factors, like Rad23 (RAD23A/B); and proteasome-associated deubiquitinating enzymes, like Ubp6 (USP14) (1,4). Finally, substrates require unfolding by the proteasomal AAA-ATPase (the Rpt proteins) and translocation to the inside of the cylindrically shaped CP where proteolysis occurs.

The ability to inhibit protein degradation by the proteasome using chemical inhibitors of the proteolytic sites has resulted in the development of the FDA-approved treatment of multiple myeloma using the proteasome inhibitor Bortezomib (5). In the cell, however, few protein-based proteasome inhibitors have been characterized. In humans, the reported proteasome inhibitors PI31/PSMF1 (6), Rpn14/PAAF1 (7) and S5b/PSMD5 (8) do not directly inhibit the 26S proteasome. PI31/PSMF1 binds to the CP, competes with RP for CP binding (6), and might have a role in regulating RP-CP association (9). Both Rpn14 and Hsm3, the yeast orthologs of Rpn14/PAAF1 and S5b/PSMD5 respectively, bind to RP and compete with CP for RP binding (10-13). They also have an important role as proteasome specific chaperones (3,14). The proteasome is also regulated by posttranslational modifications, which most likely provide an extra level of tuning in its activity (e.g. (15,16)). The closest to a non-chemical inhibitor of the 26S proteasome currently seems to be Ubp6 (USP14), a deubiquitinating enzyme that interacts with the proteasome (17). This protein delays the degradation of ubiquitinated substrates in part through a mechanism that does not require the deubiquitinating activity (18,19). Additionally, Ubp6 has been reported to stimulate gate opening in an ubiquitin-conjugate dependent fashion (20). Although the mechanisms of regulation are not well understood, Ubp6 appears to be specific for ubiquitinated substrates. One of the initial screens that identified Ubp6 as a

proteasome-associated protein in yeast also identified Ecm29 whose function has remained more elusive (17). Ecm29 and the human ortholog KIAA00368/ECM29 bind specifically to 26S proteasomes (17,21). Ecm29 has been reported to stabilize proteasomes (17,22), remodel proteasomes upon stress (23,24), be involved in membrane-associated localization of proteasomes (21,25), and, more recently, be involved in quality control or assembly of the proteasome (23,26-28). Despite these numerous associations, the molecular effects of Ecm29 binding to the 26S proteasome remain poorly understood.

In this study we show that Ecm29 preferentially binds to nucleotide-depleted as well as certain mutant proteasomes. Upon binding to proteasomes, Ecm29 inhibits the *in vivo* and *in vitro* degradation of substrates. Binding of Ecm29 to the proteasomes causes a closed gate conformation and, more importantly, causes an inhibition of proteasomal ATPase activity. The latter can explain the observed reduction in *in vivo* degradation in the presence of Ecm29.

Experimental Procedures

Yeast strains.

See Table 1 for the genotypes of strains used. DNA fragments used to generate C-terminal truncations of Rpt5 at the genomic locus were made by PCR using pYM24 (29) as template and oligos pRLs2-Rpt5 (AAT ATG TAG ATA TGT GAA TGG CGG CTT GAT AAA TCA AAA TAT TAT TAT TTA TCG ATG AAT TCG AGC TCG) and pRL-s3Rpt5d0 (GTA TAA GTG AAG TTC AAG CAA GAA AAT CGA AAT CGG TAT CCT TTT ATG CAT AGG GCG CGC CAG ATC TGT T) for *rpt5-Δ0* (i.e. no truncation control), oligos pRLs2-Rpt5 and pRL-s3Rpt5d1 (AGG GTA TAA GTG AAG TTC AAG CAA GAA AAT CGA AAT CGG TAT CCT TTT ATT AGG GCG CGC CAG ATC TGT T) for *rpt5-Δ1* (i.e. deletion of last amino acid), and oligos pRLs2-Rpt5 and pRL-s3Rpt5d3 (TCG TTG AGG GTA TAA GTG AAG TTC AAG CAA GAA AAT CGA AAT CGG TAT CCT AGG GCG CGC CAG ATC TGT T) for *rpt5-Δ3* (i.e. deletion of last three amino acids). DNA fragments used to exchange the endogenous promoter of ECM29 at the genomic locus, were made by PCR using pYM-N15 (29) as template and oligos pRL194 (TCT CCA CGA GCT GTT TTT CTT TCG CTT CGT CAG

AAG AAA TGG ATC CGG AAT GGT GAT GGT GAT GGT GGT GCA TCG ATG AAT TCT CTG TCG) and pfEcm29NtagS1 (CAA TAA TTA TAG AAA AGT TTC TAT TTC ACC ACG AAC AAC ATT CGT ACG CTG CAG GTC GAC). Standard methods for strain construction and cell culture were used. Plating assays were done as described before, using 4-fold dilutions (11).

Antibodies.

Ecm29 was detected using an Ecm29 polyclonal antibody, kindly provided by Dr. Dan Finley (Harvard Medical School, Boston, MA). Rpt4 and Rpt5 were detected using monoclonal anti-Rpt4 and anti-Rpt5, kindly provided by Dr. William Tansey (Vanderbilt-Ingram Cancer Center, Nashville, TN). Monoclonal anti-FLAG (Sigma) was used for detection of Flag-ODC. Monoclonal anti-β-Galactosidase antibody (Promega) was used for detection of β-galactosidase. Polyclonal anti-Ubiquitin antibody (Enzo) and monoclonal anti-T7 (Novagen) were used for the detection of ubiquitinated substrates, and anti-Pgk1 antibody (Invitrogen) was used as a loading control. Peroxidase conjugated secondary antibodies were used (Jackson Imuno research lab).

Imaging.

All images were acquired using a Gbox imaging system (Syngene) with GeneSnap software. To determine the relative levels of Ecm29 in figure 6, peak volumes for the different bands were determined using the Genetool analysis software from Syngene and values for each Ecm29 signal were corrected for input using the Rpt5 immunoblot. These corrected values were normalized to the signal for ATP without proteasome inhibitor (Fig. 8A) or *ecm29*Δ with ATP (Fig. 8C). Data shown are average from 2 to 4 independent experiments.

Proteasome purifications and native gels.

The affinity purification of Pre1-TeV-protein A-tagged proteasomes was performed as described before with minor modifications (17). Briefly, between 1 and 6 liters of overnight cultures (A600 = ~10) were collected, washed in H_2O, and resuspended in two pellet volumes of lysis buffer (50 mM Tris-HCl [pH 8], 1 mM EDTA, 5 mM $MgCl_2$, 1 mM ATP). The cells were lysed by French press and lysates were cleared by centrifugation (20,000 g, 4 °C for 25 min). The supernatant was filtered through a cheesecloth, IgG beads (MP Biomedicals) were added (~0.5 ml/liter of culture), and the lysate was rotated at 4 °C for 1 h. The IgG beads were collected

in an Econo Column (Bio-Rad) and washed with ice-cold wash buffer (50 column volumes; 50 mM Tris-HCl [pH 7.5], 1 mM EDTA, 100 mM NaCl, 5 mM $MgCl_2$, 1 mM ATP). Next, beads were washed with 15 column volumes of cleavage buffer (50 mM Tris-HCl [pH 7.5], 1 mM EDTA, 1 mM DTT, 5 mM $MgCl_2$, 1 mM ATP), followed by cleavage in the same buffer containing His-tagged TeV protease (Invitrogen) for 1 h at 30 °C. Talon beads were added for 20 min at 4 °C to remove TeV protease, after which the preparation was concentrated in a 10-kDa concentrator (Millipore). Proteasome preparations were stored at -80 °C. For the purifications without nucleotide, no ATP was added to any of the solutions. Proteasome preparations were analyzed using standard SDS-PAGE or on native gels prepared as described previously and run between 2 and 3 h at 4 °C (30). Total lysates for analysis on native gel were prepared as described previously (11).

Apyrase Treatment.

The apyrase treatment of purified proteasomes was performed as described previously with minor modifications (22). Purified proteasomes were diluted in 50 mM Tris-HCl [pH 7.5], 5 mM $MgCl_2$, 1 mM EDTA, and 0.25 mM ATP. Samples were incubated for 45 min at 30°C with or without apyrase (20 milliunits μl^{-1} working concentration). After treatment, proteasomes were analyzed using native gels.

β-galactosidase assay.

Cells were grown overnight in SD media without lysine and supplemented with 100 mM CuSO4. The cell equivalent to 5ml of OD_{600} 1 was collected and cells were lysed in 200 µl breaking buffer (100 mM Tris-HCl [pH 8.0], 1 mM DTT, 20% glycerol, 1 mM PMSF) by vortexing in the presence of glass beads. An additional 200 µl of breaking buffer was added and mixed. After centrifugation at 16,000 g for 5 minutes, 100 µL of the cleared lysate was mixed with 900 µl of Z buffer (60 mM Na_2HPO_4, 40 mM NaH_2PO_4, 10 mM KCl, 1 mM $MgSO_4$, 50 mM β-mercaptoethanol) and incubated for 5 min at 30°C. After incubation, 200 µl of 4 mg/ml O-nitrophenyl-β-D-galactosidase (ONPG) was added to the mixture followed by an incubation at 30°C for 30 min. The reaction was terminated by the addition of 500µl of 1 M Na_2CO_3. Absorbance was read at 420 nm.

Sic1^{PY} degradation assay.

1 µg/µl of purified proteasomes (5 µl) were incubated at 25°C in 15 µl Buffer A (50 mM Tris [pH7.5], 100 mM NaCl, 10% glycerol, 1 mM DTT) plus 10 µl 5X ATP (10 mM ATP, 50 mM $MgCl_2$, 5 mM DTT in Buffer A) for 5 min. 20 µl of T7-tagged ubiquitinated Sic1^{PY} was added to each sample (prepared as described by Saeki et al. (31)), incubation at 25 °C continued for the indicated time points. At each time point 10 µl aliquots were taken, reaction was stopped by addition of 6X sample buffer and boiling. To quantify data, images were acquired using a Gbox imaging system (Syngene) with GeneSnap software. Images were analyzed for the volumes in similar T7-antibody positive areas of the gel lanes using the Genetool analysis software from Syngene. Volume value at t=0 was set at 100% and relative amounts of signal remaining at different timepoints were averaged, using 3 to 5 independent experiments and plotted in a graph.

Cell lysis, in vivo degradation assay, and immunoblotting.

For detection of ubiquitinated substrates, cultures were grown overnight and the cell equivalent to 5ml of OD_{600} 1 was collected and lysed in 100 µl sample buffer and analyzed by SDS-PAGE, using a 14% gel. Degradation of Flag-ornithine decarboxylase (ODC) was measured as previously described (32), with minor modifications. Briefly, transformed cells were grown overnight; 5 ODs of cells were lysed in sample buffer and analyzed on a 10% SDS-PAGE. Flag-ODC abundance was revealed by Western blot.

Ecm29 recruitment assay.

4 ml of overnight culture pellets from strains, with and without proteasome tags, were lysed in 400 µl total lysis buffer (50 mM Tris-HCl [pH 8], 5 mM $MgCl_2$; 1 mM EDTA; protease inhibitors mix) in the presence of ATP or apyrase. To purify the proteasomes, lysates were incubated with IgG resin for 1 hr at 4 °C. The resin was washed three times with lysis buffer with or without ATP, followed by two washes with TeV buffer (50 mM Tris [pH7.5], 50 mM NaCl; 5 mM $MgCl_2$; 0.5 mM EDTA; 1 mM DTT) with or without ATP. Next, the resin was incubated in the presence of TeV protease for 30 min at 30 °C. After centrifugation, sample buffer was added to the supernatant, boiled, and analyzed by western blot. To look at the degradation of Ecm29 by wild-type proteasomes, the same procedure was followed with the

addition of proteasome inhibitors, 100 μM tosyl-lysylchloromethane (TLCK) and 100 nM epoxomicin (ENZO Life Sciences, NY).

ATPase activity assay.

Purified proteasomes (10 μg) were incubated in reaction buffer (50 mM Tris pH7.5, 5 mM $MgCl_2$), and 0.5 mM ATP at 30 °C in a total volume reaction of 100 ml. For each time point 20 μL of the reaction were taken, boiled for 2.5 minutes, and kept on ice. After all the time points were collected, the samples were centrifuged at RT at 13,000 g for 1 min. ADP-Glo Kinase (Promega, CA) assay was performed following manufacturers recommendation using a 384-well plate. 5 μL of each sample was incubated with 5 μL of ADP-Glo reagent for 40 minutes at room temperature. Following this incubation, 10 μL of kinase detection reagent were added to each sample, and incubated for 60 minutes at room temperature. Luminescence was read using the Victor 2 Microplate Reader (Perkin Elmer, MA).

Crosslinking.

Purified proteasomes (1 μg/μL) were incubated in phosphate buffer (50 mM phosphate-buffer [pH 7.2], 5 mM $MgCl_2$, 1 mM EDTA, 1 mM ATP) with 0.25 mM Disuccinimidyl tartarate (DST) for 15 minutes at 30 ºC. The reaction was quenched by adding 50 mM Tris-HCl [pH 7.5], followed by addition of 200 μL Urea buffer (8M Urea, 300 mM NaCl, 100 mM phosphate buffer [pH 7.9]). 25 μL of Talon resin (pre-equilibrated in urea buffer) was added to each sample, followed by 45 minutes rotation at room temperature. Resin was washed three times with urea buffer. 25 μL 2x sample buffer was added and each samples was boiled for 8 minutes prior to analysis by gel electrophoresis.

Table 3.1 Yeast Strains

Strain	Genotype[a] (*lys2-801 leu2-3, 2-112 ura3-52 his3-Δ200 trp1-1)*	Figure	Source
SUB61	MATα	3.1 (A, B, and D), 3.2, 3.3, 3.8	Ref. 60
sDL133	MAT*a rpn11::RPN11-TEVProA (HIS3)*	3.1C, 3.6, 3.8A	Ref. 17
sDL135	MATα *pre1::PRE1-TEVProA (HIS3)*	3.4A and B	Ref. 17
sMK141	MATα *ecm29::TRP*	3.1 (A, B, and D), 3.2, 3.8	This study
sJR211	MATα *ecm29::TRP rpn11::RPN11-TEVProA (HIS3)*	3.6, 3.8C	This study
sJR239	MATα *nas6::TRP rpn14::HYG*	3.1 (A, B, and D), 3.2	Ref. 11
sJR245	MATA *hsm3::KAN*	3.2	Ref. 11
sJR301	MATA *nas6::TRP rpn14::HYG ecm29::TRP*	3.1 (A, B, and D), 3.2	Ref. 26
sJR494	MATα *alpha3::alpha3ΔN alpha7::alpha7ΔN*	3.4C	Ref. 61
sJR502	MATα *nas2::NAT hsm3::KAN*	3.1 (A, B, and D), 3.2	This study
sJR504	MATA *rpt5:: rpt5Δ1 (HYG)*	3.1 (A, B, and D), 3.2, 3.8	This study
sJR544	MAT*α ecm29::TRP rpt5::rpt5Δ3 (HYG)*	3.1 (A, B, and D), 3.2	Ref. 26
sJR546	MATA *hsm3::KAN ecm29::TRP rpt5::rpt5Δ3 (HYG)*	3.1 (A, B, and D), 3.2	Ref. 26
sJR548	MATA *rpt5::rpt5Δ3 (HYG) ecm29::TRP rpn11::RPN11-TEVProA (HIS3)*	3.1C, 3.5, 3.6C	Ref. 26
sJR552	MATA *rpt5::rpt5Δ3 (HYG) rpn11::RPN11-TEVProA (HIS3)*	3.1C, 3.5	Ref. 26
sJR555	MATA *rpt5:: rpt5Δ0 (HYG)*	3.8	Ref. 26
sJR556	MATA *rpt5::rpt5Δ3 (HYG)*	3.1 (A, B, and D), 3.2, 3.8	Ref. 26
sJR558	MATA *hsm3::KAN rpt5::rpt5Δ3 (HYG)*	3.1 (A, B, and D), 3.2	Ref. 26
sJR568	MATA *nas2::NAT hsm3::KAN ecm29::TRP*	3.1 (A, B, and D), 3.2	This study
sJR570	MATα *ecm29::TRP rpt5::rpt5Δ1 (HYG)*	3.1 (A, B, and D), 3.2	This study
sJR619	MATA *rpn11::RPN11-TEVProA (HIS3)*	3.7	This study
sJR649	MATA *rpt5::rpt5Δ3 (HYG)*	3.3B	This study
sJR651	MATα *ecm29::KAN rpt5::rpt5Δ3 (HYG)*	3.3B	This study
sJR686b	MATα *rpt5::rpt5Δ3 (HYG) alpha3::alpha3ΔN alpha7::alpha7ΔN*	3.4C	This study
sJR706	MATA *pre11::pre1-TeV-ProA (HIS3) alpha3::alpha3ΔN*	3.4	This study
sJR736	MATA *rpn11::RPN11-TEVProA (HIS3) GDPp-HIS7-ECM29::NAT*	3.6, 3.7	This study
sJR743	MATα *alpha3::alpha3ΔN alpha7::alpha7ΔN ecm29Δ*	3.4C	This study
sJR744	MATα *rpt5::rpt5Δ3 (HYG) alpha3::alpha3ΔN alpha7::alpha7ΔN ecm29Δ*	3.4C	This study

a) All strains have the DF5 background genotype (lys2-801 leu2-3, 2-112 ura3-52 his3-**Δ**200 trp1-1)

Results

Ecm29 inhibits degradation of ubiquitinated substrates.

In vitro, the presence of Ecm29 causes reduced hydrolysis of the artificial peptide substrate suc-LLVY-AMC by the 26S proteasome (23,26). Therefore, we speculated that Ecm29

functions as an inhibitor of the 26S proteasome inside the cell. To test this, we transformed a wild-type strain and an *ECM29*-deletion strain (*ecm29*Δ) with a plasmid encoding the well-characterized unstable substrate ubi-K-β-galactosidase (33). While we saw a trend of reduced accumulation of β-galactosidase activity in lysates of *ecm29*Δ cells, this reduction was not significant (Fig. 3.1A). However, because only a subset of proteasomes contain Ecm29 in wild-type cells (23,26,27), any Ecm29-dependent effects may be masked. Therefore, we decided to utilize a previously characterized proteasome hypomorph, the *rpt5*-Δ*3* strain, in which 26S proteasomes are enriched with Ecm29 (Fig. 3.1B and (26)). The mutation in this strain results in a deletion of the last three amino acids of the proteasomal AAA-ATPase subunit Rpt5. These residues are important for Rpt5 binding to the CP (34,35) as well as the RP-chaperone Nas2 (26). Their absence conferred canavanine sensitivity, typically observed in proteasome hypomorphs (Fig. 3.2). *rpt5*-Δ*3* mutants showed accumulation of β-galactosidase and high levels of β-galactosidase activity in total lysate (Fig. 3.1A), indicating reduced proteasome activity in these cells. Deletion of Ecm29 from *rpt5*-Δ*3* mutants alleviated the degradation defect (Fig. 3.1A, lane 5 and 6). Because the deletion of Ecm29 did not result in increased proteasome levels (Fig. 3.1A ⟨Rpt5) and Ecm29 was bound to 26S proteasomes (Fig. 3.1B and (26)), this strongly suggests that inhibition of proteasomes by Ecm29 in the *rpt5*-Δ*3* background contributed to the accumulation of β-galactosidase activity. To confirm that the observed inhibition by Ecm29 is a direct effect on proteasomal degradation of ubiquitinated proteins, we analyzed the ability of wild-type, *rpt5*-Δ*3,* and *rpt5*-Δ*3 ecm29*Δ-derived proteasomes to degrade ubiquitinated $Sic1^{PY}$ *in vitro* (31). *rpt5*-Δ*3*-derived proteasomes showed a dramatic reduction in their capacity to degrade this substrate, and the absence of Ecm29 restored the degradation of ubiquitinated $Sic1^{PY}$, although not back to the levels of wild-type proteasomes (Fig. 3.1C and see below).

To determine if the observed inhibition by Ecm29 is specific for this proteasome hypomorph or a more general phenomenon, we tested the *nas6*Δ *rpn14*Δ strain. This strain, which contains deletions for two RP-chaperones involved in assembly of the proteasome base, showed canavanine sensitivity (Fig. 3.2 and (11)), and exhibited an enrichment of Ecm29 on 26S proteasomes (Fig. 3.1B). *nas6*Δ *rpn14*Δ cells showed an accumulation of β-galactosidase compared to wild-type (Fig. 3.1A), and deletion of *ECM*29 in this background reduced β-galactosidase levels. Thus, Ecm29 can inhibit proteasomes in a variety of mutant strains.

Like the majority of proteasome substrates, ubi-K-β-galactosidase relies on ubiquitination for its targeting to and degradation by the proteasome. When blotting for ubiquitinated proteins in total lysate, we observed a general accumulation of ubiquitinated material in the proteasome hypomorphs (Fig. 3.1D). The deletion of *ECM29* in these different backgrounds strongly reduced the levels of accumulated ubiquitinated proteins, indicating that Ecm29 inhibited the degradation of a broad range of endogenous ubiquitinated substrates inside the cell (Fig. 3.1D). Interestingly, this effect was also observed for wild-type cells deleted for *ECM29*. This suggests that Ecm29 inhibits at least a subset of wild-type proteasomes under normal physiological conditions as well.

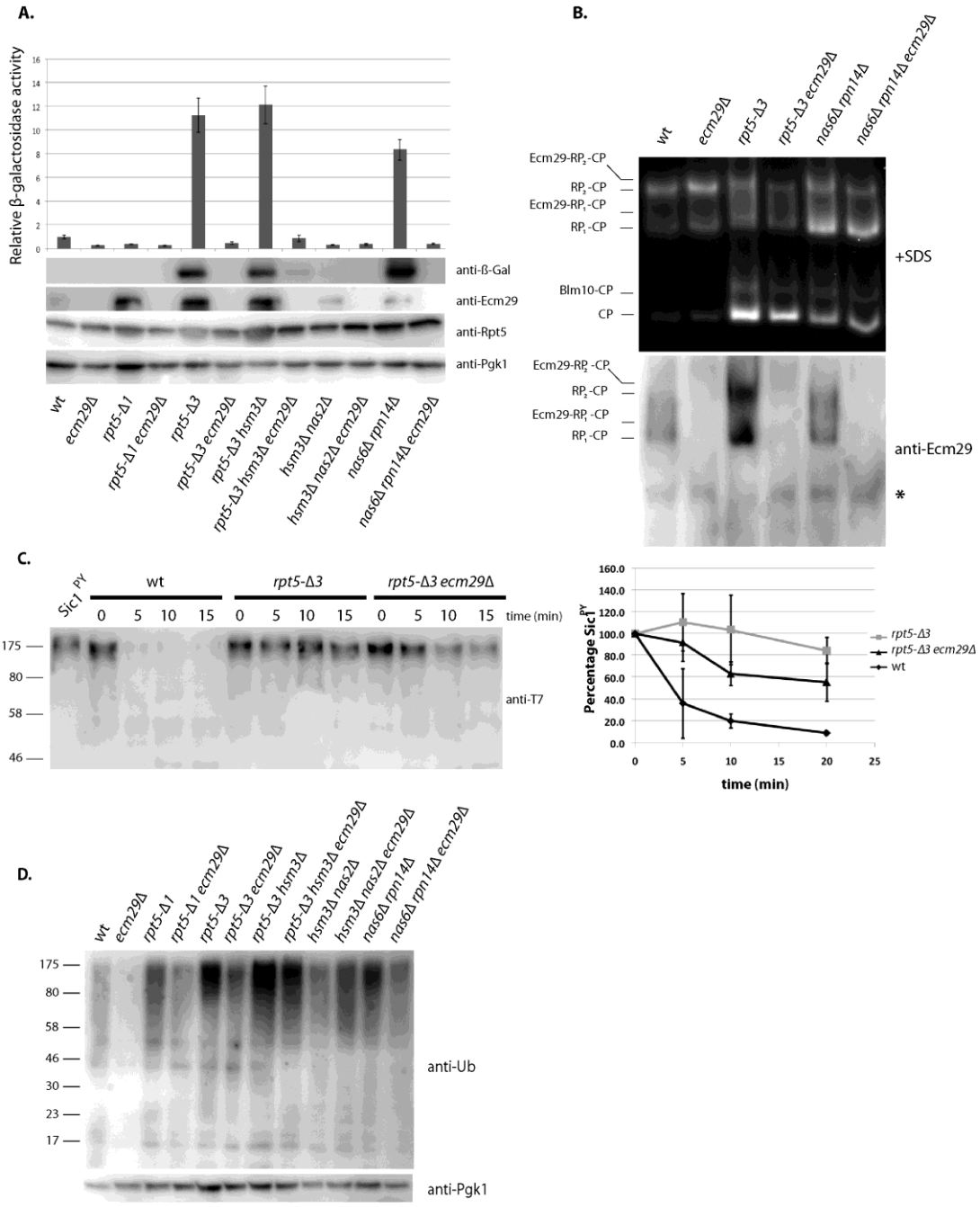

Figure 3.1 Ecm29 inhibits the degradation of ubiquitinated proteins in vivo and in vitro.

(A) Indicated strains were transformed with an unstable form of the enzyme β-galactosidase (Ub-K-βgal). β-galactosidase activity was measured in lysates and activities relative to wild-type were plotted (upper panel). Standard deviations were determined using three independent experiments. Lower panels show levels of β-galactosidase enzyme using immunoblotting (anti-β-Gal), levels of Ecm29 (anti-Ecm29), proteasome levels (anti-Rpt5) and a loading control (anti-Pgk1). (B) Cultures from indicated strains where lysed using a French press. Whole cell lysates

*were subjected to native page electrophoresis in the presence of ATP and stained for Suc-LLVY-AMC hydrolytic activity in the presence of 0.02% SDS. Gels where analyzed by Western blot using an anti-Ecm29 antibody. * Indicates a non-specific background band. (C) Purified proteasomes were incubated with ubiquitinated Sic1^{PY} for the indicated time. Levels of ubiquitinated Sic1^{PY} remaining were determined by immunoblotting using an anti-T7 antibody. Right panel shows quantification of western based on three independent experiments with T=0 normalized as 100% and standard errors shown. (D) Whole cell lysates from wild-type and mutant strains were analyzed by western blot using an anti-ubiquitin antibody.*

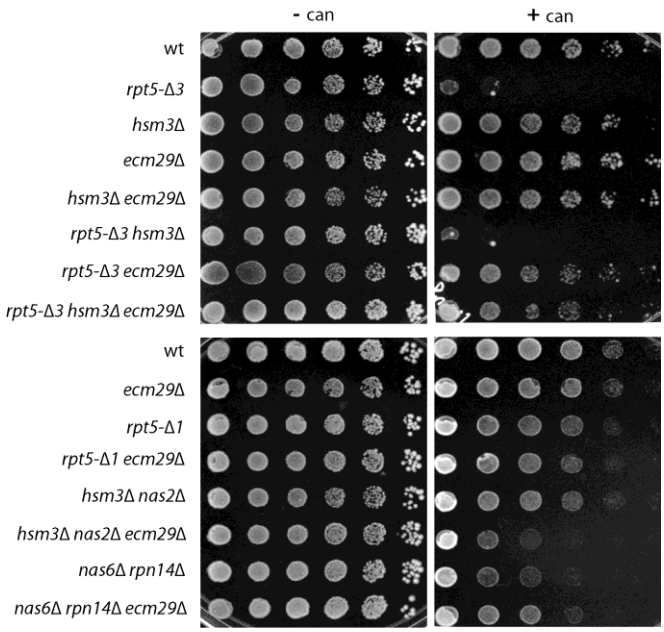

Figure 3.2 Deletion of Ecm29 rescues canavanine sensitivity of proteasome mutants.

Strains with the indicated mutations or genes deleted were spotted in 4-fold dilutions on arginine-lacking SD plates with or without 1.5 μg/ml canavanine and grown at 30 °C for 7 days. Dilution assays were performed in triplicates for two or more independent clones, each showing similar growth patterns.

Ecm29 inhibits degradation of the ubiquitin-independent substrate ODC.

If inhibition of the proteasome is specific for ubiquitinated proteins, as has been reported for Ubp6 (18), Ecm29 could potentially be interfering with the delivery or processing of ubiquitinated substrates, instead of inhibiting proteasomes more directly. Therefore, we tested the ability of the *rpt5*-Δ*3* and *rpt5*-Δ*3 ecm29Δ* strains to degrade an established, short-lived, ubiquitin-independent substrate, ornithine decarboxylase (ODC) (32,36,37). We transformed strains with a plasmid containing a Flag-tagged version of mouse ODC (32) and determined the steady-state level of ODC (Fig. 3.3A and B). As expected, ODC was barely detectable in lysates from wild-type cells. However, it accumulated in *rpt5*-Δ*3* lysates or upon treatment with proteasome inhibitors at concentrations that inhibit proteasome activity in wild-type cells (38) (Fig. 3.3A and B). Deleting *ECM29* in the *rpt5*-Δ*3* background strongly reduced the accumulation of ODC (Fig. 3.3B), albeit not back to wild-type levels. The latter suggests that the *rpt5*-Δ*3* proteasomes have an intrinsic degradation defect. This is consistent with the observations in the *in vitro* degradation assay (Fig. 3.1C) as well as the residual accumulation of ubiquitinated material in total lysate of *rpt5*-Δ*3 ecm29Δ* cells compared to wild-type cells (Fig. 3.1D). Nevertheless, the presence of Ecm29 is a major contributor to the reduced capacity of cells *rpt5*-Δ*3* cells to degrade ODC.

To assess the role of Ecm29 under proteasome stress conditions *in vivo*, we tested canavanine sensitivity for the different strains. Canavanine is an analog of arginine that leads to misfolding of proteins upon incorporation into nascent proteins. To handle the extra protein folding stress, cells show an increased dependence on molecular chaperones and the activity of protein degradation machinery. The mutants that accumulated β-galactosidase (Fig. 3.1A), like the *rpt5*-Δ*3* and the *nas6*Δ *rpn14*Δ strains, also displayed increased sensitivity to canavanine (Fig. 3.2). Deletion of *ECM*29 in these backgrounds reduced the sensitivity to canavanine, consistent with a role for Ecm29 as a proteasome inhibitor in the cell (Fig. 3.2). Note that for certain proteasome-related mutants, like *nas2*Δ *hsm3*Δ (Fig. 3.2) and *blm10*Δ (39), canavanine sensitivity is actually augmented by the deletion of *ECM29*. This pleiotropic effect most likely indicates additional roles performed by Ecm29 in the cell (see discussion). Nevertheless, the rescue of canavanine sensitivity by the deletion of *ECM*29 reiterates the point that, besides the

proteasomal mutations themselves, Ecm29 is a major contributor to degradation defects in certain mutants.

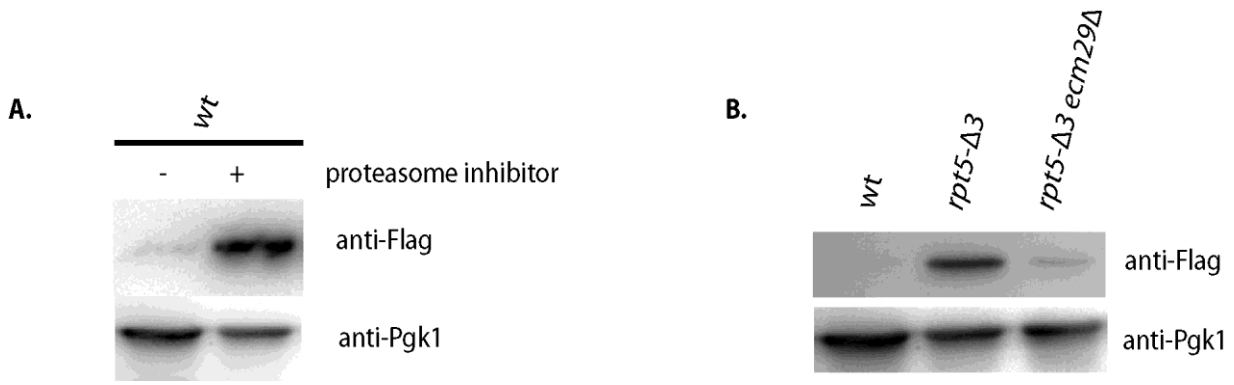

Figure 3.3 Ecm29 inhibits protein degradation of ubiquitin-independent substrates in vivo.

(A) Wild-type cells transformed with a plasmid expressing Flag-tagged mouse ODC were inoculated at OD ~0.5 and grown for 6 hours in the presence or absence of proteasome inhibitor (100 mM PS-341), lysed, and analyzed for the levels of ODC by immunoblotting using anti-Flag. (B) Indicated strains were transformed with a plasmid expressing Flag-tagged mouse ODC, grown overnight, lysed, and steady state levels of ODC were determined by immunoblotting with an anti-Flag antibody.

In vitro inhibition of degradation requires the CP gate.

We have previously reported that *in vitro* the Ecm29-dependent inhibition of suc-LLVY-AMC peptide cleavage was eliminated by the addition of 0.02% SDS (26). For free CP, this level of SDS has been shown to open the CP gate required for substrate entry (40), suggesting that Ecm29 prevents full opening of this gate. To test this directly, we used a mutant with a (partial) open-gate, the *α3ΔN* strain (40). A proteasome purification in the presence of ATP yields 26S proteasomes with and without Ecm29. In yeast only Ecm29-containing proteasomes are stable in the absence of ADP and ATP (17,22,26). Therefore, to obtain only Ecm29-containing 26S proteasomes, we purified proteasomes in the absence of nucleotide (Fig. 3.4A) or treated proteasomes purified in the presence of ATP with apyrase, which hydrolysis ATP and ADP (Fig. 3.4B). All of the resulting 26S proteasomes (Fig. 3.4A and Fig. 3.4B lane 2, 4, 6, and 8) contain Ecm29. As seen before, wild-type Ecm29-containing 26S proteasomes are inhibited, because they do not show activity in the absence of SDS (Fig. 3.4A lane 1 and Fig. 3.4B lane 2).

However, Ecm29-containing 26S proteasomes from the open-gate mutant are active (compare Fig. 3.4A lanes 1 and 2, Fig. 3.4B lanes 2 and 6), indicating that Ecm29-dependent inhibition requires a functional CP gate. Immunoblotting for Ecm29 and CP subunit α7 as well as the hydrolytic assay in the presence of SDS showed that similar levels of 26S proteasome were present in the native gel. In sum, Ecm29 inhibition of suc-LLVY-AMC hydrolysis depends on a functional CP-gate, indicating that binding of Ecm29 to 26S proteasomes reduces the time these proteasomes spend in an open-gate conformation.

To test if Ecm29 *in vivo* mainly acts through regulation of the gate, we compared accumulation of the unstable substrate β-galactosidase (see Fig. 3.1A) in an open-gate mutant strain with or without the *rpt5-Δ3* mutation. To ensure maximal disruption of the gate we used a strain containing deletions of the N-terminus of two alpha subunits, both α3 and α7 (40). The increased accumulation of substrate in the *rpt5-Δ3* background was Ecm29 dependent (Fig. 3.4C). Thus, *in vivo* the inhibition by Ecm29 is not eliminated by disruption of the CP gate, indicating Ecm29 inhibits proteasomes through a gate independent mechanism as well.

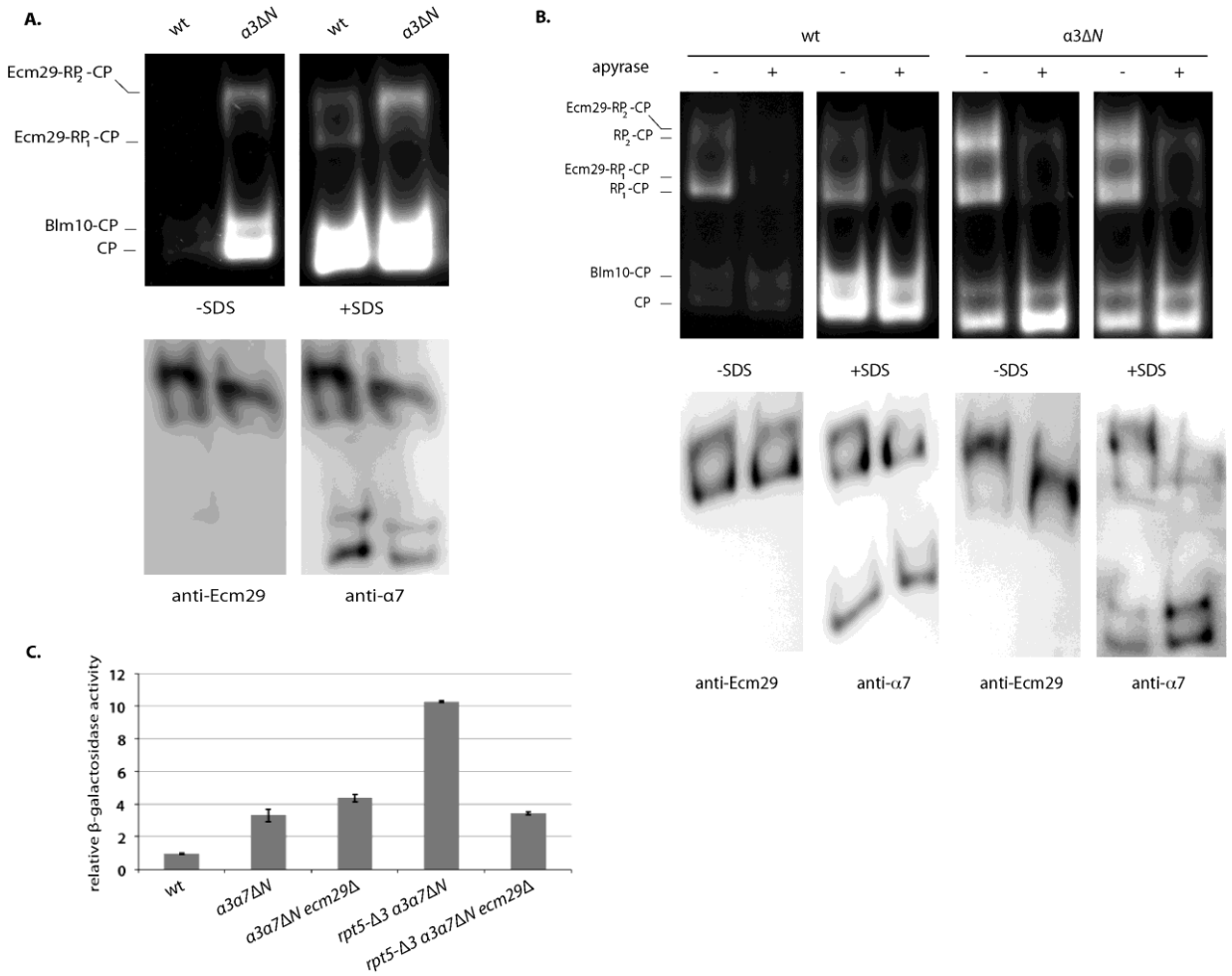

Figure 3.4 The open-gate mutant rescues Ecm29-dependent inhibition of Suc-LLVY-AMC hydrolytic activity in vitro, but not the Ecm29-dependent inhibition of in vivo substrates.

Proteasomes were affinity-purified from strains with tagged CP subunit in the absence of ATP to ensure all 26S proteasomes are associated with Ecm29 (22). The samples were subjected to native gel electrophoresis in the presence of ATP and stained for suc-LLVY-AMC hydrolytic activity in the presence or absence of 0.02% SDS. Ecm29 containing 26S proteasomes from the open-gate mutant (α3ΔN), but not wild-type cells, show suc-LLVY-AMC hydrolytic activity in the absence of SDS. The addition of SDS shows both preps contain 26S proteasomes with Suc- LLVY-AMC hydrolytic capacity. Immunoblotting of the native gels for Ecm29 and the CP subunit α7 show equal amounts of Ecm29 on the proteasome preparations. (B) Proteasomes were affinity-purified from strains with tagged CP subunit in the presence of ATP. To visualize the difference between RP-CP species with or without Ecm29, samples were treated with apyrase to remove all ATP and ADP. In apyrase treated samples all 26S proteasomes are associated with Ecm29 as shown previously (22,26). The samples were subjected to native gel electrophoresis in the presence of ATP and stained for suc-LLVY-AMC hydrolytic activity in the presence or absence of 0.02% SDS. Wild-type and mutant proteasomes show reduced 26S activity upon apyrase treatment, because only a small fraction of proteasomes contain Ecm29. Wild-type Ecm29-containing proteasomes have reduced activity in the absence of SDS (compare top panel lane 2 and 4). The open-gate (α3ΔN) Ecm29-containing proteasomes do not show increased activity upon

addition of SDS (compare lane 6 and 8), indicating that in vitro Ecm29 requires a functional gate for inhibition of suc-LLVY-AMC hydrolysis. Immunoblotting of native gels for Ecm29 and the CP subunit α7 show equal amounts of Ecm29 on the proteasome preparations with or without apyrase treatment. (C) Open-gate mutant (α3ΔN α7ΔN) does not rescue the accumulation of β-galactosidase as a result of the rpt5-Δ3 mutations. Assay identical to Fig. 1A.

Ecm29 reduces proteasomal ATPase activity of rpt5-Δ3.

Unlike peptide substrates, the degradation of folded protein substrates *in vivo* as well as *in vitro* is ATP dependent. Therefore, we tested if Ecm29 affects proteasomal ATPase activity. We purified proteasomes from *rpt5-Δ3* cells using a wash step with 25 mM or 200 mM NaCl (Fig. 3.5A). The high salt wash reduces Ecm29 levels, because the proteasomal association of Ecm29 is salt sensitive (17,23). Consistent with the reported role of Ecm29 as a stabilizer of 26S proteasomes (17,22), proteasomes with reduced levels of Ecm29 showed reduced anmounts of CP subunits (Fig. 3.5A, bands between 17 and 23 kDa). However, the level of proteasomal ATPases was similar (Fig. 3.5A lower panel). Proteasome preparations washed with 200 mM NaCl showed an increased ATPase activity (Fig. 3.5B). This suggests the presence of Ecm29 inhibits the proteasomal ATPase activity. To further test this, we purified proteasomes from *rpt5-Δ3* and *rpt5-Δ3 ecm29Δ* strains under low salt conditions. As expected the deletion of Ecm29 resulted in less CP (Fig. 3.5C, bands between 17 and 23 kDa). SDS-PAGE analysis, immunoblotting, as well as mass spectrometry analysis show, however, similar levels of RP and proteasomal ATPase subunits (Fig. 3.5C and table 3.2). To measure the ATPase activity from these preparations, we again measured ADP production over time (Fig. 3.5D). As shown in Fig. 3.5E, we observed increased ATPase activity in proteasome preparations that lack Ecm29. The mass spectrometry analysis does not show any other ATPases in the sample that could explain the difference in ATPase activity (Table 3.2). Furthermore, the observed ATPase activity shows reversed correlation with the amount of Ecm29 present (Fig. 3.5) and the observed ATPase activities are within the same range as reported by others for proteasomal ATPase activity (41). Therefore, our data strongly suggest that Ecm29 –directly or indirectly– inhibits proteasomal ATPases.

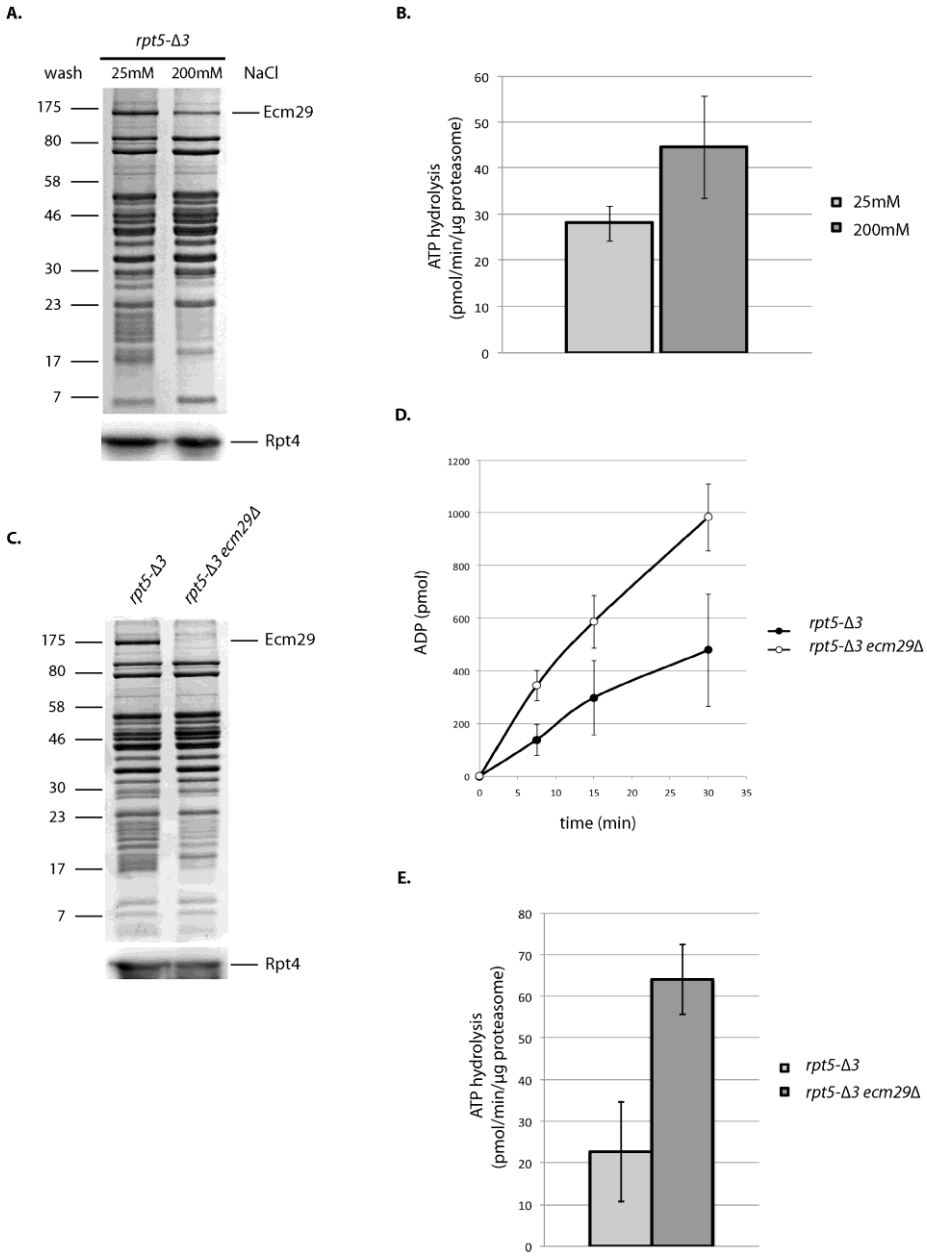

Figure 3.5 Ecm29 inhibits proteasomal ATPase activity from rpt5-Δ3 derived proteasomes.

(A) Coomassie Blue stained SDS-PAGE analysis of proteasome preparations that were purified using affinity-tagged lid subunit Rpn11 and washed with buffer containing different concentrations of NaCl. Lower panel shows levels of the ATPases subunit Rpt4 by immunoblotting (anti-Rpt4). (B) ATPase activity for purifications from (A). The activity was determined by measuring ADP produced over time. Data show average ATPase activity with standard deviation for triplicates of two independent purifications. Activity measurements have been repeated with similar results. Difference in activity was significant with $p < 0.05$ as determined by student t-test. (C) Coomassie Blue stained SDS-PAGE analysis of proteasome

preparations that were purified using affinity-tagged lid subunit Rpn11. Lower panel shows levels of the ATPases subuunit Rpt4 by immunoblotting (anti-Rpt4). (D + E) ATPase activity for purifications from (C). The activity was determined by measuring ADP produced over time. Data show average ATPase activity with standard deviation for triplicates of two independent purifications. Activity measurements have been repeated with similar results and are within the range previously reported for proteasomal ATPases (41). Difference in activity was significant with $p < 0.05$ as determined by student t-test.

Ecm29 inhibits wild-type proteasomes.

As we relied on proteasome mutants for the enrichment of Ecm29 onto proteasomes, the observed effects might be unique for the specific mutant used. The reduced accumulation of ubiquitinated proteins in total lysate of the *ecm29*Δ strain suggests, however, that Ecm29 has the same effect on wild-type cells (Fig. 3.1C). To test this more rigorously, we generated a strain that strongly overexpresses Ecm29 by replacing the endogenous promoter with the GPD promoter (29). This has been shown to cause increased Ecm29 levels onto wild-type proteasomes (23). Next, we affinity-purified proteasomes from an *ecm29*Δ strain, a strain with the endogenous promoter, or a strain overexpressing Ecm29 (Fig. 3.6A). The ATPase activity measured in these purifications again showed a reversed correlation with Ecm29 levels present; the *ecm29*Δ–derived proteasomes showed increased ATPase activity and the purifications with increased levels of Ecm29 showed reduced ATPase activity (Fig. 3.6B). Thus, association of Ecm29 with proteasomes results in reduced ATPase activity independent of the presence of proteasome mutations. To test if the increased presence of Ecm29 on wild-type proteasomes also results in degradation defects we measured, as we did for *rpt5-Δ3* derived proteasomes (Fig. 3.1C), the ability of wild-type proteasomes enriched in Ecm29 to degrade ubiquitinated $Sic1^{PY}$. Consistent with a function as inhibitor of the proteasome, we observed slower degradation of $Sic1^{PY}$ in the presence of Ecm29 (Fig. 3.6C). The overexpression of Ecm29 also caused modest canavanine sensitivity (Fig. 3.6D). These data further confirm that the presence of Ecm29 on proteasomes results in reduced ATPase activity and interferes with the ability of proteasomes to degrade substrates.

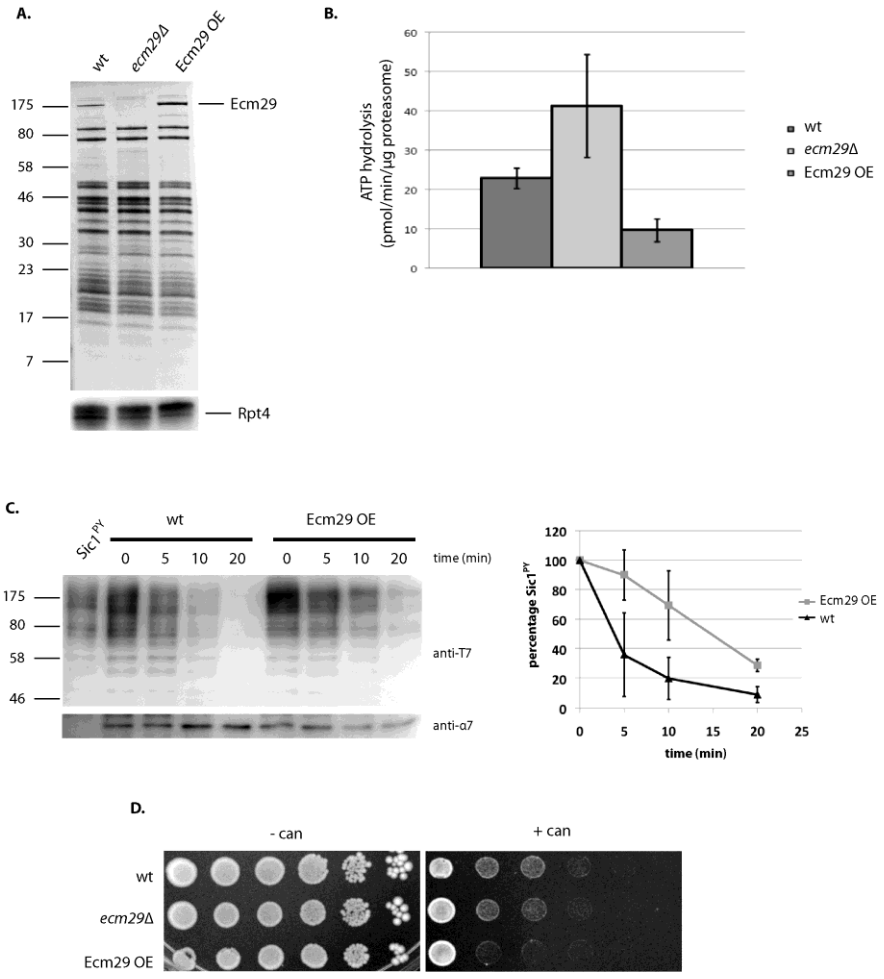

Figure 3.6 Ecm29 inhibits wild-type proteasomes.

(A) Coomassie Blue stained SDS-PAGE analysis of proteasome preparations from indicated strains that were purified using affinity-tagged lid subunit Rpn11. Lower panel shows levels of the ATPases subunit Rpt4 by immunoblotting (anti-Rpt4). (B) ATPase activity for purifications from (A). The activity was determined by measuring ADP produced over time. Data show average ATPase activity with standard deviation for triplicates of two independent purifications. Activity measurements have been repeated with similar results and are within the range previously reported for proteasomal ATPases. Difference in activity between samples was significant with $p < 0.05$ as determined by student t-test. (C) Purified proteasomes from indicated strains were incubated with ubiquitinated $Sic1^{PY}$ for the indicated time. Levels of ubiquitinated $Sic1^{PY}$ were determined by immunoblotting using an anti-T7 antibody. Right panel shows quantification of western based on three independent experiments with T=0 normalized as 100% and standard errors shown. (D) Over-expression of Ecm29 results in modest canavanine phenotype. Strains with ECM29 deletion or Ecm29 over-expression were spotted on SD plates lacking arginine with or without 1.5 µg/ml canavanine in 4-fold dilutions and grown for 7 days at 30 °C (SD plates).

Ecm29 binds close to the regulatory particle subunit Rpt5.

Ecm29 has been proposed to bind to CP as well as RP, however, no detailed binding information is available for Ecm29 (17). To identify a proteasomal binding site for Ecm29 we generated a strain that contains an N-terminally His-tagged Ecm29 in a background containing the Rpn11-tev-ProA with or without the *rpt5*-Δ*3* mutation. Proteasomes purified from both strains using the Rpn11-ProA tag show a similar subunit composition and the presence of Ecm29 (Fig. 3.7A). To identify a direct binding partner, or proteasome subunit in close proximity of Ecm29, we treated the purified proteasomes with crosslinker (DST, 6.4Å spacer arm length). Samples with or without crosslinking were denatured in 8 M urea and His-Ecm29 was purified under denaturing conditions. Samples were resolved on SDS-PAGE and stained with Coomassie (Fig. 3.7B). Lanes 3 and 5 specifically show slower migrating bands, likely indicating Ecm29 crosslinked to a proteasome subunit. Mass spectrometry analysis of gel region with crosslinked material revealed the presence of Ecm29 and Rpt5 in lanes 2 and 4, but not lanes 1, 3, or a control sample that was crosslinked but lacked His-tagged Ecm29. Western blot analysis of the different steps in the procedure confirmed Rpt5 crosslinking to Ecm29 (Fig. 3.7C). Considering the moderate levels of crosslinking (Fig. 3.7B and 3.7C), the crosslinking between Rpt5 and Ecm29 is likely direct. This is also consistent with previous work detecting more Ecm29 in proteasomes purified using tagged-Rpt5 (42). In sum, our data show that Ecm29 either binds Rpt5 directly or binds in close proximity to Rpt5.

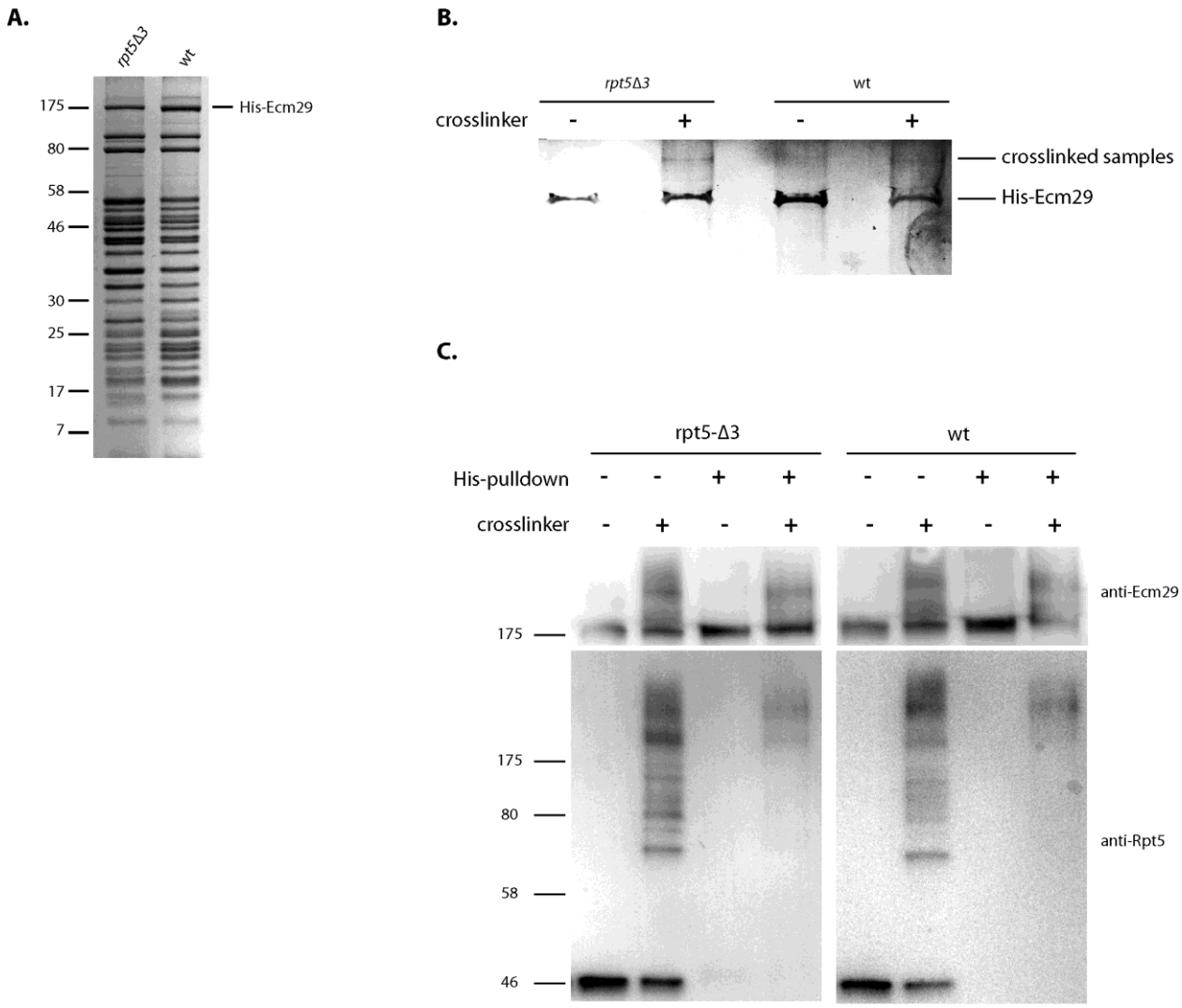

Figure 3.7 Ecm29 binds close to the AAA-ATPase subunit Rpt5.

(A) Coomassie Blue stained SDS-PAGE analysis of proteasome preparations from indicated strains that were purified using affinity-tagged lid subunit Rpn11. (B) Samples from (A) were treated with the crosslinker DST or DMSO, denatured in 8 M urea and His-Ecm29 was purified using Talon resin. Sample was resolved on gel and stained with Coomassie Blue. (C) Immunoblots are shown for Rpt5 and Ecm29 in the different steps of the crosslinking procedure. Lane 3 and 8 show Rpt5, as would be expected, crosslinked to several different proteasome subunit. Crosslinking was not excessive as ~50% of the Rpt5 was not crosslinked, hence amounts of indirect crosslinking should be low. The purification under denaturing conditions in lanes 5 and 10 show the specific crosslinking to Ecm29.

Table 3.2 Peptide numbers of proteins identified by Mass Spectrometry

			rpt5-Δ3	*rpt5-Δ3 ecm29Δ*
Ecm29	ECM29_YEAST	211610	89	0
alpha1	SCL1_YEAST	25759	23	11
alpha2	PRE8_YEAST	27145	12	5
alpha3	PRE9_YEAST	31688	10	4
alpha4	PRE6_YEAST	28697	15	
alpha5	PUP2_YEAST	28770	21	5
alpha6	PRE5_YEAST	28154		
alpha7	PRE10_YEAST	28650	10	
beta1	PRE3_YEAST	26968	17	3
beta2	PUP1_YEAST	22560	6	
beta3	PUP3_YEAST	22819	6	
beta4	PRE1_YEAST	29425	20	6
beta5	PRE2_YEAST	31902	11	6
beta6	PRE7_YEAST	23761	15	3
beta7	PRE4_YEAST	28650	4	4
Rpt1	CIM5_YEAST	52293	27	24
Rpt2	YTA5_YEAST	49026	17	12
Rpt3	YTA2_YEAST	47864	22	17
Rpt4	SUG2_YEAST	49492	15	13
Rpt5	YTA1_YEAST	48283	26	22
Rpt6	SUG1_YEAST	45471	20	14
Rpn1	RPN1_YEAST	109880	52	51
Rpn2	RPN2_YEAST	104623	58	55
Rpn3	RPN3_YEAST	60754	29	24
Rpn5	RPN5_YEAST	51850	29	16
Rpn6	RPN6_YEAST	50085	31	26
Rpn7	RPN7_YEAST	49213	29	16
Rpn8	RPN8_YEAST	38460	25	20
Rpn9	RPN9_YEAST	45811	31	27
Rpn10	RPN10_YEAST	29786	13	7
Rpn11	RPN11_YEAST	34433	19	11
Rpn12	RPN12_YEAST	31956	26	15
Rpn13	RPN13_YEAST	18005	6	7
Nas6	NAS6_YEAST	25616	12	10
Ubp6	UBP6_YEAST	57110	40	27

Hul5	HUL5_YEAST	105564	16	8
Ssa2	SSA2_YEAST	69469	4	5
Hsp70		63400	2	0

Ecm29 recruitment to the proteasome.

The enrichment of Ecm29 on mutant proteasomes can in part be explained by increased expression of Ecm29 under proteasome stress conditions (23). However, this cannot explain why we consistently observed an increased presence of Ecm29 on proteasomes purified in the absence of nucleotide as compared to proteasomes purified with ATP present (Fig. 3.8A; apyrase was used to remove endogenous ATP and ADP from lysates). This difference cannot be explained by ATP-dependent degradation of Ecm29 during the purification, because this accumulation was not observed in the presence of ADP or in the presence of proteasome inhibitors (Fig. 3.8A). Thus, Ecm29 appears to be specifically recruited to proteasomes with most or all ATPase subunits in a nucleotide-empty state.

To test if Ecm29 enrichment on proteasomes in specific strains, like the *rpt5*-Δ*3*, can be explained in part by a preferential binding of Ecm29 to such proteasomes, we tried to purify Ecm29 from bacteria. However, bacterial-expressed full-length Ecm29 was unstable and not competent in binding to proteasomes; therefore, we used a lysate of wild-type yeast cells as our source of Ecm29. To test if this Ecm29 has a preference for binding to certain proteasomes, we looked at the recruitment to affinity-tagged proteasomes from wild-type or *rpt5*-Δ*3* strains deleted for *ECM29* (Fig. 3.8B). We observed that more Ecm29 associated with *rpt5*-Δ*3*-derived proteasomes as compared to the wild-type (Fig. 3.8C). Treatment with apyrase enhanced the amount of Ecm29 bound to wild-type as well as *rpt5*-Δ*3*-derived proteasomes, but retained Ecm29's preference for mutant proteasomes (Fig. 3.8C). Strong overexpression of Ecm29 can also yield increased Ecm29 levels on wild-type proteasomes ((23) and Fig. 3.6), suggesting that the subtle difference in affinity regulates Ecm29 abundance on proteasomes. Consistent with this, more modest overexpression of Ecm29, like we observed in our control or Rpt5 truncated strains (Fig. 3.8D) only shows a modest increase of proteasome-associated Ecm29 in the control strain, while there is a strong increase for the Rpt5 truncation strains (Fig. 3.8E). In all, these experiments show that Ecm29 preferentially binds to nucleotide-depleted proteasomes as well as *rpt5*-Δ*3*-derived proteasomes.

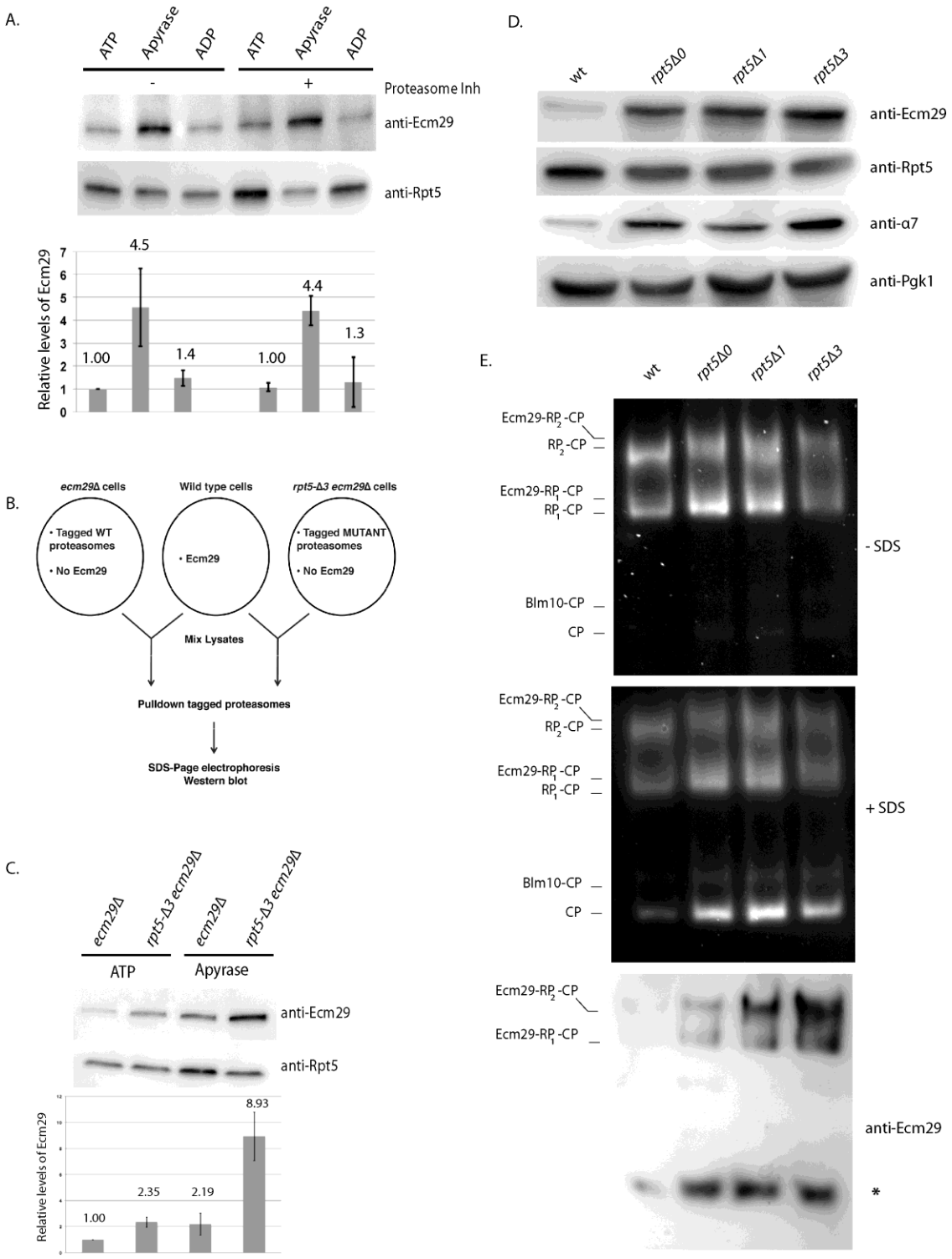

Figure 3.8 Ecm29 recognizes aberrant proteasomes.

(A) Proteasomes from wild-type cells were purified in the presence of ATP, ADP, or in the absence of these nucleotides (apyrase was used to convert endogenous ATP and ADP to AMP) using an affinity tag on the lid subunit Rpn11. Levels of co-purified Ecm29 were determined by

*immunoblotting for Ecm29 (anti-Ecm29). Proteasome levels were determined using an antibody against the proteasome subunit Rpt5. To show that the enrichment in the absence of nucleotide was not due to proteasomal degradation, the same experiment was performed in the presence of proteasome inhibitors (100 μM tosyl-lysylchloromethane and 100 nM epoxomicin). Table shows relative Ecm29 levels, corrected for input and normalized to lane 1. (B) Schematic of experiment in panel C. Wild-type lysates (middle) provide a source of Ecm29 and are mixed with lysates from ecm29Δ cells containing Rpn11-ProA tagged proteasomes (left) or ecm29Δ rpt5-Δ3 cells containing Rpn11-ProA tagged proteasomes (right). After incubation, proteasomes are affinity purified using IgG resin, separated on SDS-PAGE, and analyzed. (C) Experimental scheme, as described in B, was performed in the presence of ATP or in the absence of nucleotide (apyrase). Samples were analyzed for the levels of recruited Ecm29 and Rpt5 was used as a loading control. Results show enriched binding of Ecm29 in the absence of nucleotide as well as to the rpt5-Δ3 proteasomes. Table shows relative Ecm29 levels, corrected for input and normalized to lane 1. (D+E) Levels of proteasome associated Ecm29 and total cellular levels. Cultures from wild-type and mutant strains where lysed using a French press. (D) Whole cell lysates were subjected to SDS-PAGE followed by immunoblotting for the indicated proteins. (E) Whole cell lysates were subjected to native page electrophoresis in the presence of ATP and stained for Suc-LLVY-AMC hydrolytic activity in the presence or absence of 0.02% SDS. Next, Gels were analyzed by Western blot using an anti-Ecm29 antibody. * indicates a non-specific background band, as it is also observed in the ecm29Δ background.*

Discussion

Since its discovery as proteasome-associated protein over ten years ago, many functions have been proposed for Ecm29. This probably indicates that Ecm29 has multiple functions inside the cell. Consistent with this, the deletion of *ECM29* in the different mutant strains shows pleiotropic effects. As mentioned in the results, canavanine sensitivity can either be augmented or rescued when *ECM29* is deleted. For temperature stress, the deletion of *ECM29* has been observed to increase (e.g. *ump1*Δ strain (27)) as well as rescue (e.g. the *rpt6*-Δ*1* or the *nas2*Δ *hsm3*Δ strains (23,26)) temperature sensitivity. Interestingly, for the *nas2*Δ *hsm3*Δ strain deletion of Ecm29 shows a very robust rescue of the temperature sensitivity (26), while at the same time it shows a modest increase in canavanine sensitivity (Fig. 3.3). Clearly, different phenotypes in specific mutants each highlight a different cellular function of Ecm29.

In this study we utilized a proteasome hypomorph, the *rpt5*-Δ*3* strain, to study the function of Ecm29 in cells, because Ecm29 is highly enriched on 26S proteasomes in this strain (26). Surprisingly, our data show that the proteasomal degradation defect in this proteasome hypomorph is only partly due to the mutation of the proteasome subunit Rpt5. The increased presence of Ecm29 on proteasomes in this strain is a major contributor to this strain's inability to degrade proteasome substrates. Several other proteasome mutants also show an increase in Ecm29-bound proteasomes (23,27). As the mutations to proteasome subunits likely cause the formation of aberrant proteasomes, Ecm29 might have a more common role as inhibitor of proteasome activity for certain aberrant forms of the proteasome.

Proteasomal recruitment of Ecm29.

How would Ecm29 be able to be enriched on a variety of proteasome mutants, while in wild-type cells only a subset of proteasomes are associated with Ecm29 (22,23,26-28). One proposed model suggests that Ecm29 is degraded by the proteasome (27). If proteasome mutants have reduced proteolytic activity Ecm29 would then accumulate. This model is supported by the observation that affinity-tagged Ecm29 is unstable (27,28). However, untagged Ecm29 has been reported to be stable (23), suggesting an alternative mechanism for Ecm29 enrichment on proteasomes. A second model proposes that an increase in the ratio Ecm29 versus proteasomes in specific proteasome mutants is a determining factor in proteasomal association of Ecm29 (23).

Consistent with this, the overexpression of *ECM29* from a very strong promoter increases the association of Ecm29 to wild-type proteasomes (Fig. 3.6 and (23)). However, this model provides little dynamic control if Ecm29 is a stable protein and seems counterintuitive considering the inhibitory function described here. Furthermore, such a model cannot explain the preferential binding we observe (Fig. 3.8C), or the increase in Ecm29 recruitment upon oxidative stress (24). We propose that an important component of the recruitment of Ecm29 to proteasomes relies on the ability of Ecm29 to recognize –directly or indirectly– certain aberrant conformations of the proteasome.

Mutants in RP as well as CP have been shown to cause increased Ecm29 association. It seems unlikely that Ecm29 would be able to recognize differences in the conformation induced by proteasome mutants located at distant or opposite sites of the proteasome. We speculate that Ecm29 does not recognize each mutant specifically, but all these mutants cause a similar unfavorable alignment between CP and RP that results in increased affinity for Ecm29 to proteasomes. For certain mutants, like *rpt5*-Δ*3* or *rpt6*-Δ*1,* it is clear that they affect the CP-RP interface, since the C-terminal residues deleted in these mutants dock into pockets located on the alpha ring surface of the CP and contribute the to RP-CP interaction (13,34,35,43-47). Ecm29 also has been reported to recognize RP-CP species in which CP maturation is stalled (27). Ecm29 might recognize those by a different mechanism, because, at first glance, it appears unlikely that stalled CP maturation affects the RP-CP interface. However, the proteolytic active sites of the CP have been shown to allosterically affect the RP-CP interface (22,48). This suggests that certain CP mutations or the level of CP maturation could affect the conformation of the RP-CP interface.

The model that Ecm29 recognizes differences at the CP-RP interface is also supported by the observed increase in binding of Ecm29 to nucleotide-depleted proteasomes (Fig. 3.8). Under normal conditions, only two of the proteasomal AAA-ATPase subunits have been suggested to be free of nucleotides (49). The lack of more nucleotides probably causes a different conformation of the ATPase ring that abuts the CP, since the lack of nucleotide is known to destabilize the RP-CP interaction (22). The increased association of Ecm29 to nucleotide-depleted proteasomes, suggests Ecm29 recognizes such proteasomes prior to the RP-CP

dissociation. Another protein showing nucleotide dependent binding is AIRAP. This protein is not present in yeast, but *C. elegans* AIRAP has been shown to preferably bind and stabilize nucleotide depleted proteasomes (50). However, unlike Ecm29, AIRAP seems to increase suc-LLVY-AMC hydrolytic activity of the proteasomes with which it associates (50).

Our crosslinking of Ecm29 to Rpt5 is consistent with the model we propose as well as with recent cryo-EM structures of the proteasome. The latter show that Rpt5 is accessible for binding (51-54). Considering the large size of Ecm29 (210 kDa) and the unique binding properties (only binds to 26S proteasomes) we expect Ecm29 will interact with additional proteasome subunits. Identifying the other proteasomal binding sites of Ecm29 will further establish how the specificity of binding by Ecm29 is achieved.

The recruitment of Ecm29 to certain aberrant proteasomes fits well with previous reports proposing a function as a quality control protein (26,27). A tantalizing model is that the inhibition of the proteasome is an important component of Ecm29's quality control function, as it prevents proteolysis by aberrant proteasomes from occurring inside the cell. Next, such proteasomes would have to be either corrected or targeted for degradation, e.g. by the lysosome. The former has been suggested (27), while the latter might provide a connection to other proposed functions of Ecm29 by linking it to endosomes and transport motors (21,25). Clearly, a better understanding of the fate of Ecm29-bound proteasomes will be crucial to understand the role of Ecm29 in proteasome assembly, quality control and regulation.

Mechanism of inhibition by Ecm29.

Since recent EM structures of the proteasome (51-54) indicate that access to the CP gate is shielded by the Rpt subunits, it seems unlikely that Ecm29 can directly inhibit CP gate opening. Our data show that Ecm29 binds to the proteasome in close proximity to Rpt5. Thus, Ecm29 might restrict the conformational freedom of one or several of the proteasomal Rpt proteins thereby causing reduced ATPase activity. The binding to Rpt5 might also cause closing of the CP-gate, since the Rpt proteins abut the CP and are known to regulate gate opening (34,35,43,44). Furthermore, mutations disrupting ATP binding or hydrolysis in yeast and mammalian proteasomal ATPases have been shown to affect gating and protein degradation (55-

57). Alternatively, binding of Ecm29 to the CP directly might induce an allosteric closing of the gate. In this scenario, the inhibition of ATPase activity and gate closing are two independent events induced by Ecm29 binding to RP and CP respectively.

Understanding the mechanism of Ecm29-proteasome interactions might provide us with new targets in the search for alternative proteasome inhibitors and shows, as had previously been shown with USP14, that targeting the RP has the potential for the development of pharmaceuticals (19,58). More intriguingly, the realization that Ecm29 is an *in vivo* inhibitor of proteasome activity might provide new clues towards reduced proteasome activity observed in certain neurodegenerative diseases and during ageing (59). It will be interesting to see if there is increased binding of KIAA00368/ECM29 to proteasomes in such conditions.

A.D.L.M., S.Y.L, and J.R. conceived the experiments, S.Y.L performed experiments in figure 8. A.D.L.M conducted all other experiments with assistance or materials provided by B.P (Fig. 1, 6 and 7), P.W. (Fig. 4) and C.R.S (Fig. 1C and 7). A.D.L.M. , S.Y.L. and J.R. analyzed and interpreted the data. A.D.L.M. and J.R. wrote the manuscript with input from all coauthors.

References

1. Finley, D. (2009) Recognition and processing of ubiquitin-protein conjugates by the proteasome. *Annu Rev Biochem* **78**, 477-513
2. Schrader, E. K., Harstad, K. G., and Matouschek, A. (2009) Targeting proteins for degradation. *Nat Chem Biol* **5**, 815-822
3. Tomko Jr, R. J., and Hochstrasser, M. (2013) Molecular Architecture and Assembly of the Eukaryotic Proteasome. *Annu Rev Biochem* **82**, 415-445
4. Liu, C. W., and Jacobson, A. D. (2013) Functions of the 19S complex in proteasomal degradation. *Trends Biochem Sci* **38**, 103-110
5. Orlowski, R. Z., and Kuhn, D. J. (2008) Proteasome Inhibitors in Cancer Therapy: Lessons from the First Decade. *Clinical Cancer Research* **14**, 1649-1657
6. McCutchen-Maloney, S. L. (2000) cDNA Cloning, Expression, and Functional Characterization of PI31, a Proline-rich Inhibitor of the Proteasome. *J Biol Chem* **275**, 18557-18565
7. Park, Y., Hwang, Y. P., Lee, J. S., Seo, S. H., Yoon, S. K., and Yoon, J. B. (2005) Proteasomal ATPase-associated factor 1 negatively regulates proteasome activity by interacting with proteasomal ATPases. *Mol Cell Biol* **25**, 3842-3853
8. Shim, S. M., Lee, W. J., Kim, Y., Chang, J. W., Song, S., and Jung, Y. K. (2012) Role of S5b/PSMD5 in Proteasome Inhibition Caused by TNF-alpha/NFkappaB in Higher Eukaryotes. *Cell Rep* **2**, 603-615
9. Cho-Park, P. F., and Steller, H. (2013) Proteasome Regulation by ADP-Ribosylation. *Cell* **153**, 614-627
10. Park, S., Roelofs, J., Kim, W., Robert, J., Schmidt, M., Gygi, S. P., and Finley, D. (2009) Hexameric assembly of the proteasomal ATPases is templated through their C termini. *Nature* **459**, 866-870
11. Roelofs, J., Park, S., Haas, W., Tian, G., McAllister, F. E., Huo, Y., Lee, B. H., Zhang, F., Shi, Y., Gygi, S. P., and Finley, D. (2009) Chaperone-mediated pathway of proteasome regulatory particle assembly. *Nature* **459**, 861-865
12. Barrault, M. B., Richet, N., Godard, C., Murciano, B., Le Tallec, B., Rousseau, E., Legrand, P., Charbonnier, J. B., Le Du, M. H., Guerois, R., Ochsenbein, F., and Peyroche, A. (2012) Dual functions of the Hsm3 protein in chaperoning and scaffolding regulatory particle subunits during the proteasome assembly. *Proc Natl Acad Sci U S A* **109**, E1001-1010
13. Park, S., Li, X., Kim, H. M., Singh, C. R., Tian, G., Hoyt, M. A., Lovell, S., Battaile, K. P., Zolkiewski, M., Coffino, P., Roelofs, J., Cheng, Y., and Finley, D. (2013) Reconfiguration of the proteasome during chaperone-mediated assembly. *Nature* **497**, 512-516
14. Bedford, L., Paine, S., Sheppard, P. W., Mayer, R. J., and Roelofs, J. (2010) Assembly, structure, and function of the 26S proteasome. *Trends Cell Biol* **20**, 391-401

15. Guo, X., Engel, J. L., Xiao, J., Tagliabracci, V. S., Wang, X., Huang, L., and Dixon, J. E. (2011) UBLCP1 is a 26S proteasome phosphatase that regulates nuclear proteasome activity. *Proc Natl Acad Sci U S A* **108**, 18649-18654

16. Um, J. W., Im, E., Park, J., Oh, Y., Min, B., Lee, H. J., Yoon, J. B., and Chung, K. C. (2010) ASK1 Negatively Regulates the 26 S Proteasome. *Journal of Biological Chemistry* **285**, 36434-36446

17. Leggett, D. S., Hanna, J., Borodovsky, A., Crosas, B., Schmidt, M., Baker, R. T., Walz, T., Ploegh, H., and Finley, D. (2002) Multiple associated proteins regulate proteasome structure and function. *Mol Cell* **10**, 495-507

18. Hanna, J., Hathaway, N. A., Tone, Y., Crosas, B., Elsasser, S., Kirkpatrick, Donald S., Leggett, D. S., Gygi, S. P., King, R. W., and Finley, D. (2006) Deubiquitinating Enzyme Ubp6 Functions Noncatalytically to Delay Proteasomal Degradation. *Cell* **127**, 99-111

19. Lee, B.-H., Lee, M. J., Park, S., Oh, D.-C., Elsasser, S., Chen, P.-C., Gartner, C., Dimova, N., Hanna, J., Gygi, S. P., Wilson, S. M., King, R. W., and Finley, D. (2010) Enhancement of proteasome activity by a small-molecule inhibitor of USP14. *Nature* **467**, 179-184

20. Peth, A., Besche, H. C., and Goldberg, A. L. (2009) Ubiquitinated proteins activate the proteasome by binding to Usp14/Ubp6, which causes 20S gate opening. *Mol Cell* **36**, 794-804

21. Gorbea, C., Goellner, G. M., Teter, K., Holmes, R. K., and Rechsteiner, M. (2004) Characterization of mammalian Ecm29, a 26 S proteasome-associated protein that localizes to the nucleus and membrane vesicles. *J Biol Chem* **279**, 54849-54861

22. Kleijnen, M. F., Roelofs, J., Park, S., Hathaway, N. A., Glickman, M., King, R. W., and Finley, D. (2007) Stability of the proteasome can be regulated allosterically through engagement of its proteolytic active sites. *Nat Struct Mol Biol* **14**, 1180-1188

23. Park, S., Kim, W., Tian, G., Gygi, S. P., and Finley, D. (2011) Structural defects in the regulatory particle-core particle interface of the proteasome induce a novel proteasome stress response. *J Biol Chem* **286**, 36652-36666

24. Wang, X., Yen, J., Kaiser, P., and Huang, L. (2010) Regulation of the 26S Proteasome Complex During Oxidative Stress. *Sci Signal* **3**, ra88

25. Gorbea, C., Pratt, G., Ustrell, V., Bell, R., Sahasrabudhe, S., Hughes, R. E., and Rechsteiner, M. (2010) A protein interaction network for Ecm29 links the 26 S proteasome to molecular motors and endosomal components. *J Biol Chem* **285**, 31616-31633

26. Lee, S. Y., De la Mota-Peynado, A., and Roelofs, J. (2011) Loss of Rpt5 protein interactions with the core particle and Nas2 protein causes the formation of faulty proteasomes that are inhibited by Ecm29 protein. *J Biol Chem* **286**, 36641-36651

27. Lehmann, A., Niewienda, A., Jechow, K., Janek, K., and Enenkel, C. (2010) Ecm29 Fulfils Quality Control Functions in Proteasome Assembly. *Molecular Cell* **38**, 879-888

28. Panasenko, O. O., and Collart, M. A. (2011) Not4 E3 ligase contributes to proteasome assembly and functional integrity in part through Ecm29. *Molecular and Cellular Biology* **31**, 1610-1623

29. Janke, C., Magiera, M. M., Rathfelder, N., Taxis, C., Reber, S., Maekawa, H., Moreno-Borchart, A., Doenges, G., Schwob, E., Schiebel, E., and Knop, M. (2004) A versatile toolbox for PCR-based tagging of yeast genes: new fluorescent proteins, more markers and promoter substitution cassettes. *Yeast* **21**, 947-962

30. Elsasser, S., Schmidt, M., and Finley, D. (2005) Characterization of the Proteasome Using Native Gel Electrophoresis. *Methods in Enzymology* **398**, 353-363

31. Saeki, Y., Isono, E., and Toh, E. A. (2005) Preparation of ubiquitinated substrates by the PY motif-insertion method for monitoring 26S proteasome activity. *Methods Enzymol* **399**, 215-227

32. Erales, J., Hoyt, M. A., Troll, F., and Coffino, P. (2012) Functional asymmetries of proteasome translocase pore. *J Biol Chem* **287**, 18535-18543

33. Bachmair, A., Finley, D., and Varshavsky, A. (1986) In vivo half-life of a protein is a function of its amino-terminal residue. *Science* **234**, 179-186

34. Gillette, T. G., Kumar, B., Thompson, D., Slaughter, C. A., and DeMartino, G. N. (2008) Differential roles of the COOH termini of AAA subunits of PA700 (19 S regulator) in asymmetric assembly and activation of the 26 S proteasome. *J Biol Chem* **283**, 31813-31822

35. Smith, D. M., Chang, S.-C., Park, S., Finley, D., Cheng, Y., and Goldberg, A. L. (2007) Docking of the Proteasomal ATPases' Carboxyl Termini in the 20S Proteasome's α Ring Opens the Gate for Substrate Entry. *Molecular Cell* **27**, 731-744

36. Gandre, S., and Kahana, C. (2002) Degradation of ornithine decarboxylase in Saccharomyces cerevisiae is ubiquitin independent. *Biochem Biophys Res Commun* **293**, 139-144

37. Murakami, Y., Matsufuji, S., Kameji, T., Hayashi, S., Igarashi, K., Tamura, T., Tanaka, K., and Ichihara, A. (1992) Ornithine decarboxylase is degraded by the 26S proteasome without ubiquitination. *Nature* **360**, 597-599

38. Fleming, J. A., Lightcap, E. S., Sadis, S., Thoroddsen, V., Bulawa, C. E., and Blackman, R. K. (2002) Complementary whole-genome technologies reveal the cellular response to proteasome inhibition by PS-341. *Proc Natl Acad Sci U S A* **99**, 1461-1466

39. Schmidt, M., Haas, W., Crosas, B., Santamaria, P. G., Gygi, S. P., Walz, T., and Finley, D. (2005) The HEAT repeat protein Blm10 regulates the yeast proteasome by capping the core particle. *Nat Struct Mol Biol* **12**, 294-303

40. Groll, M., Bajorek, M., Kohler, A., Moroder, L., Rubin, D. M., Huber, R., Glickman, M. H., and Finley, D. (2000) A gated channel into the proteasome core particle. *Nat Struct Biol* **7**, 1062-1067

41. Henderson, A., Erales, J., Hoyt, M. A., and Coffino, P. (2011) Dependence of proteasome processing rate on substrate unfolding. *J Biol Chem* **286**, 17495-17502

42. Guerrero, C., Tagwerker, C., Kaiser, P., and Huang, L. (2006) An integrated mass spectrometry-based proteomic approach: quantitative analysis of tandem affinity-purified in vivo cross-linked protein complexes (QTAX) to decipher the 26 S proteasome-interacting network. *Mol Cell Proteomics* **5**, 366-378

43. Stadtmueller, B. M., Ferrell, K., Whitby, F. G., Heroux, A., Robinson, H., Myszka, D. G., and Hill, C. P. (2010) Structural models for interactions between the 20S proteasome and its PAN/19S activators. *J Biol Chem* **285**, 13-17

44. Rabl, J., Smith, D. M., Yu, Y., Chang, S.-C., Goldberg, A. L., and Cheng, Y. (2008) Mechanism of Gate Opening in the 20S Proteasome by the Proteasomal ATPases. *Molecular Cell* **30**, 360-368

45. Lander, G. C., Martin, A., and Nogales, E. (2013) The proteasome under the microscope: the regulatory particle in focus. *Curr Opin Struct Biol* **23**, 243-251

46. Matyskiela, M. E., Lander, G. C., and Martin, A. (2013) Conformational switching of the 26S proteasome enables substrate degradation. *Nat Struct Mol Biol* **20**, 781-788

47. Tian, G., Park, S., Lee, M. J., Huck, B., McAllister, F., Hill, C. P., Gygi, S. P., and Finley, D. (2011) An asymmetric interface between the regulatory and core particles of the proteasome. *Nat Struct Mol Biol* **18**, 1259-1267

48. Osmulski, P. A., Hochstrasser, M., and Gaczynska, M. (2009) A Tetrahedral Transition State at the Active Sites of the 20S Proteasome Is Coupled to Opening of the α-Ring Channel. *Structure* **17**, 1137-1147

49. Smith, D. M., Fraga, H., Reis, C., Kafri, G., and Goldberg, A. L. (2011) ATP binds to proteasomal ATPases in pairs with distinct functional effects, implying an ordered reaction cycle. *Cell* **144**, 526-538

50. Stanhill, A., Haynes, C. M., Zhang, Y., Min, G., Steele, M. C., Kalinina, J., Martinez, E., Pickart, C. M., Kong, X. P., and Ron, D. (2006) An arsenite-inducible 19S regulatory particle-associated protein adapts proteasomes to proteotoxicity. *Mol Cell* **23**, 875-885

51. Beck, F., Unverdorben, P., Bohn, S., Schweitzer, A., Pfeifer, G., Sakata, E., Nickell, S., Plitzko, J. M., Villa, E., Baumeister, W., and Forster, F. (2012) Near-atomic resolution structural model of the yeast 26S proteasome. *Proc Natl Acad Sci U S A* **109**, 14870-14875

52. da Fonseca, P. C., He, J., and Morris, E. P. (2012) Molecular model of the human 26S proteasome. *Mol Cell* **46**, 54-66

53. Lander, G. C., Estrin, E., Matyskiela, M. E., Bashore, C., Nogales, E., and Martin, A. (2012) Complete subunit architecture of the proteasome regulatory particle. *Nature* **482**, 186-191

54. Lasker, K., Forster, F., Bohn, S., Walzthoeni, T., Villa, E., Unverdorben, P., Beck, F., Aebersold, R., Sali, A., and Baumeister, W. (2012) Molecular architecture of the 26S proteasome holocomplex determined by an integrative approach. *Proc Natl Acad Sci U S A* **109**, 1380-1387

55. Kim, Y. C., Li, X., Thompson, D., and Demartino, G. N. (2012) ATP-binding by proteasomal ATPases regulates cellular assembly and substrate-induced functions of the 26S proteasome. *J Biol Chem* **288**, 3334-3345

56. Rubin, D. M., Glickman, M. H., Larsen, C. N., Dhruvakumar, S., and Finley, D. (1998) Active site mutants in the six regulatory particle ATPases reveal multiple roles for ATP in the proteasome. *EMBO J* **17**, 4909-4919

57. Lee, S. H., Moon, J. H., Yoon, S. K., and Yoon, J. B. (2012) Stable incorporation of ATPase subunits into 19 S regulatory particle of human proteasome requires nucleotide binding and C-terminal tails. *J Biol Chem* **287**, 9269-9279

58. D'Arcy, P., Brnjic, S., Olofsson, M. H., Fryknas, M., Lindsten, K., De Cesare, M., Perego, P., Sadeghi, B., Hassan, M., Larsson, R., and Linder, S. (2011) Inhibition of proteasome deubiquitinating activity as a new cancer therapy. *Nat Med* **17**, 1636-1640

59. Kourtis, N., and Tavernarakis, N. (2011) Cellular stress response pathways and ageing: intricate molecular relationships. *EMBO J* **30**, 2520-2531

60. Finley, D., Ozkaynak, E., and Varshavsky, A. (1987) The yeast polyubiquitin gene is essential for resistance to high temperatures, starvation, and other stresses. *Cell* **48**, 1035-1046

61. Bajorek, M., Finley, D., and Glickman, M. H. (2003) Proteasome Disassembly and Downregulation Is Correlated with Viability during Stationary Phase. *Current Biology* **13**, 1140-1144

Chapter 4 - Discussion

Proper proteostasis is important for human health, as its disruption is linked to cancer, neurodegeneration and aging. At the cellular level this is achieved through tightly regulated quality control networks. These networks function from the moment a protein is being synthesized, until the protein is targeted for degradation. The ubiqutin-proteasome pathway is the major pathway of selective protein degradation in the cell. Here the proteasome is the end point, where actual protein degradation happens. Since many cellular processes rely on selective degradation of proteins, understanding this pathway can provide many insights into cellular functions and homeostasis. In addition to that, the UPS has become a major target for translational research. The ability of regulating selective protein degradation is critical to many diseases, and the ubiquitin-proteasome pathway provides multiple points of regulation. Many efforts are underway to develop inhibitors for different steps in the UPS, from E1 ubiquiting-activating enzymes all the way to the proteasome (30). One important aspect in understanding proteasomal protein degradation is to elucidate how to regulate the proteasome. The studies into how this molecular machine assembles have provided new insights into proteasome function, and suggest that the assembly process can actually provide many targets for control (36).

The work described in this dissertation focuses on understanding the assembly of the proteasome by studying the interactions between the AAA-ATPase Rpt5 with the chaperone Nas2, and the quality control protein Ecm29. Rpt5 is an important subunit of the 26S proteasome, it is one of the ATPases involved in the unfolding of substrates and it is at the interface between RP and CP. Results show that Nas2 requires the last three amino acids of the Rpt5 tail for binding (15). These three amino acids are part of the unstructured 12-amino acid C-terminal tail, which has been reported to dock onto CP and induce opening of the substrate access gate and activate hydrolysis (6, 33). These results suggest that having Nas2 bound to the tail would directly prevent docking into the CP. A similar function has been shown for the other RP chaperones, Hsm3, Nas6 and Rpn14, which bind to the C-domain of their respective Rpt, but do not require the last amino acids of the tail, suggesting they inhibit binding to the CP by creating steric hindrance (4, 23, 24, 26). Considering that unlike Hsm3, Nas6 and Rpn14, Nas2 departs from assembly intermediates early in assembly, preceding full ATP ring formation, these results would imply that it is also important early in assembly to prevent the association of RP subunits with the CP.

Surprisingly, in addition to reduced binding of Nas2 in the mutant proteasomes, we observed increased binding of another proteasome-associated protein, Ecm29. Ecm29 has been reported as a stabilizing factor for the RP-CP interaction in the absence of ATP (14, 16). However, more recent publications suggest it is also a negative regulator or quality control protein for proteasome assembly (17, 21, 37). Proteasomes purified form Rpt5 mutant strains enriched in Ecm29 remained stable when ATP was removed from the system, as previously reported (14, 16). Nevertheless, these proteasomes displayed reduced suc-LLVY-AMC hydrolytic activity. Hydrolytic activity was restored in the presence of small amounts of SDS. Since SDS can artificially open the CP gate, this suggests that Ecm29 was inhibiting opening of the gate. The tail of Rpt5 is needed for opening of the gate, hence it could be argued that the reason why the gate is failing to open is due to the tail mutation of Rpt5, however deletion of ECM29 from the Rpt5 mutant relieved the degradation defects. Additionally, strains with mutations in different proteasome subunits that were also enriched in Ecm29, showed similar results (22). Our in vivo data confirmed that indeed Ecm29 inhibits the degradation of ubiquitinated as well as non-ubiquitinated substrates (3). Thus, besides stabilizing proteasomes, Ecm29 also inhibits their function. Additionally, consistent with its proposed function in quality control of the proteasome, our results show that Ecm29 preferentially binds to mutant and ATP-depleted proteasomes. Depletion of ATP (*in vitro*) results in disassociation of the RP-CP, recent studies into the structure of the 26S suggest the ATPase ring goes through conformational changes when ATP is bound, these changes affect the RP-CP interaction and substrate unfolding and translocation through the catalytic pore (2, 18, 34). Based on our findings, we propose that Ecm29 recognizes non-native conformations in assembled proteasomes. These conformations are either derived from ATP depletion on in vitro studies, or from mutations in proteasome subunits. The binding of Ecm29 to these somewhat "faulty" proteasomes, leads to inhibition of proteasomal activity, thereby ensuring no aberrant degradation of proteins occurs in the cell. The two functions we observe for Ecm29 in the proteasome, stabilizing (a positive interaction) and inhibiting (a negative interaction), can seem contradictory. However, considering Ecm29 as a quality control mechanism of proper proteasome assembly and function, these properties might be in place to ensure that only properly formed 26S can degrade cellular proteins and prevent aberrant degradation.

Ecm29 is a 210 kD protein and it's known to bind to both RP and CP. Through crosslinking and mass spectrometry we were able to identify Rpt5 as a binding partner for Ecm29 in the RP. Ecm29 stabilizes RP-CP interaction, which implies there is a binding site for Ecm29 on the CP as well. Future studies should focus on finding additional binding sites for Ecm29 in both the RP and CP, which will help draw a better picture of the mechanisms of inhibition of Ecm29. Based on the current data we propose that when there are no defects in the proteasome, the binding sites of Ecm29 in RP and CP are not positioned to allow high affinity binding of the Ecm29 molecule (Fig 4.1A). However, when there are structural misalignments of the RP-CP interface (Fig 4.1B), the Ecm29 binding sites on the RP and CP are repositioned in a way that allows for high-affinity binding of Ecm29 with the proteasome.

We are currently working on identifying the binding site for Ecm29 on the CP. Additional studies to test our hypothesis will include mutating the binding sites on CP or RP, and assess how this affects the interaction with Ecm29, as well as the inhibitory function of Ecm29 on the proteasome.

Interestingly, our phenotypic data, using the Rpt5 mutants together with Hsm3, Nas2 and Ecm29 deletion mutants, suggests that there are additional functions to both Nas2 and Ecm29 in assembly of the proteasome. If the only function of Nas2 is to prevent docking of Rpt5 onto CP, deleting *NAS2* from strains that are defective in Rpt5 docking should cause no additional phenotypes. However, deletion of Nas2 in such a background exacerbates the phenotype (Fig. 2.3).

Consistent with this, recently published structure data from our lab (32) shows that the Nas2 protein structure has patches that are conserved from yeast to humans. We believe these patches could be important for conserved protein-protein interactions, which go beyond the interaction between the Nas2 PDZ domain and the Rpt5 tail (29).

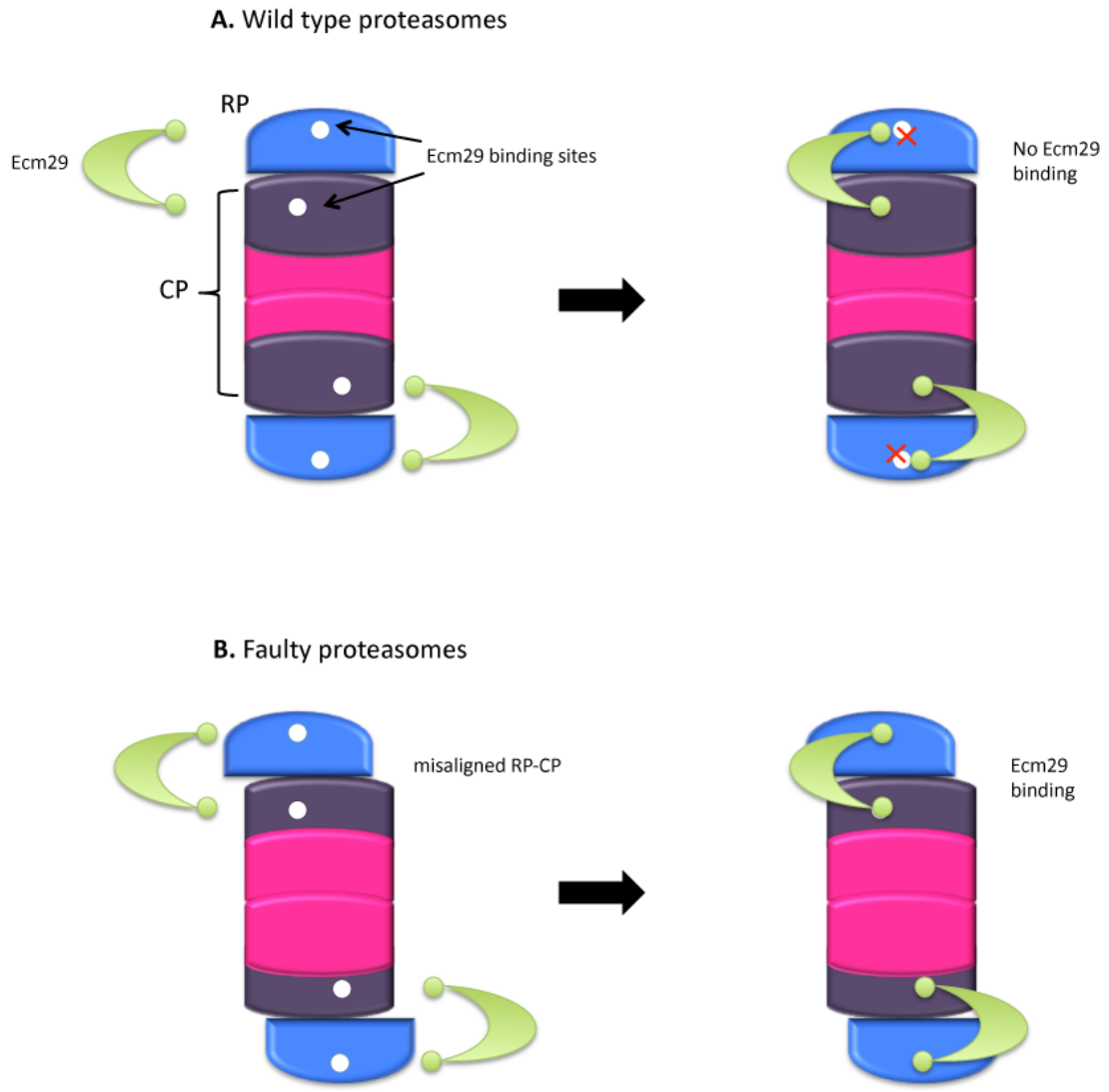

Figure 4.1 Proposed model of Ecm29 binding to proteasomes

We hypothesize that Nas2 could be working as a scaffold, facilitating the formation of specific intermediate assembly complexes, and preventing the formation of off-pathway complexes. Figure 4.2 illustrates these idea, where the RP chaperones function not only to prevent the docking into the CP, but also function in preventing premature binding of intermediate complexes. The chaperones exist in subcomplexes with one or more RP subunits (e.g. Hsm3-Rpt1-Rpt2-Rpn1, Nas2-Rpt5-Rpt4) (1, 24, 27, 35), supporting this hypothesis. However, additional studies into how the subcomplexes come together could confirm that the chaperones serve as scaffolds for the assembly.

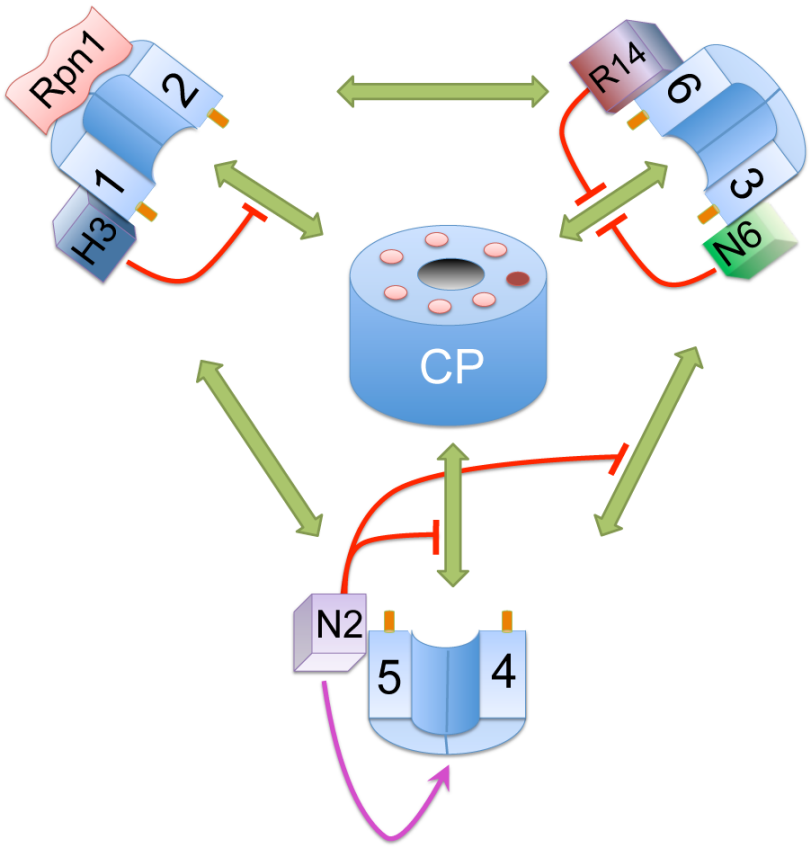

Figure 4.2 Model for chaperone function in RP assembly (2).

Our phenotypic analysis data also suggests a role for Ecm29 in assembly, something that has been proposed by other groups (17, 21, 22). We found that deletion of Ecm29 in particular RP-chaperone mutant combinations could not be explained by Ecm29 inhibitory activity. Deletion mutants of Nas6/Rpn14 and Hsm3/Nas2 are known to have phenotypes at 37ºC (12, 26). The deletion of Ecm29 has no effect on the on the Nas6/Rpn14 mutant, but rescues Hsm3/Nas2. Interestingly, when we look at the phenotypes of these strains in canavinine, the deletion of Ecm29 was able to rescue the Nas6/Rpn14 phenotype, but exacerbated the phenotype of Hsm3/Nas2. When looking for phenotypes of proteasome mutant strains, growth analyses at 37ºC or with canavinine are often used indistinctively. However, our data together with phenotypic analysis of other strains (e.g. Ubp6Δ)(11, 28) suggests phenotypes at 37ºC are representative of proteasome assembly defects, whereas the phenotypes in canavinine are representative of proteasome function defects. With this in mind, our data suggests an additional function for Ecm29 in assembly of the proteasome. Additional studies with a bigger array of

strains would be required to confirm our observations into the differences in phenotypes at 37ºC and canavinine.

With this work we have reported Ecm29 to be an inhibitor of the proteasome as part of its quality control functions. A lot of questions remain to be answered, first, what happens with the proteasomes that are enriched in Ecm29. Work in mammalian cells links Ecm29 to the endosomes (7, 8, 9), which has led us and other groups (36) to speculate that these proteasomes are transported to endosomes with the help of Ecm29, and eventually are degraded by the lysosome.

The chaperones, as well as the proteasome subunits, and Ecm29 are conserved among eukaryotes, retaining their functions from yeast to humans. In recent years there have been many reports using mammalian systems, where the RP chaperones Nas6 (Gankyrin), Hsm3 (S5b) and Rpn14 (PAAF1) have been implicated in regulation of proteasomal function, and linked to diseases that range from cancer to HIV (13, 19, 31, 39). Interestingly, recent studies suggest a direct relationship between levels of Rpt1 and tumor growth in some cancers. Here the loss of a copy of the gene that encodes for Rpt1 (PSMC2) rendered the tumors specifically sensitive to Rpt1 shRNA (20). In yeast, overexpression of Rpt1 rescues Hsm3 mutant phenotypes and vice versa (5, 26), considering that deletion of Rpt1 is lethal, it would be of interest to look at the effect of manipulating the levels of Hsm3 in these cancer cells. In general, there is increased evidence suggesting roles for the proteasome chaperones in regulation of the proteasome, with the proteasome fast becoming an important drug target for treatment of diseases (10, 25, 30, 38). Understanding the different functions of Nas2 and Ecm29 can be of critical importance. For example, it would be of great relevance to know if the inhibitory function of Ecm29 in the proteasomes is conserved in higher organisms. If so, the impact on the development of treatments for neurodegenerative diseases, and the afflictions of ageing would be great, since there are reports of lower proteasomal activity in these conditions.

Finally, figure 4.3 summarizes the findings of our studies into the role of Rpt5 in proteasome assembly and function. Like every other process in the cell, the assembly of the proteasome is subjected to multiple levels of quality control. First, during assembly of the RP there are multiple chaperones, including Nas2, that prevent premature docking onto CP, as well as prevent premature binding of subcomplexes. Once the proteasome is assembled, there is a

second quality control checkpoint, where Ecm29 senses conformational defects in the proteasome and binds to the "faulty" proteasomes inhibiting their activity.

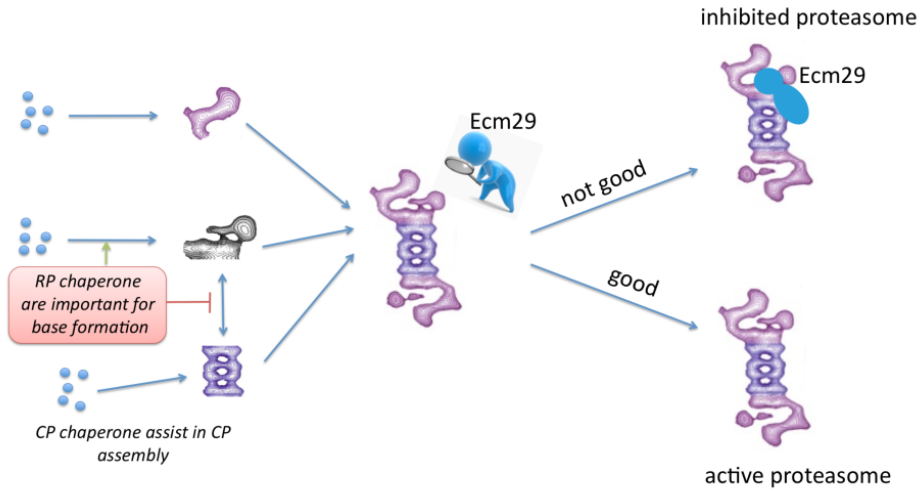

Figure 4.3 Model for quality control of proteasome assembly and function.

References

1. Barrault, M.B., Richet, N., Godard, C., Murciano, B., Le Tallec, B., Rousseau, E., Legrand, P., Charbonnier, J.B., Le Du, M.H., Guerois, R., Ochsenbein, F., and Peyroche, A. (2012) Dual functions of the Hsm3 protein in chaperoning and scaffolding regulatory particle subunits during the proteasome assembly. Proc.Natl.Acad.Sci.U.S.A. 109, E1001-10

2. Beckwith, R., Estrin, E., Worden, E.J., and Martin, A. (2013) Reconstitution of the 26S proteasome reveals functional asymmetries in its AAA+ unfoldase. Nat.Struct.Mol.Biol. 20, 1164-1172

3. De La Mota-Peynado, A., Lee, S.Y., Pierce, B.M., Wani, P., Singh, C.R., and Roelofs, J. (2013) The proteasome-associated protein Ecm29 inhibits proteasomal ATPase activity and in vivo protein degradation by the proteasome. J.Biol.Chem. 288, 29467-29481

4. Ehlinger, A., Park, S., Fahmy, A., Lary, J.W., Cole, J.L., Finley, D., and Walters, K.J. (2013) Conformational dynamics of the Rpt6 ATPase in proteasome assembly and Rpn14 binding. Structure. 21, 753-765

5. Funakoshi, M., Tomko, R.J.,Jr, Kobayashi, H., and Hochstrasser, M. (2009) Multiple assembly chaperones govern biogenesis of the proteasome regulatory particle base. Cell. 137, 887-899

6. Gillette, T.G., Kumar, B., Thompson, D., Slaughter, C.A., and DeMartino, G.N. (2008) Differential roles of the COOH termini of AAA subunits of PA700 (19 S regulator) in asymmetric assembly and activation of the 26 S proteasome. J.Biol.Chem. 283, 31813-31822

7. Gorbea, C., Goellner, G.M., Teter, K., Holmes, R.K., and Rechsteiner, M. (2004) Characterization of mammalian Ecm29, a 26 S proteasome-associated protein that localizes to the nucleus and membrane vesicles. J.Biol.Chem. 279, 54849-54861

8. Gorbea, C., Pratt, G., Ustrell, V., Bell, R., Sahasrabudhe, S., Hughes, R.E., and Rechsteiner, M. (2010) A protein interaction network for Ecm29 links the 26 S proteasome to molecular motors and endosomal components. J.Biol.Chem. 285, 31616-31633

9. Gorbea, C., Rechsteiner, M., Vallejo, J.G., and Bowles, N.E. (2013) Depletion of the 26S proteasome adaptor Ecm29 increases Toll-like receptor 3 signaling. Sci.Signal. 6, ra86

10. Gu, J.J., Hernandez-Ilizaliturri, F.J., Kaufman, G.P., Czuczman, N.M., Mavis, C., Skitzki, J.J., and Czuczman, M.S. (2013) The novel proteasome inhibitor carfilzomib induces cell cycle arrest, apoptosis and potentiates the anti-tumour activity of chemotherapy in rituximab-resistant lymphoma. Br.J.Haematol. 162, 657-669

11. Hanna, J., Hathaway, N.A., Tone, Y., Crosas, B., Elsasser, S., Kirkpatrick, D.S., Leggett, D.S., Gygi, S.P., King, R.W., and Finley, D. (2006) Deubiquitinating enzyme Ubp6 functions noncatalytically to delay proteasomal degradation. Cell. 127, 99-111

12. Kaneko, T., Hamazaki, J., Iemura, S., Sasaki, K., Furuyama, K., Natsume, T., Tanaka, K., and Murata, S. (2009) Assembly pathway of the Mammalian proteasome base subcomplex is mediated by multiple specific chaperones. Cell. 137, 914-925

13. Kim, Y.H., Kim, J.H., Choi, Y.W., Lim, S.K., Yim, H., Kang, S.Y., Chung, Y.S., Lee, G.Y., and Park, T.J. (2013) Gankyrin is frequently overexpressed in breast cancer and is associated with ErbB2 expression. Exp.Mol.Pathol. 94, 360-365

14. Kleijnen, M.F., Roelofs, J., Park, S., Hathaway, N.A., Glickman, M., King, R.W., and Finley, D. (2007) Stability of the proteasome can be regulated allosterically through engagement of its proteolytic active sites. Nat.Struct.Mol.Biol. 14, 1180-1188

15. Lee, S.Y., De la Mota-Peynado, A., and Roelofs, J. (2011) Loss of Rpt5 protein interactions with the core particle and Nas2 protein causes the formation of faulty proteasomes that are inhibited by Ecm29 protein. J.Biol.Chem. 286, 36641-36651

16. Leggett, D.S., Hanna, J., Borodovsky, A., Crosas, B., Schmidt, M., Baker, R.T., Walz, T., Ploegh, H., and Finley, D. (2002) Multiple associated proteins regulate proteasome structure and function. Mol.Cell. 10, 495-507

17. Lehmann, A., Niewienda, A., Jechow, K., Janek, K., and Enenkel, C. (2010) Ecm29 fulfils quality control functions in proteasome assembly. Mol.Cell. 38, 879-888

18. Matyskiela, M.E., Lander, G.C., and Martin, A. (2013) Conformational switching of the 26S proteasome enables substrate degradation. Nat.Struct.Mol.Biol. 20, 781-788

19. Nakamura, M., Basavarajaiah, P., Rousset, E., Beraud, C., Latreille, D., Henaoui, I.S., Lassot, I., Mari, B., and Kiernan, R. (2012) Spt6 levels are modulated by PAAF1 and proteasome to regulate the HIV-1 LTR. Retrovirology. 9, 13-4690-9-13

20. Nijhawan, D., Zack, T.I., Ren, Y., Strickland, M.R., Lamothe, R., Schumacher, S.E., Tsherniak, A., Besche, H.C., Rosenbluh, J., Shehata, S., Cowley, G.S., Weir, B.A., Goldberg, A.L., Mesirov, J.P., Root, D.E., Bhatia, S.N., Beroukhim, R., and Hahn, W.C. (2012) Cancer vulnerabilities unveiled by genomic loss. Cell. 150, 842-854

21. Panasenko, O.O., and Collart, M.A. (2011) Not4 E3 ligase contributes to proteasome assembly and functional integrity in part through Ecm29. Mol.Cell.Biol. 31, 1610-1623

22. Park, S., Kim, W., Tian, G., Gygi, S.P., and Finley, D. (2011) Structural defects in the regulatory particle-core particle interface of the proteasome induce a novel proteasome stress response. J.Biol.Chem. 286, 36652-36666

23. Park, S., Li, X., Kim, H.M., Singh, C.R., Tian, G., Hoyt, M.A., Lovell, S., Battaile, K.P., Zolkiewski, M., Coffino, P., Roelofs, J., Cheng, Y., and Finley, D. (2013) Reconfiguration of the proteasome during chaperone-mediated assembly. Nature. 497, 512-516

24. Park, S., Roelofs, J., Kim, W., Robert, J., Schmidt, M., Gygi, S.P., and Finley, D. (2009) Hexameric assembly of the proteasomal ATPases is templated through their C termini. Nature. 459, 866-870

25. Pevzner, Y., Metcalf, R., Kantor, M., Sagaro, D., and Daniel, K. (2013) Recent advances in proteasome inhibitor discovery. Expert Opin.Drug Discov. 8, 537-568

26. Roelofs, J., Park, S., Haas, W., Tian, G., McAllister, F.E., Huo, Y., Lee, B.H., Zhang, F., Shi, Y., Gygi, S.P., and Finley, D. (2009) Chaperone-mediated pathway of proteasome regulatory particle assembly. Nature. 459, 861-865

27. Saeki, Y., Toh-E, A., Kudo, T., Kawamura, H., and Tanaka, K. (2009) Multiple proteasome-interacting proteins assist the assembly of the yeast 19S regulatory particle. Cell. 137, 900-913

28. Sakata, E., Stengel, F., Fukunaga, K., Zhou, M., Saeki, Y., Forster, F., Baumeister, W., Tanaka, K., and Robinson, C.V. (2011) The catalytic activity of Ubp6 enhances maturation of the proteasomal regulatory particle. Mol.Cell. 42, 637-649

29. Satoh, T., Saeki, Y., Hiromoto, T., Wang, Y.H., Uekusa, Y., Yagi, H., Yoshihara, H., Yagi-Utsumi, M., Mizushima, T., Tanaka, K., and Kato, K. (2014) Structural Basis for Proteasome Formation Controlled by an Assembly Chaperone Nas2. Structure.

30. Shen, M., Schmitt, S., Buac, D., and Dou, Q.P. (2013) Targeting the ubiquitin-proteasome system for cancer therapy. Expert Opin.Ther.Targets. 17, 1091-1108

31. Shim, S.M., Lee, W.J., Kim, Y., Chang, J.W., Song, S., and Jung, Y.K. (2012) Role of S5b/PSMD5 in proteasome inhibition caused by TNF-alpha/NFkappaB in higher eukaryotes. Cell.Rep. 2, 603-615

32. Singh, C.R., Lovell, S., Mehzabeen, N., Chowdhury, W.Q., Geanes, E.S., Battaile, K.P., and Roelofs, J. (2014) 1.15 A resolution structure of the proteasome-assembly chaperone Nas2 PDZ domain. Acta Crystallogr.F.Struct.Biol.Commun. 70, 418-423

33. Smith, D.M., Chang, S.C., Park, S., Finley, D., Cheng, Y., and Goldberg, A.L. (2007) Docking of the proteasomal ATPases' carboxyl termini in the 20S proteasome's alpha ring opens the gate for substrate entry. Mol.Cell. 27, 731-744

34. Smith, D.M., Fraga, H., Reis, C., Kafri, G., and Goldberg, A.L. (2011) ATP binds to proteasomal ATPases in pairs with distinct functional effects, implying an ordered reaction cycle. Cell. 144, 526-538

35. Takagi, K., Kim, S., Yukii, H., Ueno, M., Morishita, R., Endo, Y., Kato, K., Tanaka, K., Saeki, Y., and Mizushima, T. (2012) Structural basis for specific recognition of Rpt1p, an ATPase subunit of 26 S proteasome, by proteasome-dedicated chaperone Hsm3p. J.Biol.Chem. 287, 12172-12182

36. Tomko, R.J.,Jr, and Hochstrasser, M. (2013) Molecular architecture and assembly of the eukaryotic proteasome. Annu.Rev.Biochem. 82, 415-445

37. Wang, X., Yen, J., Kaiser, P., and Huang, L. (2010) Regulation of the 26S proteasome complex during oxidative stress. Sci.Signal. 3, ra88

38. Weathington, N.M., and Mallampalli, R.K. (2014) Emerging therapies targeting the ubiquitin proteasome system in cancer. J.Clin.Invest. 124, 6-12

39. Zheng, T., Hong, X., Wang, J., Pei, T., Liang, Y., Yin, D., Song, R., Song, X., Lu, Z., Qi, S., Liu, J., Sun, B., Xie, C., Pan, S., Li, Y., Luo, X., Li, S., Fang, X., Bhatta, N., Jiang, H., and Liu, L. (2014) Gankyrin promotes tumor growth and metastasis through activation of IL-6/STAT3 signaling in human cholangiocarcinoma. Hepatology. 59, 935-946

Appendix A - Identification of the atypical extracellular regulated kinase 3 (Erk3) as a novel substrate for p21-activated kinase (Pak) activity.

Alina De La Mota-Peynado, Jonathan Chernoff, and Alexander Beeser

Division of Biology, Kansas State University, Manhattan, Kansas, United States of America

*Published in the Journal of Biological Chemistry, Volume 286, Issue 15, 15 April 2011, Pages 13603-13611.

Republished with permission.

Abstract

The Class I p21-activated kinases (Pak1, -2, -3) regulate many essential biological processes, including cytoskeletal rearrangement, cell cycle progression, apoptosis and cellular transformation. While many Pak substrates, including elements of mitogen-activated protein kinase (MAPK) signaling pathways, have been identified, it is likely that additional substrates remain to be discovered. Identification of such substrates, and determination of the consequences of their phosphorylation, is essential for a better understanding of Class I Pak activity. To identify novel Class I Pak substrates we used recombinant Pak2 to screen high-density protein microarrays. This approach identified the atypical MAPK Erk3 as a potential Pak2 substrate. Solution based *in vitro* kinase assays using recombinant Erk3 confirmed the protein microarray results, and phospho-specific antisera identified serine 189, within the Erk3 activation loop, as a site directly phosphorylated by Pak2 *in vitro*. Erk3 protein is known to shuttle between the cytoplasm and the nucleus, and we showed that selective inhibition of Class I Pak kinase activity in cells promoted increased nuclear accumulation of Erk3. Pak inhibition in cells reduces the extent of Erk3 phosphorylation and inhibits the formation of Erk3/Prak complexes. Collectively, our results identify the Erk3 protein as a novel Class I Pak substrate and further suggest a role for Pak kinase activity in atypical MAPK signaling.

Introduction

The Class I p21-activated kinases (Pak1, -2, -3) are established effectors of the small GTPases Rac1 and Cdc42 (1). Although initially discovered as regulators of the actin cytoskeleton, they have subsequently been implicated in a variety of different signaling pathways including those that control proliferation, apoptosis and transformation (2, 3). Not surprisingly, misregulated Pak kinase activity is associated with a variety of different pathological conditions (4-6). As Pak kinase activity contributes to a large number of different signaling pathways understanding the specific role for Paks in any biological response is greatly aided by the identification of the protein(s) they phosphorylate and the consequences of these phosphorylations. Although the list of Pak kinases substrates is quite large (3, 7), we are particularly interested in how Pak kinases modulate mitogen-activated protein kinase (MAPK) signaling cascades as these cascades are important for gene expression, cell proliferation and programmed cell death (8).

MAPK signaling is one of the most evolutionarily conserved signal transduction pathways and is critical for many biological responses (9). Various cellular stimuli lead to the phosphorylation and activation of a family of serine/threonine kinases known as MAP3Ks, initiating a three-tiered kinase cascade. Activated MAP3Ks phosphorylate and activate specific MAP2Ks. MAP2Ks are dual-specificity kinases that phosphorylate threonine and tyrosine residues within the activation loop of the MAPKs (the conserved T-X-Y motif) to activate them; phosphorylation of both activation loop residues is required for MAPK activation. Activated MAPKs then transphosphorylate a variety of different proteins including structural proteins, enzymes, and transcription factors that ultimately drive the appropriate cellular response to the initial signal (10).

In some signaling pathways the substrates for MAPK activity are themselves kinases and are defined as MAPK-activated kinases (MAPKAKs or MKs) extending the characteristic three-tiered architecture (11).

Although the central roles of the MAP3Ks, MAP2Ks and MAPK isoforms to signaling pathways are incontrovertible, the intensity and duration of MAPK signaling is additionally regulated by the activity of non-canonical proteins, including Paks. Pak kinase activity promotes

Erk1/2 signaling at two distinct points: Pak phosphorylation of the MAP3K c-Raf on serine 338 cooperates with Src-dependent phosphorylation at tyrosine 341 for maximal c-Raf kinase activity (12), and Pak phosphorylation on serine 298 of Mek1facilitates the interaction of Mek1 with Erk2 (13).

In addition to the classical MAPK families (ERK, p38 and JNK/SAPK), many cells also express atypical MAPK isoforms characterized by the Erk3, Erk4, Nlk (nemo-like kinase) and Erk7/8 proteins (14). Erk3 and 4 are most closely related to the Erk1 MAPK isoform, sharing 45 and 42% amino acid identity respectively with the catalytic domain of Erk1. Despite this similarity, Erk3 is incapable of phosphorylating known Erk1/2 substrates *in vitro* (15). One of the key characteristics that distinguish Erk3, Erk4 and NLK from the classical MAPK isoforms is the lack of the characteristic "T-X-Y" motif within their activation loops. In Erk3 and Erk4 the corresponding sequence is S-E-G, and for Nlk it is T-Q-E (14). Although Erk7 does contain a T-X-Y sequence that is phosphorylated *in vivo*, this phosphorylation is not catalyzed by any known MAP2K but results from autophosphorylation (16). As such, Erk7 is also generally considered a member of the atypical MAPK family (14).

Unlike the classical MAPKs, dual phosphorylation of the Erk3/Erk4 activation loops is not possible. It is formally possible that S189 phosphorylation of Erk3 could result from a MAP2K since Mek2, but not Mek1, poorly phosphorylated Erk3 S189 *in vitro* (17). However, using a cell-fractionation approach to identify the kinase responsible for Erk3 S189 phosphorylation, the Cobb laboratory identified a S189 kinase that did not co-fractionate with Erk1/2 kinase activity, excluding Mek1/2 from consideration as cellular Erk3 kinases (18). A similar approach based on the strong affinity of the Erk3 kinase for recombinant Erk3 excluded protein kinase C as the cellular S189 kinase despite the ability of PKC to phosphorylate Erk3 *in vitro* (18). The initial observation of Erk3 S189 phosphorylation *in vivo* occurred more than a decade ago (18) but the kinase(s) responsible for this phosphorylation remains unidentified.

Using high-density protein microarrays, we identified Erk3 as a potential Pak2 substrate. Pak2 kinase assays using recombinant full-length Erk3 protein in solution confirmed the protein microarray results and suggested that Erk3 is a direct p21-activated kinase substrate *in vitro*. We

further demonstrated that Pak2 directly targets the S189 site, within Erk3's activation loop, suggesting that p21-activated kinases contribute to Erk3 activation and furthermore may represent the elusive Erk3 S189 kinase (referred to as Kinase X in (19)). A variant of Erk3 lacking this phosphorylation site (S189A) displays an increased nuclear accumulation in fibroblasts, which can be phenocopied by wild type Erk3 with selective inhibition of Class I Pak kinase activity. Furthermore, expression of a selective Pak inhibitor in cells reduced the levels of Erk3 S189 phosphorylation. As phosphorylation of this site stabilizes the interaction of Erk3 with its effector Prak, we also demonstrated using Pak inhibitors and S189A and 189D variants of Erk3 that Pak kinase inhibition is sufficient to disrupt the interaction between Erk3 and Prak in cells. Collectively, our results identified Erk3 as a novel substrate for Class I Pak kinase activity and identified S189, within the Erk3 activation loop, as a residue phosphorylated by Class I kinase activity *in vitro* and *in vivo* suggesting a role for class I p21-activated kinases in regulating the subcellular localization and activity of the atypical MAPK Erk3.

Experimental Procedures

Human Protein Microarrays

Kinase Substrate Identification (KSI) ProtoArrays (version 4.0 arrays containing 8,274 full-length GST fusion proteins provided by Invitrogen) were processed as recommended by the manufacturer with the following modification: the supplied kinase buffer was replaced with 1X phosphobuffer (20). Recombinant His6-Pak2 expressed from *E.coli* was used as the exogenous kinase. This source of Pak2 is known to be constitutively active (Beeser and Chernoff unpublished observation) obviating the need for inclusion of Rac/Cdc42-GTP. "No-kinase" slides were identically processed in parallel as the Pak2 slides except they lacked Pak2. Radiographic images of the slides were obtained using a Fuji phosphorimager and spots were identified using GenePix Pro (Molecular devices). Data analysis was conducted in ProtoArray Prospector v.2.0 software as recommended (Invitrogen). For overlay images, spots were pseudocolored in Adobe Photoshop.

Plasmids and Plasmid Construction

The human Erk3 vector was kindly provided by Dr. Sylvain Meloche, University of Montreal. The Erk3 sequence was cloned into the N-terminal His6 baculovirus transfer vector pFBHTB (Invitrogen) and used to make high- titer baculovirus stocks (P4) as recommended. For mammalian expression vectors, the human full-length Erk3 ultimate ORF Gateway entry clone was purchased from Invitrogen, and moved to the N-terminal GFP (pcDNA6.2-EmGFP-N) and the N-terminal His6 (pDest26) Gateway destination vectors using the LR Clonase II enzyme mix as recommended (Invitrogen). Site directed point mutants of Erk3 (S189A, S189D) were created using the Erk3 ultimate ORF plasmid as template and Quick change II kit (Stratagene) with the following mutagenic oligonucleotides: SA1 (5'-cattattcccataagggtcatcttgctgaaggattggttactaaat-3'), SA2 (5'-atttagtaaccaatccttcagcaagatgacccttatgggaataatg-3'), SD1 (5'-ctcattattcccataagggtcatcttgatgaaggattggttactaaatgg-3'), SD2 (5'-ccatttagtaaccaatccttcatcaagatgacccttatgggaataatgag-3'). Plasmids encoding only the desired S189A or S189D mutations were identified by DNA sequencing and were then moved to pcDNA6.2-EmGFP-N and pDest26 vectors as described above. GFP-PID (corresponding to amino acids 83-149 of human Pak1) and GFP-PIDLl07F constructs were amplified by polymerase chain reaction using human Pak1 and Pak1L107F expression constructs as template and subsequently cloned into pEGFP-C1 (Clontech). mRFP-PID constructs were constructed by Pfusion (NEB) polymerase chain reaction using the above PID vectors as templates and the following oligonucleotides 5'-gcggatggatgcacacaattcatgtcggttttgat-3' and 5'-gcgaattcctatttatctgtaaagctcatgtattt-3'. The PCR products were digested with *Bam*HI and *Eco*RI restriction enzymes, purified from 1X TBE/agarose gels and ligated into pCS2+mRFP-N1 (a gift from Dr. Chris Thorpe, Kansas State University) similarly digested followed by DNA sequence confirmation.

Purification and Dephosphorylation of Recombinant Erk3

High titer P4 stocks were used to infect suspension cultures of Sf21 cells maintained in SFM-900 III media (Invitrogen). 48 hours post infection the cultures were pelleted by centrifugation, the supernatant discarded and the pellet was either frozen at -80° C or immediately resuspended in 30 ml of lysis buffer (15 mM $NaHPO_4$, 300 mM NaCl, 10 mM imidazole pH 8.0 containing 1mM PMSF, 1:100 aprotinin (Fisher) and 200 μl protease inhibitor cocktail (Pierce)). The pellet was subjected to 6-8 rounds of 30-second sonication, 30 seconds

on ice. The lysate was centrifuged for 10 minutes at 15000 rpm at 4°C in a SS-34 rotor. The cleared lysate was transferred to a 50 ml conical tube followed by addition of HisPur beads (Pierce) pre-equilibrated in lysis buffer and rotated for 1 hour at 4°C. The beads were collected by 3000-rpm centrifugation in a swinging bucket rotor Sorvall H1000B (5 min at 4°C) and washed 3X with lysis buffer lacking PMSF and protease inhibitors. The protein was eluted from the beads with lysis buffer containing 200 mM imidazole for 4 hours at 4°C. The 200 mM imidazole eluate containing Erk3 was concentrated using a Viva Spin 15R 30 000 molecular weight cut off (MWCO) centrifugal concentrator as recommended (Sartorius). The retentate was dialyzed against 10% glycerol/ 1 X Tris buffered saline (TBS) at 4°C overnight; then divided into single-use aliquots in 1.5 ml microfuge tubes and frozen at -80°C.

Western analyses

Protein samples were resolved on SDS-PAGE mini-gels, and transferred to PVDF membranes as recommended (BioRad). Membranes were blocked in 1X TBST, 5% BSA (Fisher) for greater than one hour at room temperature. All primary antibodies were incubated at 4°C overnight in blocking buffer. Primary antibodies used included TheHis-Tag mAb (Genscript A00186), total Erk3 (Cell Signaling # 4067), Erk3 phospho S189 (Abgent AP3098a), Prak (Santa Cruz sc-46667) and GFP (Cell signaling #2555). HRP- linked secondary antibodies were from Cell Signaling. Signal detection used the Immobilon Chemiluminescent HRP substrate (Millipore).

In vitro Pak2 kinase assays

The Erk3 protein stock was dialyzed into 1X phosphobuffer using a 10 000 MWCO mini Slide-a-lyzer (Pierce). 0, 1, 5, 10, 15 or 20 ul of the Erk3 protein were brought up to a final volume of 30 μl containing 100 μM ATP (final concentration) and 0.25 μCi of ^{32}P-ATP (NEN). Where indicated, 11 ng of recombinant His6-Pak2 was added. As a positive control for Pak2 kinase activity myelin basic protein (MBP, Upstate) was included at a final concentration of 0.17 μg/ml under identical conditions. Kinase assays were allowed to proceed for 30 minutes at 30°C followed by cooling on ice, the addition SDS-PAGE loading buffer to 1X followed by boiling for 5 minutes. Samples were resolved on 10 % acrylamide SDS-PAGE Gels, equilibrated into 40%

acetic acid/10% methanol, dried onto Whatmann 3MM paper under vacuum and exposed to phosphorimager screen (Cyclone, Perkin Elmer).

Cell culture and treatments

NIH3T3 and HEK293 cells were obtained from the ATCC. All growth media, serum and supplements were purchased from Hyclone. NIH3T3 cells were grown in 1X DMEM + 10% calf serum supplemented with penicillin/streptomycin. HEK293 cells were grown in 1X MEM + 10% fetal bovine serum supplemented with penicillin/streptomycin. Cells were grown at 37 °C, 5% CO_2 in a humidified chamber. NIH3T3 cells were transfected with 2ug DNA in a 6-well plate using Arrest-In transfection reagent as recommended (Open Biosystems). 24 hours post transfection cells were split into 4-well slides (LabTek) and allowed to attach overnight. Cells were fixed in 3.7% formaldehyde (in 1X PBS) for 20 min at room temperature, washed with PBS pH7.4, and permeabilized using 0.2% Triton X (in 1X PBS) for 10 min at room temperature. Cells were washed 3X in 1X PBS and DAPI (Roche) was added for 5 minutes prior to addition of ProLong antifade reagent (Invitrogen). Fluorescent images were acquired from a Nikon eclipse E600 microscope equipped with a Qimaging QiCAM camera using Qcapture Pro software.

HEK293 Lysis and Immobilized Metal Affinity Chromatography

For His6-Erk3 pull downs, HEK293 cells in 100 mm plates were transfected with 5μg of plasmid DNAs using TransIT-293 reagent (Mirus) or in 6 well plates with the Profection Calcium Phosphate method (Promega). 48 hours post transfection cells were lysed in RIPA buffer containing 10 mM imidazole, 1mM sodium orthovanadate, 0.5% sodium deoxycholate, 10 mM β-glycerophosphate, 5 mM sodium pyrophosphate, 50 mM sodium fluoride, 1mM PMSF and 1:100 aprotinin (Fisher). Lysates were centrifuged at 21000xg for 10 minutes at 4°C. Cleared lysate protein concentrations were determined by BCA assay (Pierce) and equilibrated with lysis buffer. HisPur beads (Pierce) were added to the cleared lysate and incubated with end/end rotation at 4° C overnight. The beads were washed twice with lysis buffer, brought to 100 μl total volume in lysis buffer followed by addition of 20 μl 6 X SDS-Page sample loading buffer.

Results

High-density Protein Microarrays Identify Erk3 as a Potential Pak2 Substrate.

Although the list of validated substrates for the p21-activated kinases is quite extensive (2, 21) it is likely that additional substrates remain to be identified. To identify novel Pak kinase substrates we used constitutively active recombinant Pak2 to screen a high-density protein array. The protein microarrays (KSI slides, Invitrogen) contain 8274 full-length human proteins including fiduciary kinases that serve as orientation landmarks spotted in duplicate onto microscope slides. Similar arrays have been used to identify novel substrates for a variety of different protein kinases, including Cdk5 (22) and the *A. thaliana* MAPKs Mkp3 and Mkp6 (23). A summary of the proteins identified from the protein microarrays is presented in appendix Figure 1. In addition to identifying proteins previously implicated involved in Rac-dependent signaling (i.e ARHGEF5 and ARHGAP15), we also identified the atypical MAPK Erk3 as a potential Pak2 substrate (Fig. A.1, Fig. A.2). The lack of a signal at the Erk3 co-ordinates in the no kinase slide suggested that the corresponding signal in the Pak2 kinase slide is not the result of Erk3 autophosphorylation and suggested that Erk3 is a Pak2 phosphoacceptor *in vitro*.

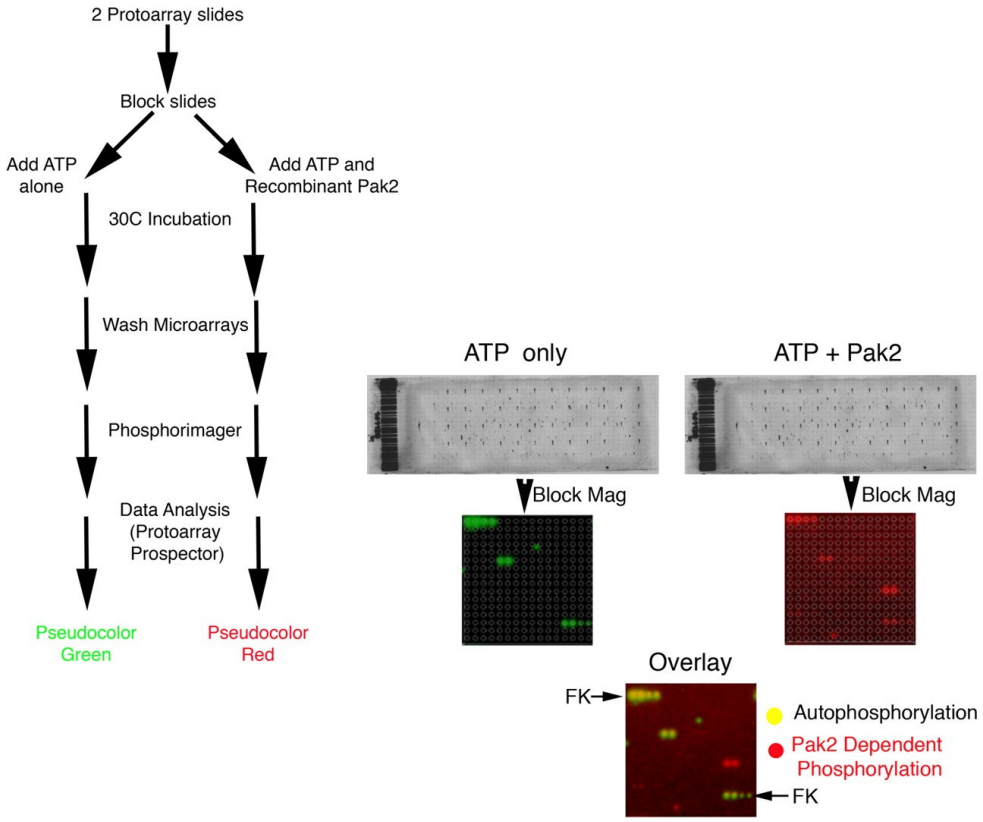

Figure A.1 High-density protein microarrays identifies the atypical MAPK Erk3 as a Pak2 phosphoacceptor.

A. Flow chart for Kinase substrate identification (KSI) slides (left) were processed as described in experimental procedures using recombinant His6-Pak2. Statistically significant spots were identified in Protoarray Prospector. B. A single block of the array from the ATP alone and ATP +Pak2 slides are shown at higher magnification (middle). All substrate proteins are spotted in duplicate, single spots or spots that do not align with the printing grid (grey circles) are excluded from consideration The ^{33}P- spots obtained from the phosphorimager were pseudocolored, and overlaid (bottom). Yellow signals in the overlay result from autophosphorylation, either by spotted protein kinases or by fiduciary kinases (FK) that are arrayed in the upper left and lower right of each block for orientation landmarks. Red signals appearing in the overlay, including Erk3, identify proteins transphosphorylated by recombinant Pak2

Lot Number = HA20021
Array Type = Human Experimental Array
Application = Kinase Substrate Identification

Protein Cut-Off Value calculated by = Larger then Median plus 3 times the Standard Deviation
Protein Cut-Off Value = 5866.97

Common Name	Database	Database ID	Ultimate ORF ID	Array ID	Block	Row	Column	Protein Concentration	Signal	Background	Signal Used	Signal Rank	Z-Score	NC P-Value	Sig
PCTK1	MGC	BC001048.1	IOH4605	B03R10C13	03	10	13	0	43053	34334	11261	33	5.80819	0.00312	Hit
	MGC	BC001048.1	IOH4605	B03R10C14	03	10	14	0	45096	45110	13095.1	23	6.76305	0.00312	Hit
Adducin	MGC	BC013393.2	IOH13082	B06R05C03	06	05	03	0	32985	27519	6892.84	70	3.53408	0.00937	Hit
	MGC	BC013393.2	IOH13082	B06R05C04	06	05	04	0	35061	27912	9152.78	49	4.71063	0.00312	Hit
FXR1	MGC	BC028983.1	IOH22379	B07R05C03	07	05	03	0	41541	35715	13285	22	6.86192	0.00312	Hit
	MGC	BC028983.1	IOH22379	B07R05C04	07	05	04	0	36752	33255	9151.52	50	4.70997	0.00312	Hit
ARHGAP15	MGC	BC038976.1	IOH28763	B09R09C01	09	09	01	0	38786	33449	11438.2	30	5.90043	0.00312	Hit
	MGC	BC038976.1	IOH28763	B09R09C02	09	09	02	0	38531	31226	10908.7	37	5.62480	0.00312	Hit
cORF42	Ref	NM_138333.1	IOH10239	B17R03C09	17	03	09	0	36047	27732	10663.5	39	5.49713	0.00312	Hit
	Ref	NM_138333.1	IOH10239	B17R03C10	17	03	10	0	34892	28994	9326.46	48	4.80105	0.00312	Hit
Rps29	MGC	BC032813.1	IOH28699	B22R10C15	22	10	15	0	34332	29351	8264.72	55	4.24829	0.00728	Hit
	MGC	BC032813.1	IOH28699	B22R10C16	22	10	16	0	35452	33731	9662.22	46	4.97584	0.00312	Hit
Erk3	Ref	NM_002748.2		B27R06C07	27	06	07	0	52664	42973	22178.7	3	11.49204	0.00104	Hit
	Ref	NM_002748.2		B27R06C08	27	06	08	0	54282	51907	23563.7	1	12.21310	0.00104	Hit
OR8D2	MGC	XM_208541.2	IOH28446	B27R07C07	27	07	07	0	39225	36233	8462.34	53	4.35118	0.00520	Hit
	MGC	XM_208541.2	IOH28446	B27R07C08	27	07	08	0	41423	41098	10551.8	41	5.43898	0.00312	Hit
LARP1	MGC	BC033856.1	IOH21797	B28R10C07	28	10	07	0	34929	29315	8475.58	52	4.35807	0.00520	Hit
	MGC	BC033856.1	IOH21797	B28R10C08	28	10	08	0	32655	30008	6124.7	75	3.13418	0.01353	Hit
Hypothetical	Ref	NM_032694.1	IOH6500	B32R06C01	32	06	01	0	34491	27995	8043.04	58	4.13289	0.00728	Hit
	Ref	NM_032694.1	IOH6500	B32R06C02	32	06	02	0	36943	29193	10408.8	42	5.36452	0.00312	Hit
c18orf25	Ref	NM_145055.1	IOH12956	B39R03C15	39	03	15	0	43034	33311	14245.2	18	7.36179	0.00208	Hit
	Ref	NM_145055.1	IOH12956	B39R03C16	39	03	16	0	42623	40321	13771.4	19	7.11512	0.00208	Hit
PCTK1	Ref	NM_033019.1	IOH6258	B43R05C13	43	05	13	0	54073	52060	21617.4	4	11.19985	0.00104	Hit
	Ref	NM_033019.1	IOH6258	B43R05C14	43	05	14	0	55037	53201	23474.6	2	12.16668	0.00104	Hit
ARHGEF5	Ref	NM_005435.2	IOH14526	B47R04C05	47	04	05	0	42373	31470	14538.3	16	7.51438	0.00208	Hit
	Ref	NM_005435.2	IOH14526	B47R04C06	47	04	06	0	42727	32302	14867.9	14	7.68599	0.00208	Hit

Figure A.2 Proteins identified as Pak2 substrates by the Kinase Substrate Identification (KSI) microarrays.

Output file of protoarray prospector for ATP + Pak2 protein microarray. Each protein is spotted in duplicate and evaluated independently. The common name of the accession numbers, when known, appears at the left.

Pak2 Phosphorylates Full-length Erk3 in Solution.

Although KSI slides can rapidly identify potential new kinase substrates, we wanted to confirm that Erk3 was a Pak2 phosphoacceptor in solution. This is an important consideration as not every protein identified from protein microarrays recapitulates in solution. KSI experiments using recombinant p38alpha, CK2 and PKA kinases identified 26 potential substrates, 5 of which (19%), failed confirmation when tested in solution (Invitrogen). Human Erk3 is an inherently unstable protein subject to proteasome-mediated degradation (24). As the protein microarrays do not reveal which residues of Erk3 are phosphorylated, we chose to use a baculovirus expression system similar to what has been previously reported for expression of full-length Erk3(25) and Erk4 (26) (Fig. A.3A). Although our Erk3 preparation is not homogenous, it is highly enriched and cross-reactive with both anti-Erk3 antisera (directed towards residues surrounding leucine 410) and anti-His6 antibodies directed towards the extreme N-terminus of the protein (Fig. A.3B). Our Erk3 preparations therefore contain presumably full-length (based on electrophoretic mobility) as well as discrete C-terminal truncations that do not extend beyond amino acid 410 (Fig. A.3B). We used this source of recombinant Erk3 for Pak2 *in vitro* kinase assays to confirm the initial protein microarray result. As expected, in the absence of exogenous substrates recombinant Pak2 undergoes autophosphorylation as monitored by ^{32}P incorporation (Fig. A.3C, lane 1). Inclusion of myelin basic protein (MBP), led to both Pak2 autophosphorylation and MBP transphosphorylation (Fig. A.3C, lane 2). The increased autophosphorylation of Paks by substrates has previously been reported (27) and we have previously observed that high concentrations of Paktide can lead to Pak activation independently of small GTPases (28). Inclusion of increasing amounts of recombinant Erk3 with a fixed amount of recombinant Pak2 lead to an increase in the extent of Erk3 phosphorylation (Fig. A.3C, lanes 3-7, Erk3 signal is denoted by an asterisk). Exclusion of recombinant Pak2 from samples containing the highest amount of Erk3 (Fig. A.3C, lane 8) indicated that the phospho-Erk3 signal is dependent on Pak2 and argues against Erk3 phosphorylation resulting from autophosphorylation or by an unknown contaminating kinase in our Erk3 preparations. Additionally, although both the His6 and total ERK3 antisera reveal the presence of three major cross-reactive species, the *in vitro* kinase assays predominantly what appears to be a single phosphorylated species. We do not know whether this results from the inability to specifically resolve the three Erk3 species (each approximately 100 kDa) or whether the different C-terminal truncations have differential ability

to be phosphorylated by Pak2, as is the case for the phosphorylation of the C-terminal of ERK3 by Cdk1to regulate its stability in mitosis (29). Together, these results demonstrate that Pak2 kinase is able to selectively phosphorylate GST-Erk3 on protein microarrays (Fig. A.1 and A.2) and His6-Erk3 (Fig. A.3C) *in vitro*.

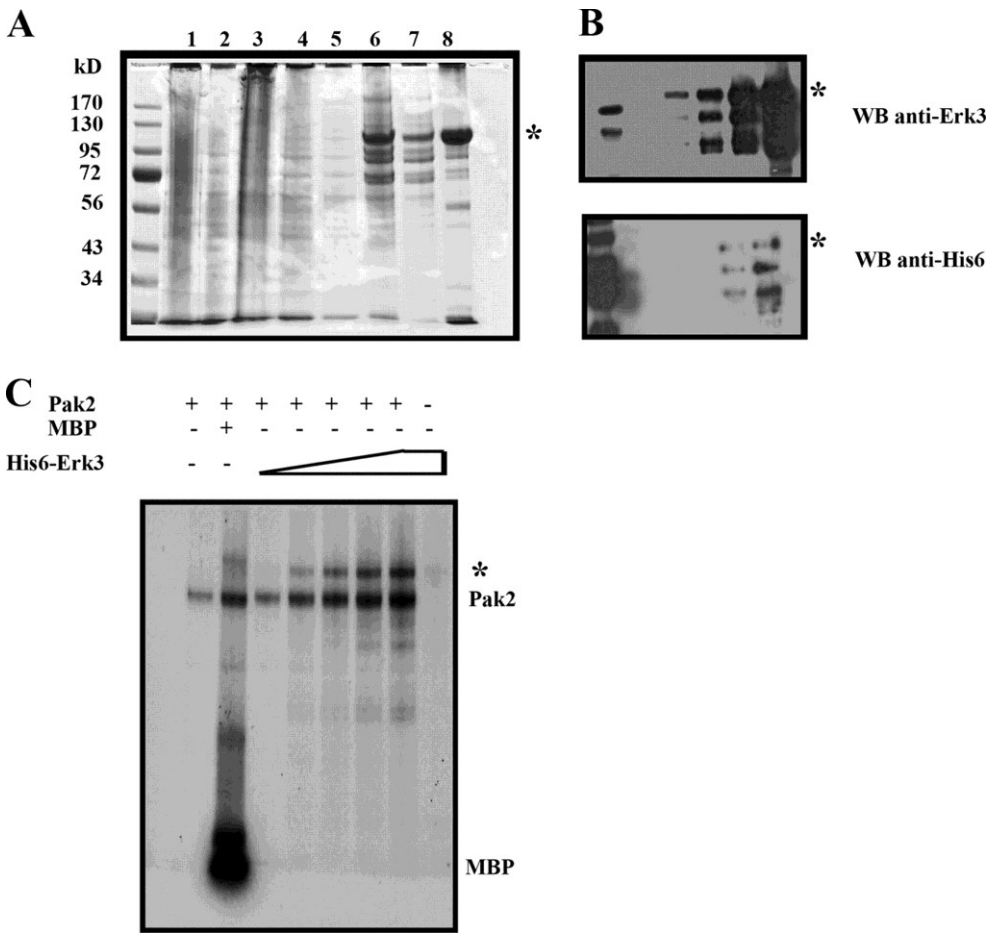

Figure A.3 Erk3 is a Pak2 substrate in solution

A. Purification scheme of recombinant Erk3 from baculovirus infected insect cells. Cell pellets were collected 48 hours post infection with high-titer baculovirus stocks and lysed by sonication. Specific fractions were collected and evaluated for purity by electrophoresis on a 10% SDS-Page gel followed by Coomassie staining. Lane 1 = total cell lysate, lane 2= cleared lysate, lane 3= HisPur non-binding fraction, lane 4= HisPur wash1, lane 5= HisPur wash 2, lane 6= 200 mM imidazole elution fraction, lane 7= Vivaspin 30 000 MWCO filtrate, lane 8= Vivaspin 30 000 MWCO retentate. The asterisk denotes the slowest migrating, and presumably full-length Erk3. B. Purified ERK3 protein is recognized by N-terminal hexahistidine and total Erk3 antibodies. Increasing amounts of the 30 000 MWCO retentate (Fig. 2A, lane 8) were resolved by electrophoresis on an 8% SDS-PAGE gel and subjected to Western analyses using anti-Erk3 (top) and anti-His6 antibodies (bottom). C. ^{32}P-ATP Autoradiogram of Pak2 in vitro kinase assays. For all lanes the amount of Pak2 added remained constant. Lane 1= Pak2 protein alone, lane 2= Pak2 + MBP, lane 3-7= Pak2 with increasing amounts of Erk3 protein. Lane 8= Equivalent amounts of ERK3 as in lane 7 but lacking Pak2. ^{32}P- Erk3 is denoted by asterisk, ^{32}P-Pak2 and ^{32}P-MBP signals are also identified.

Pak2 Phosphorylates Erk3 on Serine 189.

Erk3 is a member of the atypical MAPK family, lacking the characteristic "T-X-Y" motif within the activation loop (in Erk3, the corresponding sequence is S189-E190-G191). Although the S189 site is phosphorylated in cells (18, 19) the kinase responsible for this phosphorylation has yet to be identified. As Pak2 can phosphorylate Erk3 *in vitro* (Fig. A.1, Fig. A.3C), we asked whether Pak2 could specifically phosphorylate S189. Using phospho-specific S189 antibodies, we demonstrate that recombinant Erk3 derived from insect cells is pre-phosphorylated at this position (Fig. A.4, lane 1), consistent with previous observations for recombinant full-length Erk4 purified from insect cells (26). Addition of ATP alone led to a small increase in the extent of the phospho-S189 signal, as did the inclusion of ATP and Pak2 (Fig. A.4, lanes 2, 3). Although S189 cross reactivity is clearly observed in our ERK3 preparations, we cannot determine the stoichiometry of this phosphorylation by Western blot. In order to more clearly evaluate whether Pak2 can phosphorylate S189 we first dephosphorylated Erk3 with lambda phosphatase followed by inactivation of the phosphatase by addition of sodium orthovanadate. This treatment completely abolished phospho S189 cross-reactivity (Fig. A.4, lane 4 top panel) without affecting the total amount of Erk3 (Fig. A.4, bottom panel). Addition of ATP alone to the dephosphorylated Erk3 did not promote an increase in phospho S189 cross-reactivity suggesting again that the increased S189 signal was not the result of Erk3 autophosphorylation, consistent with our previous results (Fig. A.1). Addition of Pak2 and ATP to the dephosphorylated Erk3 protein led to an increase in S189 phosphorylation (Fig. A.4, lane 6). Collectively, these results demonstrate that Erk3 is a suitable substrate for Pak2 kinase activity *in vitro*, and that at least one of the residues phosphorylated by Pak2 is serine 189.

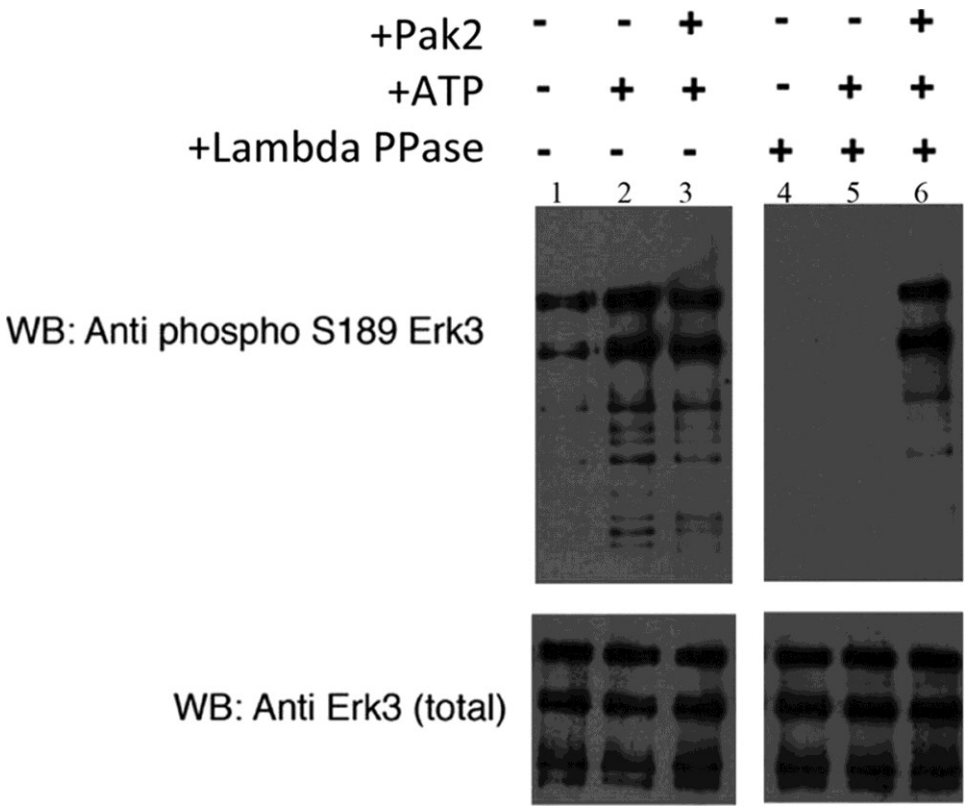

Figure A.4 Pak2 phosphorylates serine 189 within the Erk3 activation loop in vitro.

The Erk3 protein purified from insect cells is pre-phosphorylated on serine 189. Recombinant Erk3 protein (Fig. 2A, lane 8) was dialyzed into 1X phosphobuffer and subjected to an in vitro kinase assay using recombinant Pak2. Proteins were resolved by electrophoresis on an 8% SDS-PAGE gel and subjected to Western analyses using phospho-S189 specific antisera (upper panel) and total Erk3 antibodies (lower panel) to ensure equivalent loading of Erk3. Lane 1= Erk3 protein in 1X phosphobuffer, lane 2 = Erk3 protein after 30 minutes incubation with ATP, Lane 3 = Erk3 protein after 30 minutes incubation with ATP and Pak2. Lanes 4-6 are similar to lanes 1-3 with the exception that the Erk3 source was first dephosphorylated by lambda phosphatase followed by inactivation of the phosphatase by the addition of sodium orthovanadate.

Pak Kinase Inhibition Promotes Erk3 Nuclear Accumulation.

Erk3 is known to shuttle between the nucleus and the cytoplasm through a CRM1-dependent mechanism (30). To determine whether S189 phosphorylation contributes to the localization of Erk3, we assessed the subcellular localization of GFP-Erk3, as well as the GFP-Erk3S189A and GFP-Erk3S189D variants in transiently transfected NIH3T3 cells. Wild type and S189D variants are predominantly cytoplasmic whereas the GFP-Erk3S189A variant displays an increased nuclear localization (Fig. A.5A, B). To determine whether this differential localization was dependent on Pak kinase activity, we co- transfected NIH3T3 cells with wild type GFP-Erk3 and various monomeric red fluorescent protein (mRFP) constructs expressing the Pak1 protein inhibitory domain (PID). The PID corresponds to residues 83-149 of human Pak1 and acts as a highly selective pan-Class I (Pak1, -2 and -3) inhibitor when expressed *in trans* by exploiting Class I Pak's activation mechanism (31). Co-expression of mRFP-PID, but not mRFP alone or the inactive mRFP-PIDL107F, significantly increased the extent of nuclear Erk3 (Fig. A.5C, D). These results implicated Pak kinase activity in regulating the subcellular distribution of Erk3.

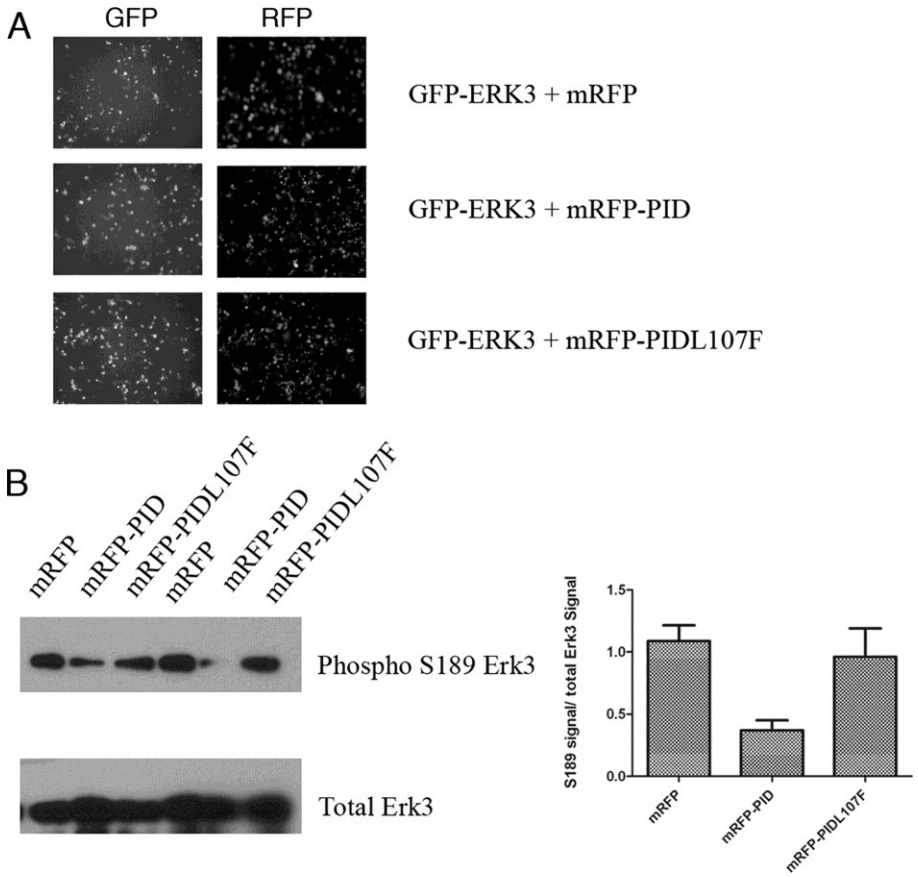

Figure A.5 Erk3 S189 phosphorylation promotes its cytoplasmic redistribution in NIH3T3 cells.

A. NIH3T3 cells were transfected with GFP tagged expression plasmids for wild type Erk3, Erk3S189A and Erk3S189D. 48 hours post transfection cells were fixed and counterstained with DAPI to unambiguously identify the nucleus. B. Quantification of the subcellular distribution of Erk3. The subcellular localization of the GFP-Erk3 signals was determined for greater than 100 transfected cells. Each GFP positive cell was scored blind and assigned into one of three categories: uniform GFP signal in the cytoplasm and the nucleus (N=C), predominantly nuclear (N>C) or predominant cytoplasmic staining (N<C). C. Inhibition of Pak kinase activity promotes the nuclear retention of GFP-Erk3. NIH3T3 cells were co-transfected with wild type GFP-Erk3 expression plasmids and expression plasmids encoding mRFP, mRFP-PID or mRFP-PIDL107F. 48 hours later the cells were fixed and analyzed as described above. D, Quantification of the subcellular distribution of GFP-Erk3 in cells expressing the indicated mRFP constructs. Bar graphs represent the mean and +/- SEM of at least three different transfections.

Inhibition of Pak kinase activity reduces the extent of Erk3 S189 phosphorylation in cells.

Our biochemical results suggesting that recombinant Erk3 was phosphorylated by recombinant Pak2 and that at least one of the sites phosphorylated *in vitro* is within Erk3's presumptive activation loop prompted us to determine whether this also occurred in cells. As endogenous ERK3 is subjected to degradation by the 26S proteasome we relied on co-transfecting HEK293 cells with plasmids encoding emGFP-ERK3 and the following mRFP constructs: mRFP (empty vector control), mRFP-PID (active Class I inhibitor) or mRFP-PIDL107F (inactive class I inhibitor). Approaches to evaluate the relative levels of S189 phosphorylation require that the vast majority of GFP positive cells are also RFP positive which we confirmed by immunofluorescence (Fig. A.6A); we estimate that the proportion of GFP+/RFP- transfected cells is less than 5% of the total number of GFP positive cells.

These cells were then lysed and subjected to Western blots using total Erk3 antibodies. Although we generally load equivalent amounts of total protein lysates for Western blots, in this case we had to empirically adjust the amount of lysate loaded to approach equivalent levels of total Erk3 protein as it appears that co-expression of the RFP-PID leads to a decrease in the amount of GFP-Erk3 expressed. Once conditions achieved approximate equivalent loading of ERK3 were achieved these same conditions were probed with the phospho S189 antibody and the relative S189 and total ERK3 signals were determined by densitometry. Figure A.6B shoes that co-expression of the PID leads to a decrease in the extent of S189 cross-reactivity, quantification of three independent transfections suggests that expression of the PID can reduce the S189/ total Erk3 signal ratio approximately two fold. These data suggest that selective Pak inhibition in cells leads to a decrease in Erk3 S189 phosphorylation and suggests that ERK3 is a Class I Pak substrate in cells.

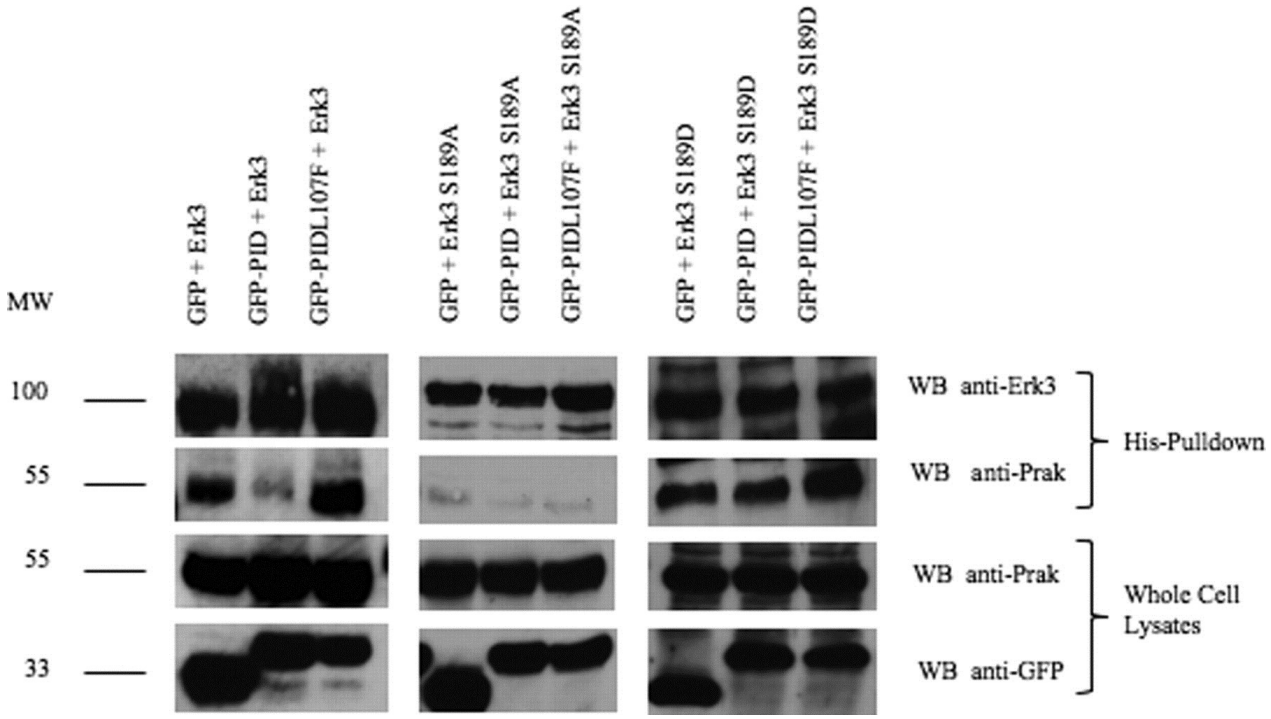

Figure A.6 Pak kinase inhibition reduces the extent of Erk3 S189 phosphorylation in cells.

HEK293 cells were cotransfected with expression contructs for EmGFP-Erk3 and monomeric RFP, monomeric RFP-PID or monomeric RFP-PIDL107F. A. 48 hours post transfection, the cells were imaged on an inverted fluorescent microscope to ensure that the majority of cells expressing GFP-ERK3 also expressed a mRFP variant. B. Cell lysates were prepared from replicate independent transfections including cells imaged in A, and separated by electrophoresis prior to Western analyses with variable amounts of lysate loaded to empirically achieve approximately equal levels of total Erk3. These conditions were then used to probe a replicate blot with the phospho S189 specific antibody. C. The densitometric ratios of the phospho S189/ total Erk3 signals for three independent transfecrions were acquired in Image J (NIH) using recommended protocols.

S189 Phosphorylation Modulates the Interaction of Erk3 and Prak.

Although the kinases responsible for S189 phosphorylation had heretofore been uncharacterized, site directed mutants (S189A) had previously demonstrated that S189 phosphorylation was essential for the ability of Erk3 to interact with and activate Prak (19, 26), the only known Erk3 substrate. As S189 phosphorylation is required for a productive Erk3/Prak interaction and Pak inhibition leads to decreased S189 cross reactivity in cells (Figure A.6B), we asked whether Pak inhibition also led to a decreased Erk3/Prak interaction. To address this we co-transfected HEK293 cells with a His6-Erk3 expression plasmid and plasmids expressing GFP, GFP-PID or GFP-PIDL107F. The His6-Erk3 was adsorbed by IMAC and the extent of endogenous Prak co-purifying with His6-Erk3 was determined by Western analysis. Focusing on the wild type allele (Fig. A.7, *leftmost panels*), expression of the PID, but not GFP alone or the inactive GFP-PIDL107F variant, reduced the amount of Prak co-precipitating with His6-Erk3. This was not due to reduced Prak expression as the levels of endogenous Prak in whole cell lysates was not affected by expression of the PID (Fig. A.6). To ensure that the ability of Pak inhibition to reduce the stability of the Erk3/Prak complexes did not result from other residues of Erk3 being phosphorylated by Paks, we repeated the experiments described above using the non-phosphorylatable (S189A) and phospho-mimetic (S189D) variants of His6-Erk3. Consistent with the model proposed for Erk3/Prak interaction (19) mutation of serine 189 to alanine strongly reduced the extent of Prak co-precipitating with His6-Erk3 (Fig. A.7 *middle panels*). Substituting serine 189 with aspartic acid restored the interaction between Erk3 and Prak. Importantly, and unlike the wild type allele, the Erk3S189D/Prak interaction was insensitive to the expression of the PID (Fig. A.7 *rightmost panels*). These results demonstrated that selective Class I kinase inhibition in cells modulates the interaction of Erk3 with its only known effector Prak, in a mechanism that is dependent on S189 phosphorylation, and provides the first evidence that Class I activity modulates the activity of Erk3 in cells.

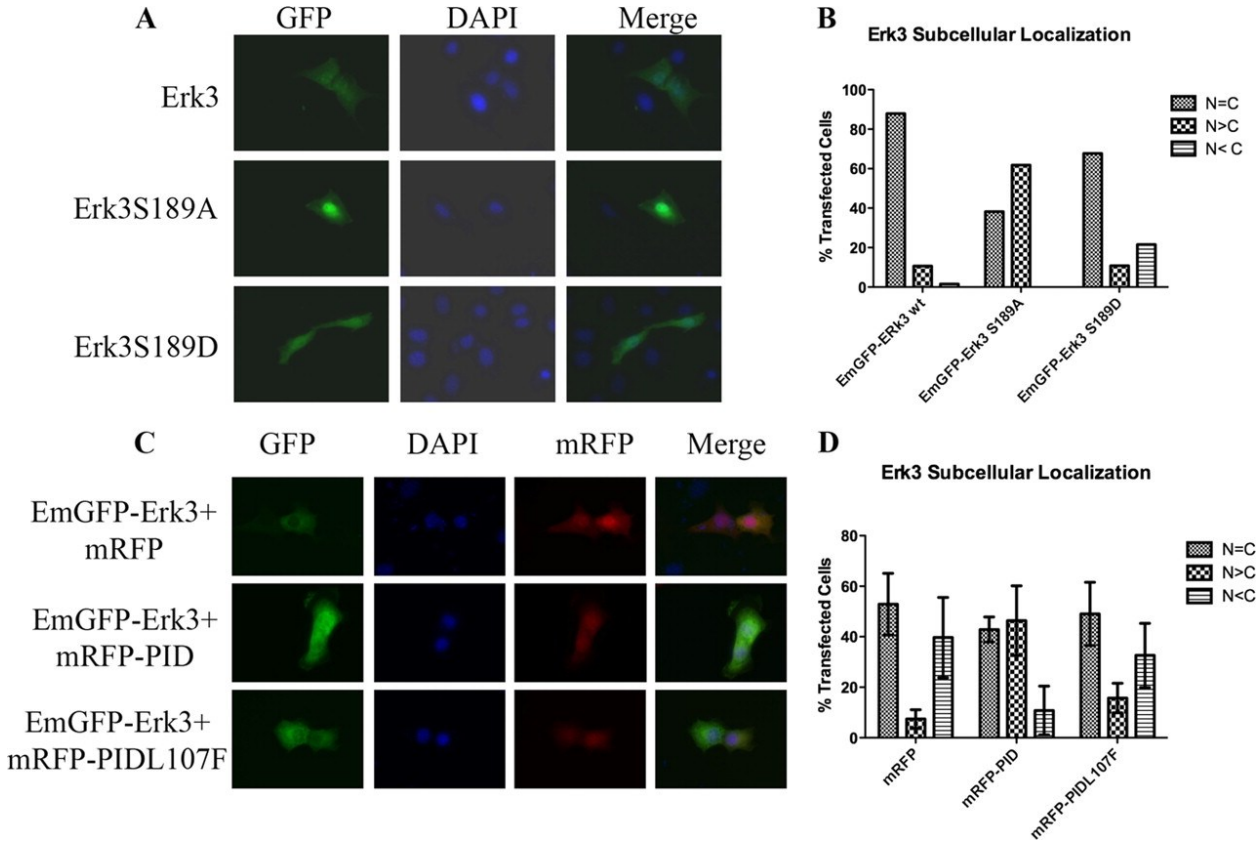

Figure A.7 Pak kinase inhibition prevents the association of Erk3 with its known effector Prak in an S189-dependent manner.

HEK293 cells were co-transfected with expression constructs for His6-Erk3, His6-Erk3S189A or His6-Erk3S189D along with expression constructs for GFP, GFP-PID or GFP-PIDL107F as indicated. 48 hours post transfection; His6 proteins were affinity adsorbed to HisPur beads. The amount of His6-Erk3 in the His pulldowns was determined by Western analysis using total anti-Erk3 antibodies and the amount of endogenous Prak was similarly determined using anti-Prak antibodies (upper six panels). To ensure appropriate expression of indicated GFP constructs and that the experimental treatments did not alter the total levels of endogenous Prak, Western analyses of whole cell lysates were conducted using anti-GFP and anti-Prak antibodies (lower six panels). Numbers on the right represent the molecular mass as determined by pre-stained SDS-Page loading standards. Results are representative of three independent co-transfections.

Discussion

A number of different groups have investigated the requirements for Erk3 and Erk4 activation loop phosphorylation and kinase activity in atypical MAPK signaling pathways. These pathways remain enigmatic with respect to both the cellular upstream activating signals (functioning analogously to MAP2Ks) and to a slightly lesser extent in regards to downstream effectors (the MAPK activated kinases or MKs). Models for Erk3/Erk4 function have so far been generally restricted to the following common properties: i) the ability of variants of Erk3/Erk4 to bind to Prak ii) the ability of Erk3/Erk4 variants to promote Prak T182 phosphorylation and/or activate the kinase activity of Prak and iii) the ability of these variants to modulate their own subcellular localization or the subcellular localization of Prak.

The Erk3 literature is not entirely consistent with regards to the requirements of S189 phosphorylation and Erk3 kinase activity for Prak activation (25, 26, 32, 33). This is somewhat surprising in light of the similarity of experimental approaches used to support or to reject a role for either Erk3 catalytic activity or S189 phosphorylation. The observation that Erk3 and Erk4 can be detected in oligomers containing Prak may be sufficient to reconcile some of the previous discrepancies (34). Nonetheless, the inability to selectively promote or inhibit atypical MAPK signaling remains a significant hurdle against a better understanding of Erk3 function and has led some to suggest that the ability of ERK3 mutants to activate MK5 depends on the experimental system applied (34).

Using high-density protein microarrays and recombinant Erk3 and Pak2 proteins we found that Erk3 is a Pak2 substrate *in vitro*. Phospho-specific antibodies against residues within the Erk3 activation loop further indicated that serine 189 is a site phosphorylated by Pak2 *in vitro*. Additionally selective class I kinase inhibition led to a decrease in the extent of S189 phosphorylation in HEK293 cells (Fig. A.6B) suggesting that this kinase substrate relationship between Pak and Erk3 is retained *in vivo*. Specific inhibition of class I kinase activity in fibroblasts led to an increased nuclear retention of GFP-Erk3, suggesting a role for Paks in regulating the subcellular localization of Erk3. This result was rather surprising as the Meloche laboratory had previously reported that nuclear export of Erk3 was independent of both activation loop phosphorylation and kinase activity in NIH3T3 cells (30), the same cell line used

in our studies. The one obvious difference between the two approaches was the way in which Erk3 was detected; the Meloche group detected the localization of myc-tagged Erk3 by indirect immunofluorescence whereas we used GFP-Erk3. We do not know whether this accounts for the observed differences, but GFP tagged variants of Erk3 have been used by other groups that display very similar subcellular localization in HEK293 cells as we observe in NIH3T3 cells (34). We also believe that the similarity in subcellular localization of the GFP-Erk3S189A variant to that seen for GFP-Erk3 in cells co-expressing mRFP-PID (Fig. A.5C,D) supports our conclusion that S189 phosphorylation modulates Erk3 subcellular localization.

Finally, as Erk3 S189 phosphorylation is required for the interaction with Prak, we further demonstrated that specific inhibition of Class I kinase activity in cells decreases the interaction between His6-Erk3 and endogenous Prak in HEK293 cells (Fig. A.6). This effect was specific to the phosphorylation status of S189 as Prak interacted poorly with the Erk3S189A variant, whereas Prak interacted strongly with Erk3 phosphomimetic variant (S189D). Importantly, the interaction between Prak and Erk3S189D was insensitive to PID expression indicating that the ability of Pak to stabilize Erk3/Prak complexes derives exclusively from the ability to promote S189 phosphorylation. Collectively, our results are the first to demonstrate a relationship between the p21-activated kinases and Erk3 and further suggest a role for class I kinase activity in regulating atypical MAPK pathways by promoting S189 phosphorylation.

The specific consequences of atypical MAPK signaling are not well understood, but the biological importance of Erk3 is suggested from the following observations: i) Expression of stabilized versions of Erk3 can promote cell cycle arrest in fibroblasts and Erk3 is stabilized and accumulates to high levels during muscle differentiation (24) ii) differential Erk3 expression is observed in many cancers including those harboring BRAFV600E mutations (35), iii) Erk3 is essential for neonatal development in mice (36). An important question remains- how does S189 phosphorylation promote the interaction with Prak? Previous work has demonstrated that the residues of Erk3 required for Prak binding map to a region characterized by the sequence ^{328}FRIEDE^{333} (32) distinct from the common docking (CD) domain used by classical ERK's to bind to both their respective MAP2Ks and their cognate substrates (37). Molecular modeling suggests that Erk4 S186 phosphorylation (analogous the Erk3 S189) might promote a

conformational change that increases the solvent accessibility of isoleucine 330 (within the conserved FRIEDE motif) allowing for efficient interaction with the C-terminal of Prak (32).

This is not the first time that Paks have been implicated in promoting the interaction of proteins functioning within a sequential kinase cascade. Paks facilitate the interaction between Mek1 and Erk1/2 via phosphorylation of Mek1 S289 (13, 38). Unlike the situation for Erk3 S189, S298 is not part of the Mek1 activation loop (consisting of serines 218 and 222) but is contained within the Mek1 proline rich sequence (residues 270 to 307). Interestingly, the Catling laboratory has demonstrated that Pak-dependent phosphorylation of Mek1 on serine 298 leads to an autocatalytic phosphorylation of the Mek1 activation loop residues and increased kinase activity against recombinant Erk1/2 *in vitro* (39). Similar to Erk3 S189 phosphorylation, Mek1 S298 phosphorylation does not respond to growth factor stimulation (31, 39) but activated by cellular attachment signals (40). To the best of our knowledge a role for cellular attachment in Erk3 S189 phosphorylation has never been addressed.

We believe that the identification of Paks as kinases responsible for Erk3 S189 phosphorylation represents an important step forward in our understanding of atypical MAPK signaling cascades. Its identification affords the ability to modulate atypical MAPK signaling pathways in physiologically relevant settings by specific Pak inhibition. In our opinion, use of the PID affords several important advantages over other experimental approaches, such as pharmacological inhibition or siRNA knockdowns. These advantages include, lack of isoform selectivity, high target specificity, lack of dominant negative effects and the ability to inhibit endogenous Class I activity *in trans* in tissue culture (31) and in transgenic animals (5). Specific mutants of the PID (L107F) that no longer function as Pak inhibitors further provide an important control to evaluate the specific contribution of Pak kinase activity.

Even with the identification of Paks as S189 kinases, previous reports of the kinetics of S189 phosphorylation raise some important questions. As Erk3 S189 phosphorylation does not respond to signals that activate the classical MAPKs (19), S189 phosphorylation persists in HEK293 cells rendered quiescent by serum starvation (19). Although the signals that activate Class I kinase activity differ from cell type to cell type, serum starvation is sufficient to reduce

Pak kinase activity in most cells as demonstrated by both Pak1 activation specific anti-sera as well as in-gel kinase assays (20, 31). It is important to note that although we commonly think of Pak kinase activity being "off" in quiescent cells, this activity is still readily detected albeit as much lower levels than in cells stimulated with the appropriate growth factors. As the relative levels of the inherently unstable Erk3 and Class I Paks are unknown, and likely to be cell type specific, basal Class I kinase activity may still be sufficient to promote S189 phosphorylation in quiescence cells.

Alternatively S189 could be targeted by kinases other than Pak. Although entirely speculative, possible candidates include the group II Paks (Pak4, -5, -6), which are constitutively active kinases sharing similar substrate specificity with the class I Paks (28) or the related mammalian sterile 20-like kinase (Mst-1) as Erk3 was identified in a KSI protein microarray screen using recombinant Mst-1 (S. Jalan and J. Chernoff, unpublished observations). It is important to note that although these proteins are all members of the Ste20 superfamily, neither the class II Paks nor Mst1 are inhibited by expression of the PID. Irrespective of whether the ability to phosphorylate S189 is unique to Call I Paks, our results strongly suggest that Class I kinase activity is critical for the formation of Erk3/Prak complex in cells, and suggests and important role for Class I kinase activity in regulating atypical MAPK signaling.

References

1. Cotteret, S. and Chernoff, J. (2002) *Genome Biol* **3**, REVIEWS0002
2. Kumar, R., Gururaj, A. E. and Barnes, C. J. (2006) *Nat Rev Cancer* **6**, 459-471
3. Szczepanowska, J. (2009) *Acta Biochim Pol* **56**, 225-234
4. Allen, J. D., Jaffer, Z. M., Park, S. J., Burgin, S., Hofmann, C., Sells, M. A., Chen, S., Derr-Yellin, E., Michels, E. G., McDaniel, A., Bessler, W. K., Ingram, D. A., Atkinson, S. J., Travers, J. B., Chernoff, J. and Clapp, D. W. (2009) *Blood* **113**, 2695-2705
5. Hayashi, M. L., Rao, B. S., Seo, J. S., Choi, H. S., Dolan, B. M., Choi, S. Y., Chattarji, S. and Tonegawa, S. (2007) *Proc Natl Acad Sci U S A* **104**, 11489-11494
6. Nguyen, D. G., Wolff, K. C., Yin, H., Caldwell, J. S. and Kuhen, K. L. (2006) *J Virol* **80**, 130-137
7. Dummler, B., Ohshiro, K., Kumar, R. and Field, J. (2009) *Cancer Metastasis Rev* **28**, 51-63
8. Chang, L. and Karin, M. (2001) *Nature* **410**, 37-40
9. Krishna, M. and Narang, H. (2008) *Cell Mol Life Sci* **65**, 3525-3544
10. Chen, Z., Gibson, T. B., Robinson, F., Silvestro, L., Pearson, G., Xu, B., Wright, A., Vanderbilt, C. and Cobb, M. H. (2001) *Chem Rev* **101**, 2449-2476
11. Roux, P. P. and Blenis, J. (2004) *Microbiol Mol Biol Rev* **68**, 320-344
12. Mason, C. S., Springer, C. J., Cooper, R. G., Superti-Furga, G., Marshall, C. J. and Marais, R. (1999) *EMBO J* **18**, 2137-2148
13. Eblen, S. T., Slack, J. K., Weber, M. J. and Catling, A. D. (2002) *Mol Cell Biol* **22**, 6023-6033
14. Coulombe, P. and Meloche, S. (2007) *Biochim Biophys Acta* **1773**, 1376-1387
15. Cheng, M., Boulton, T. G. and Cobb, M. H. (1996) *J Biol Chem* **271**, 8951-8958
16. Abe, M. K., Kuo, W. L., Hershenson, M. B. and Rosner, M. R. (1999) *Mol Cell Biol* **19**, 1301-1312
17. Robinson, M. J., Cheng, M., Khokhlatchev, A., Ebert, D., Ahn, N., Guan, K. L., Stein, B., Goldsmith, E. and Cobb, M. H. (1996) *J Biol Chem* **271**, 29734-29739
18. Cheng, M., Zhen, E., Robinson, M. J., Ebert, D., Goldsmith, E. and Cobb, M. H. (1996) *J Biol Chem* **271**, 12057-12062
19. Deleris, P., Rousseau, J., Coulombe, P., Rodier, G., Tanguay, P. L. and Meloche, S. (2008) *J Cell Physiol* **217**, 778-788
20. Deacon, S. W., Beeser, A., Fukui, J. A., Rennefahrt, U. E., Myers, C., Chernoff, J. and Peterson, J. R. (2008) *Chem Biol* **15**, 322-331
21. Hofmann, C., Shepelev, M. and Chernoff, J. (2004) *J Cell Sci* **117**, 4343-4354
22. Schnack, C., Hengerer, B. and Gillardon, F. (2008) *Proteomics* **8**, 1980-1986

23. Feilner, T., Hultschig, C., Lee, J., Meyer, S., Immink, R. G., Koenig, A., Possling, A., Seitz, H., Beveridge, A., Scheel, D., Cahill, D. J., Lehrach, H., Kreutzberger, J. and Kersten, B. (2005) *Mol Cell Proteomics* **4**, 1558-1568

24. Coulombe, P., Rodier, G., Pelletier, S., Pellerin, J. and Meloche, S. (2003) *Mol Cell Biol* **23**, 4542-4558

25. Seternes, O. M., Mikalsen, T., Johansen, B., Michaelsen, E., Armstrong, C. G., Morrice, N. A., Turgeon, B., Meloche, S., Moens, U. and Keyse, S. M. (2004) *EMBO J* **23**, 4780-4791

26. Perander, M., Aberg, E., Johansen, B., Dreyer, B., Guldvik, I. J., Outzen, H., Keyse, S. M. and Seternes, O. M. (2008) *Biochem J* **411**, 613-622

27. Jakobi, R., Huang, Z., Walter, B. N., Tuazon, P. T. and Traugh, J. A. (2000) *Eur J Biochem* **267**, 4414-4421

28. Rennefahrt, U. E., Deacon, S. W., Parker, S. A., Devarajan, K., Beeser, A., Chernoff, J., Knapp, S., Turk, B. E. and Peterson, J. R. (2007) *J Biol Chem* **282**, 15667-15678

29. Tanguay, P. L., Rodier, G. and Meloche, S. (2010) *Biochem J* **428**, 103-111

30. Julien, C., Coulombe, P. and Meloche, S. (2003) *J Biol Chem* **278**, 42615-42624

31. Beeser, A., Jaffer, Z. M., Hofmann, C. and Chernoff, J. (2005) *J Biol Chem* **280**, 36609-36615

32. Aberg, E., Torgersen, K. M., Johansen, B., Keyse, S. M., Perander, M. and Seternes, O. M. (2009) *J Biol Chem* **284**, 19392-19401

33. Schumacher, S., Laass, K., Kant, S., Shi, Y., Visel, A., Gruber, A. D., Kotlyarov, A. and Gaestel, M. (2004) *EMBO J* **23**, 4770-4779

34. Kant, S., Schumacher, S., Singh, M. K., Kispert, A., Kotlyarov, A. and Gaestel, M. (2006) *J Biol Chem* **281**, 35511-35519

35. Hoeflich, K. P., Eby, M. T., Forrest, W. F., Gray, D. C., Tien, J. Y., Stern, H. M., Murray, L. J., Davis, D. P., Modrusan, Z. and Seshagiri, S. (2006) *Int J Oncol* **29**, 839-849

36. Klinger, S., Turgeon, B., Levesque, K., Wood, G. A., Aagaard-Tillery, K. M. and Meloche, S. (2009) *Proc Natl Acad Sci U S A* **106**, 16710-16715

37. Bardwell, A. J., Frankson, E. and Bardwell, L. (2009) *J Biol Chem* **284**, 13165-13173

38. Eblen, S. T., Slack-Davis, J. K., Tarcsafalvi, A., Parsons, J. T., Weber, M. J. and Catling, A. D. (2004) *Mol Cell Biol* **24**, 2308-2317

39. Park, E. R., Eblen, S. T. and Catling, A. D. (2007) *Cell Signal* **19**, 1488-1496

40. Slack-Davis, J. K., Eblen, S. T., Zecevic, M., Boerner, S. A., Tarcsafalvi, A., Diaz, H. B., Marshall, M. S., Weber, M. J., Parsons, J. T. and Catling, A. D. (2003) *J Cell Biol* **162**, 281-291